UNIVERSIDAD AUTÓNOMA DE MÉXICO

PROGRAMA DE POSGRADO EN CIENCIAS BIOMÉDICAS

INSTITUTO DE FISIOLOGÍA CELULAR

TESIS

PARA OPTAR POR EL GRADO DE DOCTOR EN CIENCIAS

IDENTIFICACIÓN DE LOS AMINOÁCIDOS RESPONSABLES DE LAS DIFERENCIAS EN SUSCEPTIBILIDAD A REACTIVOS SULFHIDRILO DE LA CISTEÍNA DE INTERFASE EN LAS TRIOSAFOSFATO ISOMERASAS DE *TRYPANOSOMA CRUZI* Y *T. BRUCEI.*

PRESENTA

SELMA DÍAZ MAZARIEGOS

DIRECTOR DE TESIS

DR. RUY ENRIQUE PÉREZ MONTFORT
INSTITUTO DE FISIOLOGÍA CELULAR

CIUDAD DE MÉXICO, NOVIEMBRE 2020

Universidad Nacional Autónoma de México
UNAM
Biblioteca Central
Dirección General de Bibliotecas de la UNAM

UNAM – Dirección General de Bibliotecas
Tesis Digitales
Restricciones de uso

DERECHOS RESERVADOS ©
PROHIBIDA SU REPRODUCCIÓN TOTAL O PARCIAL

Todo el material contenido en esta tesis esta protegido por la Ley Federal del Derecho de Autor (LFDA) de los Estados Unidos Mexicanos (México).

El uso de imágenes, fragmentos de videos, y demás material que sea objeto de protección de los derechos de autor, será exclusivamente para fines educativos e informativos y deberá citar la fuente donde la obtuvo mencionando el autor o autores. Cualquier uso distinto como el lucro, reproducción, edición o modificación, será perseguido y sancionado por el respectivo titular de los Derechos de Autor.

Reconocimiento

Esta tesis estuvo dirigida por el Dr. Ruy Pérez Montfort del laboratorio 201 oriente del Departamento de Bioquímica y Biología Estructural del Instituto de Fisiología Celular de la Universidad Autónoma de México.

El comité encargado de asesorar el desarrollo de la tesis estuvo conformado por:

Dr. Ruy Pérez Montfort	Instituto de Fisiología Celular (UNAM)
Dr. Daniel Alejandro Fernández Velasco	Facultad de Medicina (UNAM)
Dr. José de Jesús García Trejo	Facultad de Química (UNAM)

El proyecto fue apoyado por el donativo número 254694 del Consejo Nacional de Ciencia y Tecnología (CONACyT) y el donativo número IN206816 de la Direccion General de Asuntos del Personal Académico Universidad Nacional Autónoma de México. Además, agradezco el apoyo de la beca de estudios otorgada por CONACyT con número 263707.

Agradezco la ayuda técnica de la Bióloga Elizabeth Nallely Cabrera González en el presente trabajo.

El jurado de examen de grado estuvo constituido por:

Presidente: Dra. Adela Rodríguez Romero

Secretario: Dr. José de Jesús García Trejo

Vocal. Dra. Alejandra Hernández Santoyo

Vocal. Dr. Diego González Halphen

Vocal. Dr. Enrique Ortega Soto

Agradecimientos

Técnica académica Nallely Cabrera González

No me alcanzarán las palabras para agradecer las asesorías académicas en protocolos de experimentos, funciones y manejo de equipo. En ocasiones no lo sabías, pero lo investigabas. Gracias por compartir tu formación y experiencia académica.

Agradezco a la amiga que encontré en ti. Tú siempre estabas dispuesta a escucharme y compartir anécdotas de tu vida. Eres una maravillosa persona, ha sido muy disfrutable compartir contigo estos años que ha durado el doctorado.

“Eres como el arco iris, alegras nuestras vidas”

Agradecimientos

Para mi formación académica fueron necesarias las funciones de varias personas que laboran en el Instituto de Fisiología Celular y quiero agradecer a cada uno de ellos.

Técnico del laboratorista. Alejandro Flores, te doy un agradecimiento especial por tus excelentes funciones en la preparación de medios de cultivos, amortiguadores, limpieza de materiales y equipos de laboratorio. Gracias por mantener un laboratorio limpio y disfrutable.

Técnico Académico. Ingeniero Manuel Ortínez Benavides, agradezco la maravillosa disposición para solucionar el mal funcionamiento de las centrífugas, incubadoras, detalles con los baños refrigerantes y otros equipos con problemas eléctricos o mecánicos. Gracias por tener una excelente atención y un magnifico trabajo, ya que sin sus soluciones hubiera sido imposible realizar en tiempo y forma muchos de los experimentos reportados en ésta tesis.

Dr. Alfredo Torres Larios. Hay varias cosas por las que te quiero agradecer: una de ellas es la ayuda que me brindaste en la búsqueda de alternativas para mejorar el diseño de experimentos; en esas ocasiones donde no funcionaba el protocolo empleado normalmente en TIMs. Gracias por el compromiso personal que invertiste, la generosidad de donar tus propios reactivos y apoyarme con el préstamo de equipo: columnas, matraces e incubadora.

También quiero agradecer el ejemplo de trabajo en lo académico. Gracias por ser un modelo a seguir.

¡Gracias por todo!

Dra. Andrea Gutiérrez Quezada.

Es muy emocionante para mí escribirte esto. Agradezco a la amiga que siempre estuvo para compartir sus conocimientos y experiencias académicas. Gracias por enseñarme a trabajar ideas, organizar y discutir resultados de los experimentos, sentarte conmigo a discutir sobre ellos. Realizaste el trabajo más difícil: “enseñarme a estructurar los resultados obtenidos”; has sido fundamental en este trabajo, no me alcanzan las palabras para agradecerte. Gracias por todo el tiempo donado para que aprendiera a escribir este trabajo.

Dra. Alma Reina Escalona Montaño.
Almita siempre estaré agradecida contigo por brindarme tu amistad y enseñarme un lugar en donde vivir. Recuerdo aquella ocasión en la que buscaste la forma para que pudiera practicar la candidatura con tu grupo de trabajo.

Por otro lado, agradezco tus consejos y cuidados respecto a mi salud, por compartir los menjurjes, acompañarme al médico, cuidar que nada me faltara cuando enfermaba, siempre estaré agradecida por cada uno de los detalles que tuviste conmigo, los llevo en el corazón. Eres una maravillosa persona, gracias por compartir tus conocimientos, anécdotas y familia.

¡Gracias por todo!

Dr. José María Farías Sánchez

Doctor José. A usted le quiero dedicar la tesis completa, ha sido una de las mejores personas que he podido conocer en la vida. Voy a estar enteramente agradecida por impulsarme a seguir estudiando y terminar el doctorado con éxito. Gracias por su ejemplo maravilloso y el apoyo en aspectos que no conocía, gracias por compartirme sus libros y sus experiencias.

Usted me ha brindado todo lo bueno que puede tener un estudiante de doctorado: libros, tips de experimentos, consejos de cómo ser mejor persona, estrategias para manejar la tensión nerviosa, tiempo para leer mis reportes y para corregir mi mala forma de escribir. Para expresarle mi agradecimiento el apoyo que me ha brindado para poder culminar el doctorado. Su disposición para ayudar en todo lo que usted podía siempre lo tuve, aunque no siempre usé todas las ventajas que eso me traería. Gracias por el ejemplo de humildad, muy pocos doctores en ciencia tienen lo que usted tiene, esa pasión por la ciencia. ¡Estaré agradecida toda la vida!

Nelly Raquel Gonzales Arena

Agradezco tu maravillosa amistad, en varias ocasiones te he agradecido por compartirme a tu familia, hacerme parte de tu familia espiritual, cuidarme cuando enfermaba y estar al pendiente que nada me faltará. Ha sido maravillo compartir la etapa del doctorado con tu compañía, ir por los cafés, reír juntas, llorar juntas etc.

Nuestra amistad es eterna, en el cielo sólo recordaremos todo lo que pasamos en el doctorado y nos reiremos. Cada uno de los procesos que vivimos en este período doctoral no fueron nada sencillos ni fáciles de procesar, pero han servido para que seamos mejores personas, sabias y maduras en carácter, no creo que lo lográramos todo, pero tenemos esperanza de un dia llegar a la plenitud de Cristo.

Aminoácidos responsables de las diferencias en inactivación al metil metano tiosulfonato

ABREVIATURAS

TIM	triosafosfato isomerasa
TcTIM	triosafosfato isomerasa de *Trypanosoma cruzí*
TbTIM	triosafosfato isomerasa de *Trypanosoma brucei*
MMTS	metil metano tiosulfonato
PDB	Protein Data Bank
NaCl	cloruro de sodio
MES.Na	sal sódica del ácido 2-N-morfolino etanosulfónico
IPTG	isopropil-β-D tiogalactopiranósido
$(NH_4)_2SO_4$	sulfato de amonio
TEA	trietanolamina
EDTA	ácido etilendiamino tetracético
GAP	gliceraldehído 3-fosfato
DHAP	dihidroxiacetona-fosfato
α-GDH	α-glicerolfosfato deshidrogenasa
NADH	nicotin adenin dinucleótido o nicotinamida adenina dinucleótido
Km	concentración de sustrato para la cual la velocidad de reacción es la mitad de la velocidad máxima.
Vmax	velocidad máxima
K_{cat}	constante catalítica
K_{cat}/Km	eficiencia catalítica
Ln	logaritmo natural
pH	potencial de iones hidronio
M	molar
mL	mililitro

Resumen

Las proteínas con un alto grado de similitud en su secuencia de aminoácidos generalmente también tienen similitud en su estructura, función y otras propiedades físico-químicas. Sin embargo, algunas proteínas homólogas difieren en una o más propiedades funcionales o fisicoquímicas. Para comprender mejor cómo uno o más aminoácidos pueden determinar una propiedad específica en las proteínas, deben identificarse esos residuos responsables. Nosotros estudiamos a la triosafosfato isomerasa de dos parásitos, *Trypanosoma cruzi* y *Trypanosoma brucei* que tienen un alto grado de similitud en su secuencia de aminoácidos, para estudiar específicamente la diferencia en la reactividad de la cisteína de interfaz al reactivo metilmetano tiosulfonato entre ambas enzimas. Para ello, desarrollamos una estrategia usando mutaciones aditivas y mutantes con aminoácidos seleccionados para localizar e identificar los residuos que influencian directamente esa reactividad. Encontramos que ésta depende de tres residuos ubicados lejos de la cisteína de interfaz, los cuales parecen inducir cambios en su reactividad, al aumentar o disminuir el *pKa* aparente de esa cisteína de interfaz. Es muy probable que el papel modulador sobre la reactividad de la cisteína de interfaz por estos tres aminoácidos no podría haberse predicho usando otros métodos. La realización de este trabajo mejoró una estrategia para identificar residuos específicos que modulan respuestas diferentes de una propiedad biofísica determinada de dos proteínas homólogas. La estrategia podría aplicarse en otros estudios sobre la estructura y función de proteínas.

Abstract

Proteins with high degree of similarity in their amino acid sequence also have similarity in their structure, function and other physicochemical properties. Nevertheless, in some homologous proteins differ in one or more functional or physicochemical properties. To better understand how one or more parameters can determine a specific property in proteins, the residues responsible for those differences must be identified. We studied the triosephosphate isomerases from *Trypanosoma cruzi* and *Trypanosoma brucei*, which have a high degree of similarity in their amino acid sequence, to specifically investigate the difference in the reactivity of their interface cysteine to the thiol reagent: methyl methane thiosulfonate. We therefore developed a strategy using enzymes with additive mutations and site directed mutant enzymes with selected amino acids, to locate and identify residues that directly influence that reactivity. We found that this depends on three residues located at a distance from the interface cysteine, which induce changes in its reactivity, by increasing or decreasing the apparent *pKa* of this interface cysteine. It is almost certain that the modulating role on the reactivity of the interface cysteine by these three amino acids could not have been predicted using other current methods. This work completed a strategy to identify specific residues that modulate different responses of a specific biophysical property for two homologous proteins. The strategy could be applied in other studies on the structure and function of proteins.

1. Introducción

Las enzimas que provienen de una misma familia, generalmente, presentan una alta identidad en secuencia de aminoácidos, similitudes en su estructura, funciones y características físico-químicas. También pueden mostrar similitud en su susceptibilidad o inactivación con agentes químicos y físicos [1–4]. Sin embargo, no todas las enzimas pertenecientes a la misma familia siguen el mismo patrón, y a veces presentan grandes diferencias en su estabilidad, o en su susceptibilidad a la inactivación, al ser tratadas con desnaturalizantes químicos y físicos. Estas diferencias pueden variar en intervalos de varios órdenes de magnitud. Un ejemplo de ello puede observarse en una enzima de la vía glucolítica, la triosafosfato isomerasa (TIM), cuya secuencia de aminoácidos se encuentra altamente conservada en dos tripanosomas patógenos para los humanos. La TIM es una enzima de la vía glucolítica que se encarga de la interconversión de gliceraldehído-3-fosfato a dihidroxiacetona fosfato, que tiene una estructura de barril $(\beta/\alpha)_8$ y que es activa sólo como un homodímero [5–7].

La triosafosfato isomerasas de *T. cruzi* y *T. brucei*

Similitudes y diferencias

Las secuencias de aminoácidos de las triosafosfato isomerasas de *T. cruzi* (TcTIM) y *T. brucei* (TbTIM) presentan un 73.9% de identidad. A pesar de que TcTIM tiene en su secuencia 251 aminoácidos y TbTIM tiene 250 aminoácidos, entre ambas existe una similitud de secuencia del 92.4% con únicamente 65 diferencias; de las cuales 36 aminoácidos son de sustitución conservativa (:), 11 aminoácidos son de sustitución

semiconservativa (.) y 18 aminoácidos no tienen homología (fig. 1.1). Ambas enzimas tienen una alta similitud estructural, ya que la desviación de la raíz cuadrática media de las posiciones atómicas (RMSD), al comparar entre sí sus estructuras cristalográficas, es de únicamente 0.98 Å. (fig. 1.1) [8]

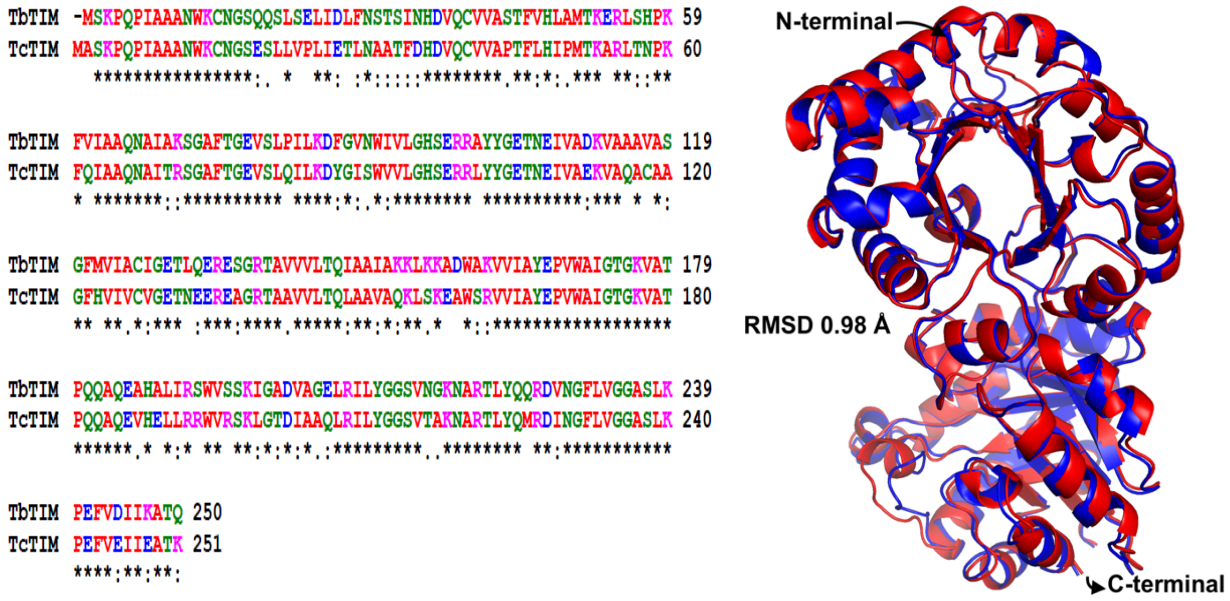

Figura 1.1. **Similitudes y diferencias en TbTIM y TcTIM**. Las secuencias de TcTIM y TbTIM fueron introducidas en el servidor ClustalW2 para el alineamiento. En este alineamiento los aminoácidos marcados en la parte inferior con: (*) son idénticos en ambas enzimas, (:) son conservados, (.) son semiconservados y los que no tienen homología no están marcados. Además, los aminoácidos pequeños e hidrofóbicos se encuentran en rojo (AVFPMILW), los de carga negativa ácida en azul (DE), los de carga positiva básica (RK), los que poseen grupos sulfhidrilo, hidroxilo y/o aminas, y también se incluye la glicina en verde (STYHCNGQ). En el lado derecho se presenta una superposición de las estructuras cristalográficas de TcTIM (rojo) y TbTIM (azul). La superposición de 497 carbonos alfa equivalentes entre TcTIM y TbTIM presenta un RMSD de 0.98 Å y las coordenadas empleadas se encuentran depositadas en el PDB con código 5TIM para TbTIM y 1TCD para TcTIM.

En estas enzimas hay aminoácidos responsables de características específicas y funciones generales en ambas, por ejemplo: los aminoácidos K13, H95 y E167 del sitio activo (según la numeración de TbTIM, que es la que se usará en todo el trabajo) y los aminoácidos que determinan la flexibilidad del asa 6 (residuos 162 a 166), los cuales son idénticos en estas dos TIMs [9,10].

A pesar de que TbTIM y TcTIM son extremadamente similares, presentan diferencias en los patrones de digestión por la proteasa subtilisina [11], y sus monómeros desplegados con hidrocloruro de guanidina también tienen distinta velocidad y grado de reactivación al eliminar el agente desnaturalizante [12]. Además, presentan diferencias cuantitativas en su susceptibilidad a la acción inactivante de varios agentes de bajo peso molecular y, en particular, a reactivos con grupos sulfhidrilo. Estas enzimas también difieren en su estabilidad cinética medida por energía de activación (Eact) [13], temperatura de desnaturalización térmica, punto isoeléctrico y, cantidad de cisteínas presentes en su secuencia de aminoácidos.

Distinta reactividad o inactivación por reactivos de sulfhidrilo

Como se mencionó arriba, TbTIM y TcTIM presentan diferencias cuantitativas en su susceptibilidad a agentes que reaccionan con grupos sulfhidrilo como el metilmetano tiosulfonato (MMTS) y el ácido 5,5'-ditiobis (2-nitrobenzoico) (DTNB). La TcTIM es 70 veces más susceptible que la TbTIM. Es decir que, para que la TcTIM pierda el 100% de su actividad catalítica por alquilación de sus cisteínas por el MMTS, se necesita una concentración 70 veces menor de reactivo que para la TbTIM en un ensayo

estandarizado de inactivación de ambas enzimas con este reactivo [14,15]. Por lo tanto, la TcTIM se inactiva en un 100% a una concentración de 100 μM de MMTS, mientras que la pérdida de actividad para la TbTIM es de aproximadamente 20% a la misma concentración (fig. 1.2).

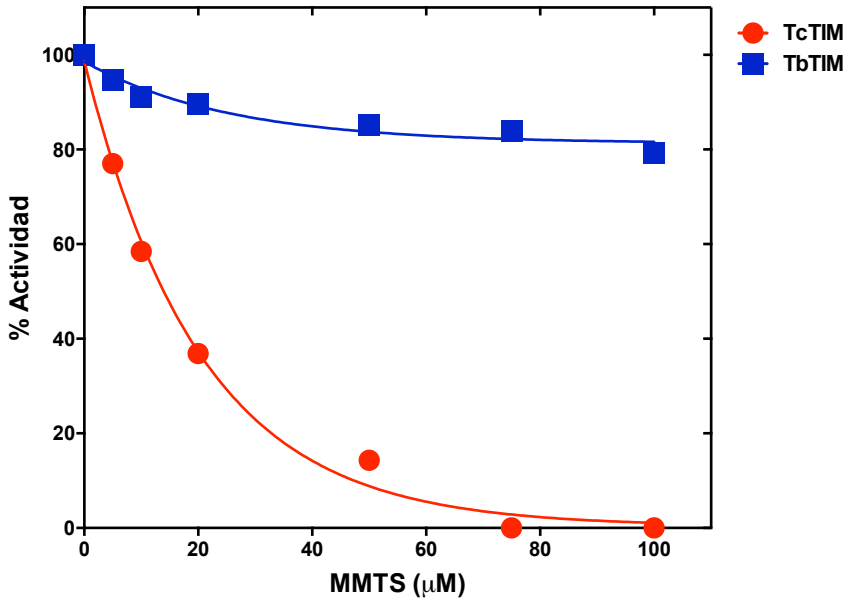

Figura 1.2**. Inactivación de TcTIM y TbTIM con metilmetano tiosulfonato**. La enzimas se incubaron a 250 μg/mL con 5-100 μM de MMTS en 100 mM de trietanolamina, 10 mM de EDTA a pH 7.4 durante 2 horas a 25 ºC, incluida una muestra sin MMTS para calcular el 100% de la actividad. Transcurrido el tiempo de incubación se determinó su actividad catalítica residual y se graficó en función de las concentraciones de MMTS. Figura modificada de [14,16,17].

Una pregunta que surgió al observar esta gran diferencia fue: ¿es posible determinar qué aminoácido(s) en la secuencia de ambas enzimas es (son) responsable (s) de causar esta susceptibilidad tan dispar entre la TbTIM y la TcTIM?

2. Antecedentes

La búsqueda de los aminoácidos responsables de la distinta reactividad de la cisteína 14 de la triosafosfato isomerasa de *T. cruzi* y *T. brucei*

Nuestro grupo de investigación ha trabajado durante muchos años para encontrar una respuesta a la distinta reactividad de las triosafosfato isomerasas de TcTIM y TbTIM al ser inactivadas con MMTS. Se ha estudiado a estas enzimas utilizando mutagénesis dirigida de diversos aminoácidos que se consideraron que podrían estar involucrados en la diferencia en susceptibilidad a la inactivación.

Las cisteínas en las secuencias de aminoácidos de TbTIM y TcTIM

En primer lugar, se analizaron las cisteínas que existen en las secuencias de aminoácidos de TbTIM y TcTIM. Ambas tienen tres cisteínas en las mismas posiciones de su secuencia (14, 39 y 126) pero, TcTIM tiene una cuarta cisteína. La cisteína 117 (numeración de TbTIM) que se encuentra presente en TcTIM pero ausente en TbTIM. Se sustituyó esta cisteína de TcTIM por una valina, el aminoácido en la posición equivalente de TbTIM, y viceversa. Sin embargo, las proteínas mutantes obtenidas presentaron la misma susceptibilidad a ser inhibidas por el MMTS que las enzimas silvestres correspondientes (tabla 2.1). Estos resultados indicaron que la diferencia en reactividad no se debía a la cisteína adicional presente en la secuencia de aminoácidos de TcTIM, si no probablemente a otros factores [16].

Tabla 2.1. **Constantes de inactivación de segundo orden para la reacción de inactivación de diversas TbTIM y TcTIM con MMTS.**

TIM	k_2 ($M^{-1}s^{-1}$) por MMTS
TbTIM	0.6
TcTIM	40
TbTIM V117C	~ 0.6
TcTIM C117V	~ 40
TcTIM P24E	> 40
TcTIM E19Q	90
TcTIM Q82P	32
TcTIM T70A/R71K/Q82P	18
TcTIM interfaz TbTIM	~ 40
TbTIM interfaz TcTIM	1.74

Paralelo a estos estudios se demostró que la cisteína 14 de interfaz en la secuencia de TbTIM es la primera cisteína que alquila el MMTS [18–20], es decir, el agente MMTS agrega un grupo tiol (SH) al azufre de la cisteína 14 de interfaz, produciendo un grupo disulfuro que produce la inactivación de esa TIM [20]. Estudios subsecuentes se centraron sobre este residuo y se generaron un importante número de enzimas mutantes en las cuales se monitorearon diferencias estructurales entre los aminoácidos circundantes a la cisteína 14 de interfaz tanto de TcTIM como de TbTIM.

Una cavidad cercana a la cisteína 14 de interfaz

Al resolverse la estructura tridimensional de la TcTIM (Maldonado E., *et al*., 1998), se pudo comparar ésta con la que existía previamente de TbTIM [21]. En este caso se analizaron las diferencias estructurales de una cavidad que se localiza cercana a la cisteína 14, al inicio de la hélice 1 y el asa 3 de la subunidad adyacente, la cual es mayor en TcTIM, que en TbTIM (fig. 2.1 indicado por flechas y modificado de Maldonado E., *et al*., 1998). Como se puede apreciar en la figura 2.2, el aminoácido en la posición 18 en la cavidad tiene diferencias estructurales y es un ácido glutámico en TcTIM y una glutamina en TbTIM. Por lo que se sustituyó el ácido glutámico de TcTIM por la glutamina de TbTIM en la mutante E19Q. Sin embargo, esta mutante resultó con una inactivación mayor a diferentes concentraciones de MMTS que la TcTIM silvestre (tabla 2.1). De tal forma, que el aminoácido en la posición 18 tampoco influye en la marcada diferencia en sensibilidad al MMTS entre TbTIM y TcTIM [11].

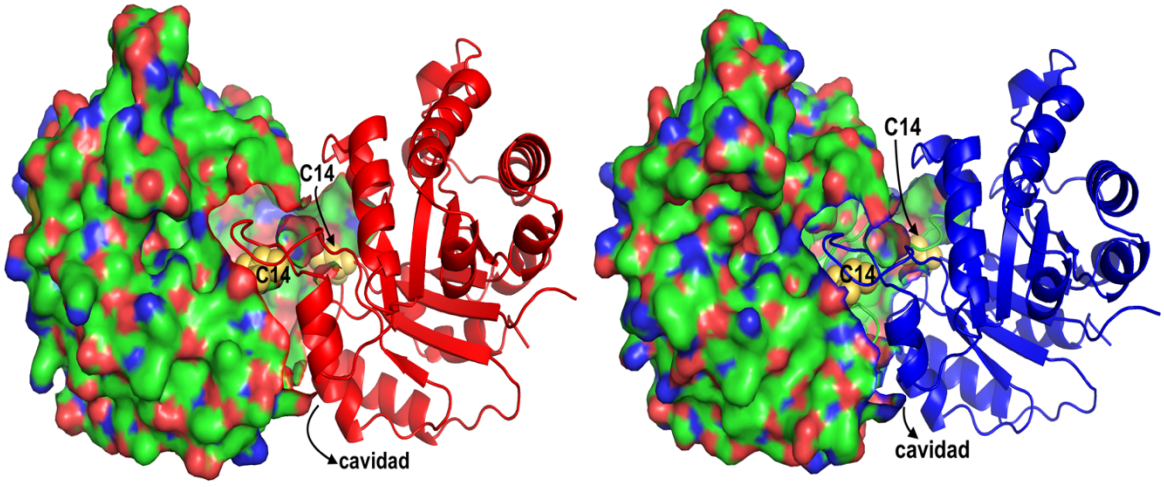

Figura 2.1. **Cavidad entre el asa 1 y el asa 3 en TbTIM (azul) y TcTIM (rojo).** En TcTIM se observa que la cavidad es mayor que en TbTIM. Modificado de Maldonado E., *et al*., 1998.

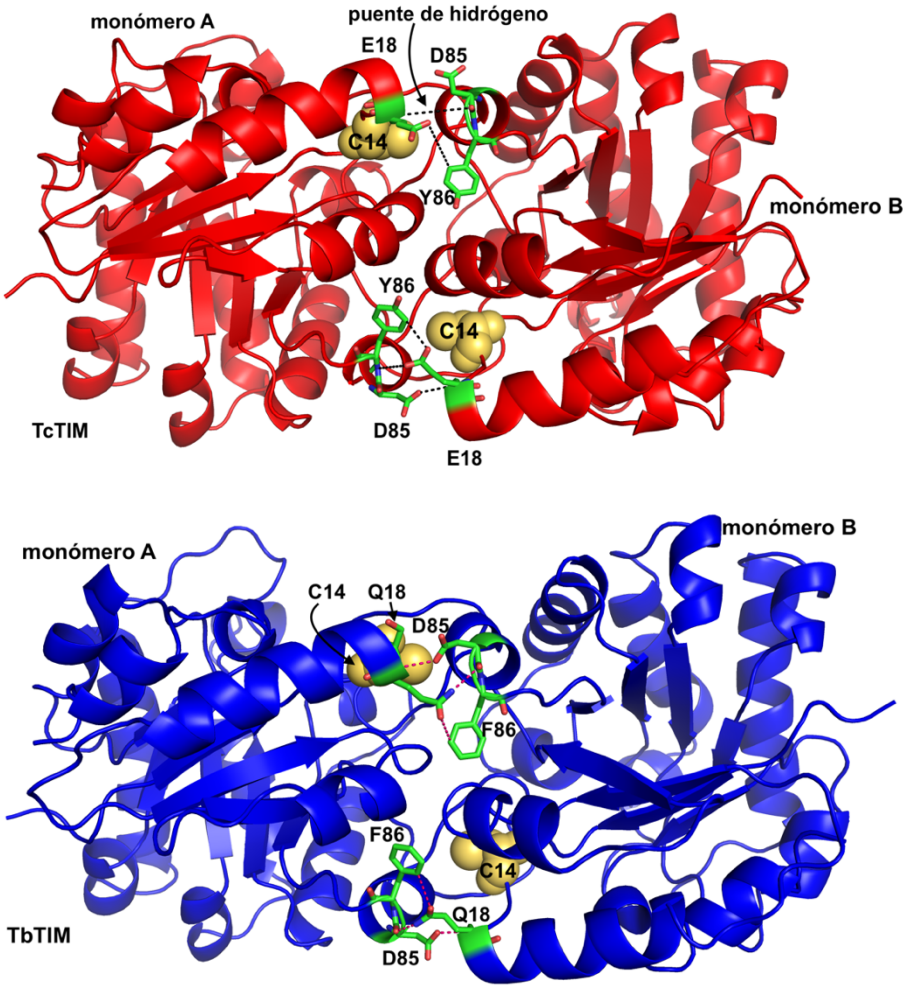

Figura 2.2. **Diferencias estructurales en la cavidad entre el asa 1 y el asa 3.** En TcTIM (rojo) la cavidad está formada por las interacciones del nitrógeno del enlace péptico del ácido glutámico 18 del monómero A que forma un puente de hidrógeno a una distancia de 3.4 Å con el oxígeno de la cadena lateral del aspártico 85 (ausente en el monómero B). Además, el oxígeno de la cadena lateral del ácido glutámico se encuentra a una distancia de 3.5 Å (6.9 Å en el monómero B) de la tirosina 86**.** En TbTIM (azul) la cavidad está formada por las interacciones de la glutamina 18 del monómero A con aminoácidos del monómero B: El nitrógeno del enlace peptídico de la glutamina 18 se encuentra a una distancia de 3.0 Å (2.7 Å para el monómero B) del oxígeno de la cadena lateral del aspártico 85 formando un enlace de hidrógeno. El nitrógeno de la cadena lateral de la glutamina 18 se encuentra a 3.3 Å (2.8 Å para el monómero B) del oxígeno del enlace peptídico del aspártico 85. El oxígeno de la cadena lateral de la glutamina 18 se encuentra a una distancia de 4.1 Å (3.9 Å para el monómero B) de fenilalanina 86. Modificado de Maldonado E., *et al*., 1998.

Aumento del tamaño de la cavidad con la mutante TcTIMP24E

En tercer lugar, con la finalidad de incrementar la accesibilidad de la cisteína 14 a moléculas pequeñas disueltas en el solvente, se construyó la mutante TcTIMP24E. La posición 24 en la secuencia de aminoácidos está ubicada en la hélice 1 y la mutación la acorta por 1.2 Å, sin perturbar las interacciones hidrofóbicas de la hélice 1 con la hebra beta interna, de tal forma que la cavidad se agrandaría. El ácido glutámico 23 en TbTIM forma un puente de hidrógeno con la glutamina 19, el cual está ausente en TcTIM por que posee una prolina en esa posición. Esta enzima mutante tuvo un aumento de 5 veces en la susceptibilidad a los agentes de sulfhidrilo (fig. 2.3 y tabla 2.1) [8]. De esta manera se concluyó que un aumento en la separación entre el inicio de la hélice 1 y el final de la hélice 3 es importante para la accesibilidad de los agentes que perturban la cisteína 14 de interfaz. La distinta reactividad que presentan las enzimas ante derivatizantes de cisteínas puede deberse al distinto grado de accesibilidad de las mismas en pequeño grado.

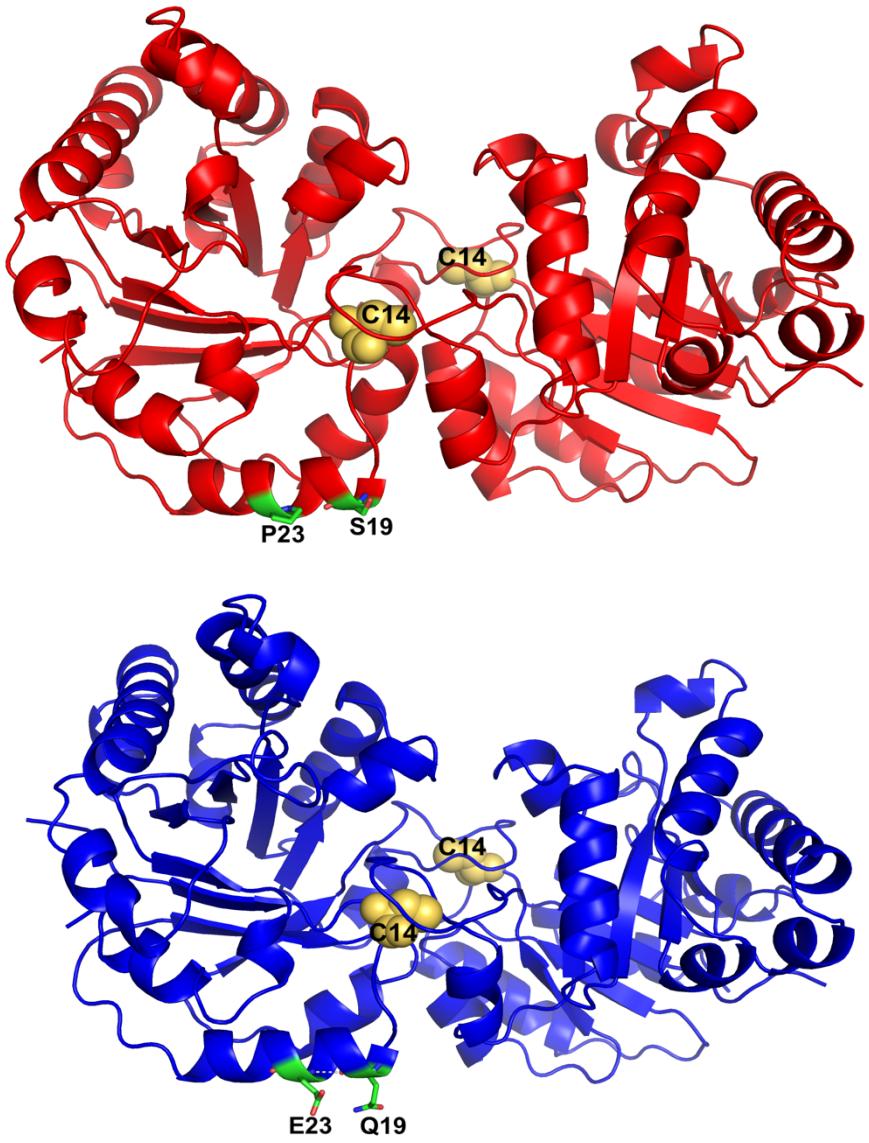

Figura 2.3. **Estrategia para acortar la hélice 1.** En TbTIM, al final de la hélice 1, se encuentra un ácido glutámico 23 formando un puente de hidrógeno con la glutamina 19. En cambio, en TcTIM, en las posiciones equivalentes, hay una serina en la posición 19 y una prolina en la posición 23; por lo que no se forma un puente de hidrógeno.

Mutantes del asa 3

En cuarto lugar, en varios experimentos se determinó que la constante de inactivación de la TIM de *Leishmania mexicana* (LmTIM) con MMTS es 3 veces menor que TbTIM y 250 veces menor que TcTIM. Con base en este resultado se comparó la secuencia de aminoácidos del asa 3 entre LmTIM, TbTIM y TcTIM, y se encontró que son casi idénticas y que sólo difiere de TcTIM en las posiciones 70 y 71. Se construyeron dos mutantes en TcTIM; en una mutante se sustituyó glutamina 82 por prolina (TcTIMQ82P) y en otra se construyó una triple mutante con los residuos de TbTIM y LmTIM en esas posiciones TcTIMT70A/R71L/Q82P. La constante de inactivación con MMTS de la mutante TcTIMQ82P fue aproximadamente 30% menor que la de TcTIM silvestre. La constante de inactivación en la triple mutante resultó mucho menor (tabla 2.1) lo que sugirió que la secuencia de aminoácidos del asa 3, y los aminoácidos adyacentes, contribuyen parcialmente a la susceptibilidad de la cisteína de interfaz a los reactivos sulfhidrilo [11]. Estos resultados, aunque mostraban un efecto sobre las diferencias en susceptibilidad a la inactivación por MMTS entre TbTIM y TcTIM, no eran satisfactorios, pues la magnitud de esas diferencias era muy pequeña y podían deberse también a otros factores.

Intercambio de los aminoácidos diferentes en la interfaz de las triosafosfato isomerasas de *T. cruzi* y *T. brucei*

La búsqueda de una respuesta satisfactoria continuó, y, sabiendo que las TIMs sólo son activas en su forma dimérica, y que los aminoácidos de la interfaz juegan un papel crucial para mantener la integridad de las interacciones entre ambas subunidades [22–24], se analizaron las interfaces de TcTIM y TbTIM en sus estructuras cristalográficas. Se

encontró que están formadas por 40 aminoácidos que, al ser comparados entre sí, presentan una identidad del 82%. Los siete aminoácidos que son diferentes en ambas interfaces se muestran en la tabla 2.2 marcados con asterisco.

Tabla 2.2. **Aminoácidos que forman las interfaces de TcTIM y TbTIM**

	11	13	14	15	16	17	18	19	44	45	46	47	48	49	50	65	66	68	71	72
TcTIM	Q	K	C	N	G	S	E	S	T	F	L	H	I	P	M	Q	N	I	S	G
TbTIM	Q	K	C	N	G	S	Q	Q	T	F	V	H	L	A	M	Q	N	I	S	G
							*	*			*		*	*						

	73	74	75	76	77	78	79	82	83	85	86	88	92	95	97	98	101	102	172	174
TcTIM	A	F	T	G	E	V	S	I	L	D	T	I	V	H	E	R	Y	Y	I	G
TbTIM	A	F	T	G	E	V	S	I	L	D	F	V	V	H	E	R	Y	Y	I	G
											*	*								

Los residuos marcados con * son diferentes entre ambas enzimas.

Con base en esas siete diferencias de aminoácidos se produjeron dos enzimas con siete mutaciones intercambiando la secuencia de la interfaz de TcTIM por la secuencia de interfaz de TbTIM y viceversa. Sin embargo, al determinar la susceptibilidad de las mutantes obtenidas a diferentes concentraciones de MMTS, la mutante de TcTIM con interfaz de TbTIM tenía un patrón de inactivación similar a la TcTIM silvestre. En cambio, la mutante de TbTIM con interfaz de TcTIM tuvo una constante de inactivación tres veces mayor respecto a la enzima silvestre (tabla 2.1). La diferencia en susceptibilidad todavía era muy pequeña, por lo que se concluyó que las diferencias de la interfaz no estaban involucradas en la diferencia de comportamiento de las enzimas ante el MMTS [25].

Después de haber monitoreado con mutagénesis dirigida diversas regiones de TcTIM y TbTIM sin que las mutantes revelaran por qué las enzimas, siendo tan similares, se comportan de forma diferente al ser tratadas con MMTS; se concluyó que esas diferencias no parecen deberse a un efecto a corta distancia, ya que se habían monitoreado varias posibilidades cercanas a la cisteína 14. Con base en estos resultados, la siguiente estrategia fue explorar zonas distantes de la cisteína de interfaz. Lo que se hizo fue, con base en su estructura de barril $(\beta/\alpha)_8$, dividir a las enzimas en ocho partes con el fin de encontrar las regiones responsables de causar las diferencias en susceptibilidad entre la TcTIM y TbTIM.

Diseño de secuencias quiméricas de TcTIM y TbTIM

Iniciamos el trabajo de García-Torres et, al. [17] dividiendo el barril de la TIM en ocho regiones. Cada región quedó constituida por una hélice alfa, una lámina beta y su correspondiente asa de unión. Luego, mediante el diseño de secuencias quiméricas de TcTIM y TbTIM, insertamos progresivamente diferentes regiones de TbTIM en la región equivalente de TcTIM (fig. 2.4).

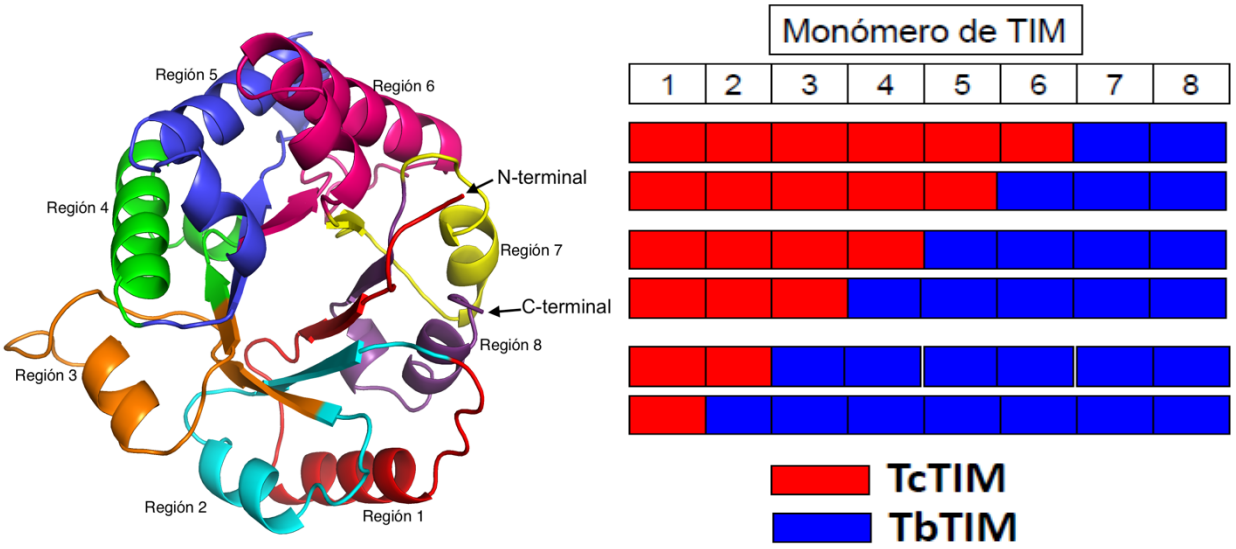

Figura 2.4. **Estrategia para estudiar las diferencias de inactivación mediante quimeras.** Las secuencias de TbTIM y TcTIM se dividieron en 8 regiones y mediante el diseño de secuencias quiméricas de ambas enzimas se sustituyeron gradualmente de una a seis regiones de TbTIM en la secuencia de aminoácidos de TcTIM.

Siguiendo este procedimiento, analizando los resultados, y posteriormente construyendo una quimera de TcTIM con dos regiones de TbTIM, descubrimos que la región 1 (con los aminoácidos en posiciones 1 a 35) y la región 4 (con los aminoácidos en las posiciones 92 a 119) de TbTIM, son las responsables de causar la diferencia en la susceptibilidad a la inactivación de la actividad enzimática con MMTS (fig. 2.5).

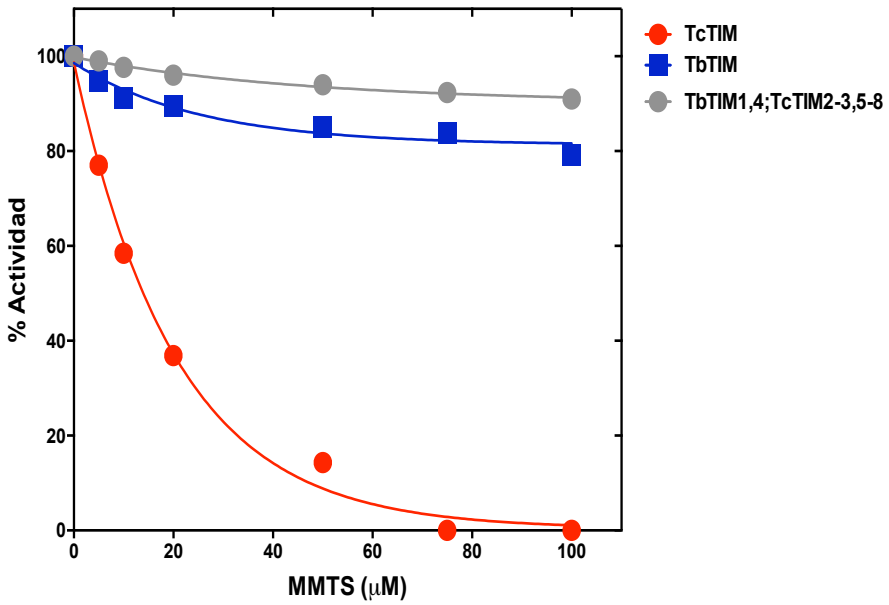

Figura 2.5. **Efecto del MMTS en la enzima quimérica con las regiones 1 y 4 de TbTIM y las regiones 2, 3, 5, 6, 7, y 8 de TcTIM.** Todas las enzimas se incubaron a 250 µg/mL con 5-100 µM de MMTS, 100 mM de trietanolamina, 10 mM de EDTA a pH 7.4 durante 2 horas a 25 °C. Los ensayos de MMTS para cada mutante se realizaron tres veces de forma independiente, incluida una muestra sin MMTS, para calcular el 100% de la actividad. Trascurrido el tiempo de incubación se determinó la actividad catalítica residual y se graficó en función de la concentración de MMTS. Figura modificada de [17].

Estructuralmente, las regiones 1 y 4 no se encuentran cercanas entre sí y no interaccionan. La cisteína 14 se encuentra dentro de la región 1 y no tiene contacto con la región 4. Los aminoácidos diferentes en estas dos regiones, de alguna forma compleja, afectan la susceptibilidad que tiene la cisteína de interfaz hacia el MMTS en ambas enzimas. Comparando las secuencias de aminoácidos de TbTIM y TcTIM, hay trece residuos diferentes en la región 1 y cinco residuos diferentes en la región 4, respectivamente. Nuestra conclusión de ese trabajo fue que podríamos asignar la susceptibilidad alta o baja a la inactivación en presencia de MMTS a los dieciocho aminoácidos diferentes ubicados en las regiones 1 y 4, de un total de sesenta y cinco

diferencias entre las secuencias de aminoácidos de las dos TIMS de tripanosomas. Pero, en ese momento, la pregunta seguía siendo si esos dieciocho residuos eran todos necesarios para producir los efectos observados, o si podían ser un número menor de ellos. La localización de las regiones 1 y 4 en la estructura de la TbTIM, así como las diferencias en los aminoácidos que forman su secuencia se muestran en la figura 2.6.

En esta tesis se utilizó una estrategia similar al diseño de las enzimas quiméricas, pero utilizando mutagénesis dirigida, para contestar la pregunta mencionada anteriormente de si los dieciocho aminoácidos diferentes en las regiones 1 y 4 de las enzimas eran todos necesarios para determinar la diferente susceptibilidad de TcTIM y TbTIM a la inactivación con MMTS, o si podían ser un número menor. También intentamos determinar cuántos y cuáles son necesarios y suficientes para tener ese efecto.

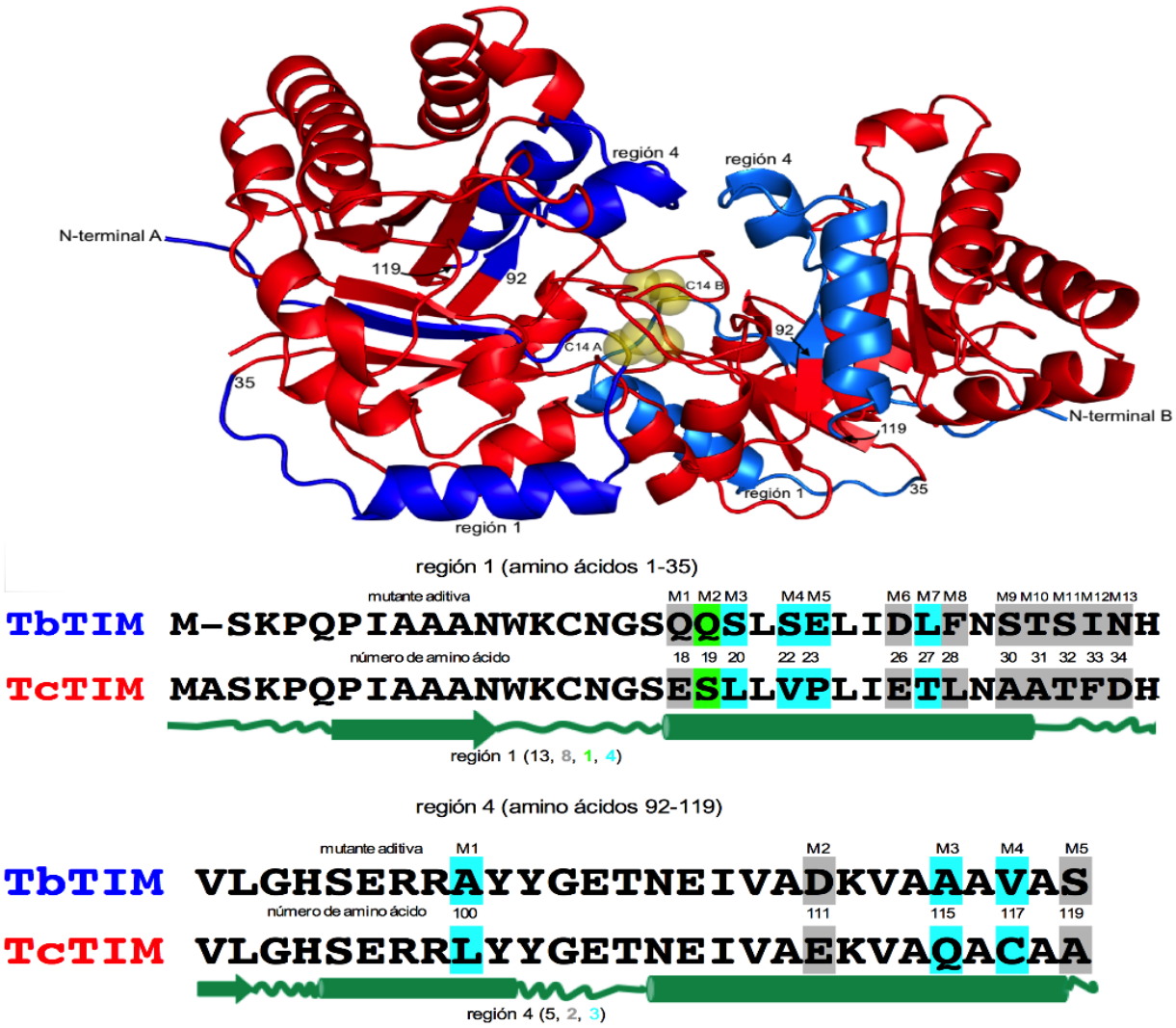

Figura 2.6. **Localización de la región 1 y 4 en la estructura de TbTIM y alineamiento de aminoácidos de las regiones 1 y 4 de TbTIM y TcTIM.** La estructura con código 5TIM del PDB correspondiente TbTIM se muestra en rojo. Las regiones 1 y 4 se muestran en azul y azul marino para los monómeros A y B, respectivamente. Los extremos amino y carboxilo terminal de cada monómero, y la posición de los aminoácidos 35, 92 y 119 están indicados con el número correspondiente, algunas veces se señalan usando una flecha en el diagrama. Las cisteínas de interfaz de ambos monómeros se muestran como esferas amarillas. En el alineamiento, las diferencias en los aminoácidos se encuentran resaltados así: los aminoácidos conservados en gris (tamaño y/o polaridad similar), los aminoácidos semi-conservados en verde (polaridad similar) y los aminoácidos sin similitud en azul claro. Los elementos de estructura secundaria como líneas verdes (asas), flechas verdes (hojas beta) y cilindros verdes (alfa hélices).

3. Hipótesis

Los aminoácidos responsables de la diferencia en susceptibilidad a la inactivación por el metilmetano tiosulfonato en TbTIM y en TcTIM son menos de dieciocho aminoácidos.

4. Objetivo general

Encontrar los aminoácidos en la secuencia de las regiones 1 y 4 que son responsables de causar las diferencias en susceptibilidad a la inactivación por el metilmetano tiosulfonato en TbTIM y en TcTIM.

Objetivos particulares

1. Diseño y sobreexpresión de mutantes aditivas de las regiones 1 y 4.
2. Diseño y sobreexpresión de mutantes con aminoácidos seleccionados de las regiones 1 y 4 en TbTIM y en TcTIM.
3. Purificar todas las mutantes obtenidas.
4. Realizar ensayos de inactivación con metilmetano tiosulfonato para todas las mutantes obtenidas.

5. Materiales y Métodos

En este trabajo modificamos de forma sistemática la susceptibilidad de la TcTIM a la inactivación con MMTS hasta obtener una enzima tan resistente como la TbTIM. De igual manera, modificamos la resistencia relativa de TbTIM a la inactivación con MMTS hasta obtener una enzima con una alta susceptibilidad, similar a la de TcTIM. Para ello, realizamos mutaciones de forma aditiva en dos enzimas quiméricas que involucraron a las regiones 1 y 4, y también mutaciones puntuales de algunos aminoácidos seleccionados de las regiones 1 y 4 sobre las enzimas silvestres.

Diseño de los genes de las mutantes

Se puede considerar que este trabajo es una continuación del trabajo de García-Torres, et al. [17]. Nosotros usamos algunas de las proteínas quiméricas producidas en esa investigación. Para la conclusión principal del trabajo de Itzhel García-Torres, se generó la enzima quimérica TbTIM1,4; TcTIM 2,3,5 (llamada TcTIM 2,3, 5-8 en esa publicación) que tenía un patrón de susceptibilidad igual, o ligeramente más resistente, a la inactivación con MMTS que la TbTIM silvestre. La secuencia de TbTIM1,4; TcTIM 2,3,5 tiene dieciocho aminoácidos diferentes a la secuencia de TcTIM: trece se localizan en la región 1, y cinco en la región 4.

Nuestra estrategia fue la de introducir de forma gradual las trece diferencias de la región 1 en “mutantes aditivas”. Para ello utilizamos la secuencia de DNA de la quimera TbTIM 4; TcTIM1-3,5-8 como templado para las mutantes R1M1-R1M5 (la explicación de la

nomenclatura de las mutantes aditivas RXMX se da a continuación). La nomenclatura de las mutantes aditivas tiene la forma RXMX, donde: la R es la región en que se introdujo la mutación, y M es el número de mutantes aditivas que contiene. Por lo tanto, la mutante R1M12, tiene doce mutaciones en la región 1 y la mutante R4M1 tiene una mutación en la región 4 (ver, por ejemplo, la tabla 5.1). En la tabla 5 del anexo se describen detalles de los templados de DNA utilizados para producir las mutantes aditivas de la región 1. De la misma forma, los cinco aminoácidos diferentes de la región 4 se introdujeron de forma secuencial en “mutantes aditivas”, utilizando como templado el DNA de la quimera TcTIM4 para la mutante R4M1; los templados para las mutantes R4M2-R4M5 se describen en la tabla 5, en el anexo. Las estrategias para la producción de las mutantes aditivas de las regiones 1 y 4 se ilustran en las tablas 5.1 y 5.2, respectivamente.

Los resultados de la inactivación con MMTS de las mutantes aditivas de la región 1 y 4 nos llevó a producir una serie de mutantes sitio-dirigidas las cuales tenían combinaciones de residuos de la región 1 y 4, tanto en la secuencia de TcTIM como en la secuencia de TbTIM (tablas 5.3 y 5.4). Estas mutantes sitio-dirigidas se produjeron para probar la importancia de aminoácidos individuales, o combinaciones de aminoácidos, en la susceptibilidad y/o resistencia a la inactivación de TbTIM y TcTIM con MMTS.

Cabe mencionar que el templado de DNA utilizado para introducir las mutantes simples en TcTIM y TbTIM tienen los códigos X03921 y U53867 en la base de datos del PDB, respectivamente. En total se produjeron 18 mutantes-sitio dirigidas de la TcTIM y 8 de la TbTIM. Estas mutantes se nombraron utilizando el nombre de la secuencia (TcTIM o

TbTIM), seguido de las diferencias introducidas. Por ejemplo, la mutante TcTIM: E27D, T28L, L29F, L101A posee tres mutaciones (E27D, T28L, L29F) en la región 1 y una mutación (L101A) en la región 4. Las mutantes sitio-dirigidas de las regiones 1 y 4 en la secuencia de TcTIM se muestran en la tabla 5.3 y las mutantes sitio-dirigidas en la secuencia de la TbTIM se muestran en la tabla 5.4

Tabla 5.1. **Mutantes aditivas de la región 1**. Los aminoácidos mutados se encuentran resaltados.

Mutante aditiva	Región de TbTIM	Regiones de TcTIM	mutación(s) resaltadas	número de residuo(s) mutados
R1M1	4	1-3 y 5-8	TbTIM NGSQQSLSELIDLFNSTSINH TcTIM NGSESLLVPLIETLNAATFDH	18
R1M2	4	1-3 y 5-8	TbTIM NGSQQSLSELIDLFNSTSINH TcTIM NGSESLLVPLIETLNAATFDH	18-19
R1M3	4	1-3 y 5-8	TbTIM NGSQQSLSELIDLFNSTSINH TcTIM NGSESLLVPLIETLNAATFDH	18-20
R1M4	4	1-3 y 5-8	TbTIM NGSQQSLSELIDLFNSTSINH TcTIM NGSESLLVPLIETLNAATFDH	18-20, 22
R1M5	4	1-3 y 5-8	TbTIM NGSQQSLSELIDLFNSTSINH TcTIM NGSESLLVPLIETLNAATFDH	18-20, 22-23
R1M6	4	1-3 y 5-8	TbTIM NGSQQSLSELIDLFNSTSINH TcTIM NGSESLLVPLIETLNAATFDH	18-20, 22-23,26
R1M7	4	1-3 y 5-8	TbTIM NGSQQSLSELIDLFNSTSINH TcTIM NGSESLLVPLIETLNAATFDH	18-20, 22-23,26-27
R1M8	4	1-3 y 5-8	TbTIM NGSQQSLSELIDLFNSTSINH TcTIM NGSESLLVPLIETLNAATFDH	18-20, 22-23,26-28
R1M9	4	1-3 y 5-8	TbTIM NGSQQSLSELIDLFNSTSINH TcTIM NGSESLLVPLIETLNAATFDH	18-20, 22-23,26-28,30
R1M10	4	1-3 y 5-8	TbTIM NGSQQSLSELIDLFNSTSINH TcTIM NGSESLLVPLIETLNAATFDH	18-20, 22-23,26-28,30-31
R1M11	4	1-3 y 5-8	TbTIM NGSQQSLSELIDLFNSTSINH TcTIM NGSESLLVPLIETLNAATFDH	18-20, 22-23,26-28,30-32
R1M12	4	1-3 y 5-8	TbTIM NGSQQSLSELIDLFNSTSINH TcTIM NGSESLLVPLIETLNAATFDH	18-20, 22-23,26-28,30-33
R1M13	4	1-3 y 5-8	TbTIM NGSQQSLSELIDLFNSTSINH TcTIM NGSESLLVPLIETLNAATFDH	18-20, 22-23,26-28,30-34

Tabla 5.2 **Mutantes aditivas de la región 4**. Los aminoácidos mutados se encuentran resaltados.

Mutante aditiva	Regiones de TbTIM	Región de TcTIM	mutación(s) resaltadas	número de residuos
R4M1	1-3 y 5-8	4	TbTIM VLGHSERRAYYGETNEIVADKVAAAVAS TcTIM VLGHSERRLYYGETNEIVAEKVAQACAA	100
R4M2	1-3 y 5-8	4	TbTIM VLGHSERRAYYGETNEIVADKVAAAVAS TcTIM VLGHSERRLYYGETNEIVAEKVAQACAA	100,111
R4M3	1-3 y 5-8	4	TbTIM VLGHSERRAYYGETNEIVADKVAAAVAS TcTIM VLGHSERRLYYGETNEIVAEKVAQACAA	100,111,115
R4M4	1-3 y 5-8	4	TbTIM VLGHSERRAYYGETNEIVADKVAAAVAS TcTIM VLGHSERRLYYGETNEIVAEKVAQACAA	100,111,117
R4M5	1-3 y 5-8	4	TbTIM VLGHSERRAYYGETNEIVADKVAAAVAS TcTIM VLGHSERRLYYGETNEIVAEKVAQACAA	100,111,117,119

Tabla 5.3. **Mutantes sitio-dirigidas de las regiones 1 y 4 en la secuencia de TcTIM**

Nombre	Aminoácidos de TcTIM a TbTIM	Aminoácidos de TcTIM
TcTIM: E26D, T27L, L28F, L100A	E26D, T27L, L28F, L100A	Resto de TcTIM
TcTIM: E26D, T27L, L28F, A30S, L100A	E26D, T27L, L28F, A30S, L100A	Resto de TcTIM
TcTIM: E26D, T27L, L28F, A30S, T33S, L100A	E26D, T27L, L28F, A30S, T32S, L100A	Resto de TcTIM
TcTIM: E26D, T27L, L28F, A30S, L100A, Q115A	E26D, T27L, L28F, A30S, L100A, Q115A	Resto de TcTIM
TcTIM: E26D, T27L, L28F, A30S, T32S, L100A, Q115A	E26D, T27L, L28F, A30S, T32S, L100A, Q115A	Resto de TcTIM
TcTIM: E26D, T27L, L28F, L100A, Q115A	E26D, T27L, L28F, L100A, Q115A	Resto de TcTIM
TcTIM: T27L, L28F, L100A, Q115A	T27L, L28F, L100A, Q115A	Resto de TcTIM
TcTIM: E26D, L28F, L100A, Q115A	E26D, L28F, L100A, Q115A	Resto de TcTIM
TcTIM: E26D, T27L, L100A, Q115A	E26D, T27L, L100A, Q115A	Resto de TcTIM
TcTIM: T27L, L28F, L100A	T27L, L28F, L100A	Resto de TcTIM
TcTIM: L28F, L100A, Q115A	L28F, L100A, Q115A	Resto de TcTIM
TcTIM: T27L, L100A, Q115A	T27L, L100A, Q115A	Resto de TcTIM
TcTIM: L28F, L100A	L28F, L100A	Resto de TcTIM
TcTIM: L28F, Q115A	L28F, Q115A	Resto de TcTIM
TcTIM: L100A, Q115A	L100A, Q115A	Resto de TcTIM
TcTIM: L28F	L28F	Resto de TcTIM
TcTIM: L100A	L100A	Resto de TcTIM
TcTIM: Q115A	Q115A	Resto de TcTIM

Tabla 5.4. **Mutantes sitio-dirigidas de las regiones 1 y 4 en la secuencia de TbTIM**

Nombre	Aminoácidos de TcTIM	Aminoácidos de TbTIM
TbTIM: F28L	F28L	Resto de TbTIM
TbTIM: A100L	A100L	Resto de TbTIM
TbTIM: A115Q	A115Q	Resto de TbTIM
TbTIM: F28L, A100L	F28L, A100L	Resto de TbTIM
TbTIM: F28L, A115Q	F28L, A115Q	Resto de TbTIM
TbTIM: A100L, A115Q	A100L, A115Q	Resto de TbTIM
TbTIM: F28L, A100L, A115Q	F28L, A100L, A115Q	Resto de TbTIM

Los oligonucleótidos con las mutaciones correspondientes utilizados para construir las enzimas mutantes aditivas de la región 1, la región 4 y las mutantes sitio-dirigidas en las secuencias de TcTIM y TbTIM se presentan en las tablas 2, 3, 4 y 5 del anexo. En las tablas 6 y 7 del anexo se describen detalles de los templados de DNA utilizados para producir las mutantes sitio-dirigidas en TcTIM y TbTIM.

Expresión y purificación de proteínas

Todos los genes de las mutantes se clonaron en el plásmido de expresión pET3a entre los sitios de restricción *Nde-1* y *BamHI*. Los genes de las mutantes se secuenciaron y transformaron en células de *E. coli* BL21 (DE3) pLysS (Novagen, Madison Wisconsin, USA).

Las bacterias transformadas se inocularon en un litro de medio Luria Bertani con una concentración de ampicilina de 100 µg/mL y se incubaron a 37 °C. Una vez que el cultivo alcanzó un valor de absorbencia A_{600nm}= 0.8 se adicionó isopropil-β-D tiogalactopiranósido (IPTG) a una concentración final de 1 mM y se incubó durante 12 horas a 30 °C. En seguida, el litro de cultivo se centrifugó a 6400 x g durante 20 minutos. El paquete celular compactado de bacterias se separó y homogenizó en 40 mL de amortiguador que contenía MES 100 mM, e IPTG 0.5 mM, pH 6.3 [26].

Las bacterias homogeneizadas se sonicaron en un sonicador BRANSON al 40% de potencia. Las bacterias *E. coli* BL21 (DE3) pLysS se sometieron a cinco ciclos de sonido con una duración de 40 segundos y un minuto de descanso entre cada ciclo. El extracto total obtenido se centrifugó a 11,0660 x g durante 40 minutos para separar los restos celulares del sobrenadante.

Los sobrenadantes se inyectaron a una columna de intercambio catiónico SP-Sepharose (fast flow) equilibrada con amortiguador de MES 50 mM, pH 6.3. Las proteínas se separaron con un gradiente de concentración de NaCl entre 0-500 mM en el mismo

amortiguador. Las fracciones con las proteínas de interés se colectaron, se precipitaron con sulfato de amonio al 70% y se colocaron en agitación a 4 °C durante 12 horas. Las proteínas precipitadas se obtuvieron por centrifugación a 23,000 x g durante 20 minutos y se disolvieron en 10 mL de amortiguador con 100 mM de trietanolamina y EDTA 1 mM, pH 7.4. Finalmente, a la suspensión obtenida se le adicionó la cantidad necesaria de $(NH_4)_2SO_4$ para alcanzar una concentración final de 2.2 M de $(NH_4)_2SO_4$.

El siguiente paso de purificación consistió en pasar las proteínas por una columna hidrofóbica (Toyopearl), equilibrada con amortiguador con trietanolamina (TEA) 100 mM, EDTA 1 mM y $(NH_4)_2SO_4$ 2.2 M. Las proteínas se separaron con un gradiente de 2.2-0 M de $(NH_4)_2SO_4$. Las fracciones con las proteínas de interés se concentraron a una concentración igual o mayor de 1 mg/mL.

Los pasos de purificación de todas las mutantes se siguieron verificando la pureza de las proteínas con geles de poliacrilamida al 16%, teñidos con azul de Coomassie y midiendo la actividad catalítica. La concentración de las proteínas puras se determinó registrando la absorbencia a 280 nm y usando el coeficiente de extinción molar para TbTIM ε = 34,950 M^{-1} cm^{-1} y ε= 36,440 M^{-1} cm^{-1} para TcTIM. Los coeficientes de extinción molar de las quimeras y mutantes se calcularon a partir de su secuencia de aminoácidos, utilizando el programa Expasy ProtParam.

Determinación de la actividad catalítica

La actividad enzimática de las proteínas se determinó a 25 °C siguiendo la conversión de gliceraldehído 3-fosfato (GAP) a dihidroxiaacetona-fosfato (DHAP). Utilizamos la enzima α-glicerolfosfato deshidrogenasa (α-GDH) como enzima acoplada y cuantificamos la disminución de absorbencia a 340 nm debido a la oxidación del NADH. El amortiguador en que se realizó la reacción enzimática contenía 100 mM de TEA, 10 mM EDTA, 1 mM de GAP, 0.20 mM NADH y 20 µl/mL de α-GDH. La reacción para medir la actividad catalítica se inició al añadir 5 ng/mL de enzima a la celda [27].

Parámetros cinéticos

Los parámetros cinéticos se determinaron variando la concentración de GAP de 0.04 a 3 mM. Los datos obtenidos se ajustaron al modelo de Michaelis-Menten, mediante una regresión no lineal, para obtener la concentración de sustrato en la cual la enzima alcanza la mitad de la velocidad media (Km) y la velocidad máxima (Vmax). A partir de estos datos se calcularon también la constante catalítica (K_{cat}) y la eficiencia catalítica (K_{cat}/Km) [28].

Ensayos de inactivación con MMTS

Las enzimas mutantes se incubaron a una concentración de 250 µg/mL con MMTS 5-100 µM, TEA 100 mM y EDTA 10 mM a 25 °C durante 2 horas. Transcurrido el tiempo de incubación, la actividad catalítica residual se determinó a 340 nm en un

espectrofotómetro Agilent Tecnologies Kary 60 (Santa Clara, California, USA). Las actividades catalíticas residuales obtenidas se transformaron a porcentaje de actividad catalítica. El porcentaje de actividad catalítica se graficó contra concentración de MMTS con el programa Prism Graphad versión 6.0. La actividad catalítica en ausencia de MMTS se tomó como el 100% [17].

Determinación del *pKa* aparente de la cisteína de interfaz

Las mutantes TcTIM: E26D, T27L, L28F, L100A, Q115A; TcTIM: T27L, L28F, L100A, Q115A; TcTIM: E26D, L28F, L100A, Q115A; TcTIM: L28F, L100A, Q115A; TcTIM: E26D, T27L, L100A, Q115A y TbTIM: F28L, A100L, A115Q, a una concentración de 250 µg/mL se incubaron con MMTS 80 µM en TEA 100 mM y EDTA 10 mM a diferentes pH (7.0 7.4, 7.8, 8.0 8.4, 8.8, 9.0, 9.2 y 9.5, respectivamente) durante 1 minuto a 25 °C. Transcurrido el tiempo de incubación, se determinó la actividad catalítica residual a 340 nm en el espectrofotómetro. El logaritmo natural del porcentaje de actividad [ln (% actividad)] se determinó con la actividad catalítica residual obtenida, y se graficó en función del pH usando el programa OriginPro 8.6 32bit. El *pKa* se determinó ajustando los datos de la gráfica obtenida a la ecuación derivada de la fórmula de la ecuación de Henderson-Hasselbalch [11].

$$\ln(\%\ \text{actividad}) = (Y_1 + Y_h \times 10^{Pka\text{-pH}})/(1 + 10^{Pka\text{-pH}})$$

Donde Y_1 y Y_h representan las actividades inicial y final, respectivamente.

6. Resultados

TcTIM y TbTIM presentan diferentes grados de inactivación catalítica, al ser expuestas a diferentes concentraciones de MMTS. La TcTIM es 70 veces más sensible que la TbTIM. Es decir, a una concentración de 100 μM de MMTS la TcTIM pierde el 100% de su actividad, mientras que TbTIM mantiene 80% de su actividad residual.

Como se explicó anteriormente en la introducción, los barriles $(\beta/\alpha)_8$ de la TbTIM y la TcTIM se dividieron en ocho regiones. Cada región tiene una lámina beta, una hélice alfa y un asa de unión (los residuos que conforman cada región se encuentran listados en la tabla 8 de los anexos). Esta división se utilizó para construir una serie de quimeras en que la mayoría de las regiones de una TcTIM silvestre se sustituyeron de forma gradual por las regiones correspondientes de la TbTIM. Utilizando estas quimeras, se determinó que las regiones 1 y 4 de TbTIM son necesarias y suficientes para hacer una enzima quimérica con secuencia mayoritariamente de TcTIM, pero con una resistencia a la inactivación en presencia de MMTS muy similar a la de TbTIM silvestre.

La enzima quimerica TbTIM1,4; TcTIM2-3,5-8 (con las regiones 1 y 4 de TbTIM) tiene una secuencia que tiene 92.8% de los aminoácidos de la secuencia de TcTIM. Es decir, posee 13 aminoácidos que son diferentes en la región 1 y 5 aminoácidos diferentes en la región 4, lo que hace un total de 18 diferencias. Estos cambios son necesarios y suficientes para cambiar el comportamiento de la enzima mutante a que tenga un patrón más resitente a la inactivación en presencia del MMTS fig. 2.5.

Construcción de mutantes aditivas y puntuales.

La estrategia empleada para determinar cuáles y cuántos aminoácidos se encuentran implicados en la susceptibilidad a la inactivación por el MMTS, consistió inicialmente en el diseño y construcción de mutantes aditivas. En el caso de las mutantes aditivas de la región 1 se utilizó la quimera TbTIM4 como enzima inicial y para las mutantes de la región 4 se utilizó la quimera TcTIM4; ambas enzimas tienen una resistencia baja a la inactivación por el MMTS, similar a la de TcTIM [17]. De estas mutantes se lograron identificar algunos aminoácidos que aumentaban la resistencia ante la inactivación por el agente alquilante. Después, se realizaron mutaciones puntuales combinadas de aminoácidos selectos de las regiones 1 y 4 sobre las secuencias de las enzimas silvestres de TcTIM y TbTIM. De esta manera, se logró encontrar un número mínimo de residuos que son los responsables de provocar la diferencia en la respuesta a la inactivación por el MMTS entre TbTIM y TcTIM.

Inactivación con MMTS de las mutantes aditivas de la región 1

Para identificar cuales aminoácidos en la región 1 son importantes en la susceptibilidad de TbTIM y TcTIM a la inactivación por MMTS, se introdujeron de forma gradual las 13 diferencias de la región 1 en la enzima quimérica TbTIM 4; TcTIM 1-3; 5-8. Esta proteína tiene un patrón de inactivación similar a TcTIM [fig. 2c en [17] y Fig. 6.1a]. En las curvas de inactivación de las trece mutantes aditivas de la región 1 observamos que los aminoácidos 18Q, 19Q, 20S, 22S y 23E en la secuencia de TbTIM no tienen ningún efecto sobre el patrón de inactivación en la quimera TbTIM 4; TcTIM 1-3; 5-8 (fig. 6.1a).

Esto se demostró con la actividad residual que presentan las enzimas mutantes R1M1, R1M2, R1M3, R1M4 y R1M5 que son prácticamente iguales a la de la quimera TbTIM 4; TcTIM 1-3; 5-8. Por lo tanto, estos aminoácidos se descartaron de contribuir un incremento en la resistencia a la inactivación con MMTS.

Por otro lado, la mutante R1M6, que tiene la mutación adicional E26D, tuvo una menor susceptibilidad a la inactivación, pues mostró una curva de inactivación diferente a las mutantes aditivas anteriores. Su actividad residual fue del 11% a una concentración de MMTS 100 μM (tabla 9 del anexo y fig. 6.1b). La mutante R1M7 con la mutación adicional T27L produjo una enzima que es ligeramente más resistente que las mutantes anteriores, su actividad residual fue del 18% (fig. 6.1b). El papel de estos dos aminoácidos, en estos momentos, no es todavía muy evidente y, más adelante, se describirá su importancia, cuando se produjeron enzimas con mutaciones sitio-dirigidas con combinaciones de aminoácidos de las regiones 1 y 4 en las enzimas silvestres TcTIM y TbTIM.

La importancia de la F28 se notó inmediatamente al observar el comportamiento de la mutante aditiva R1M8 (con la mutación L28F), la cual resiste la inactivación a una concentración de MMTS 100 μM. Su resistencia fue similar al comportamiento de la TbTIM silvestre y conservó una actividad residual del 72.8% (fig. 6.1b). Es decir, que esta mutación aumentó en un 54% la actividad residual con respecto a la mutante R1M7 (fig. 6.1b y tabla 9 del anexo). En este caso, es necesario mencionar que, más adelante, se describirá el efecto de la mutación L28F sobre las secuencias de TcTIM y TbTIM silvestres.

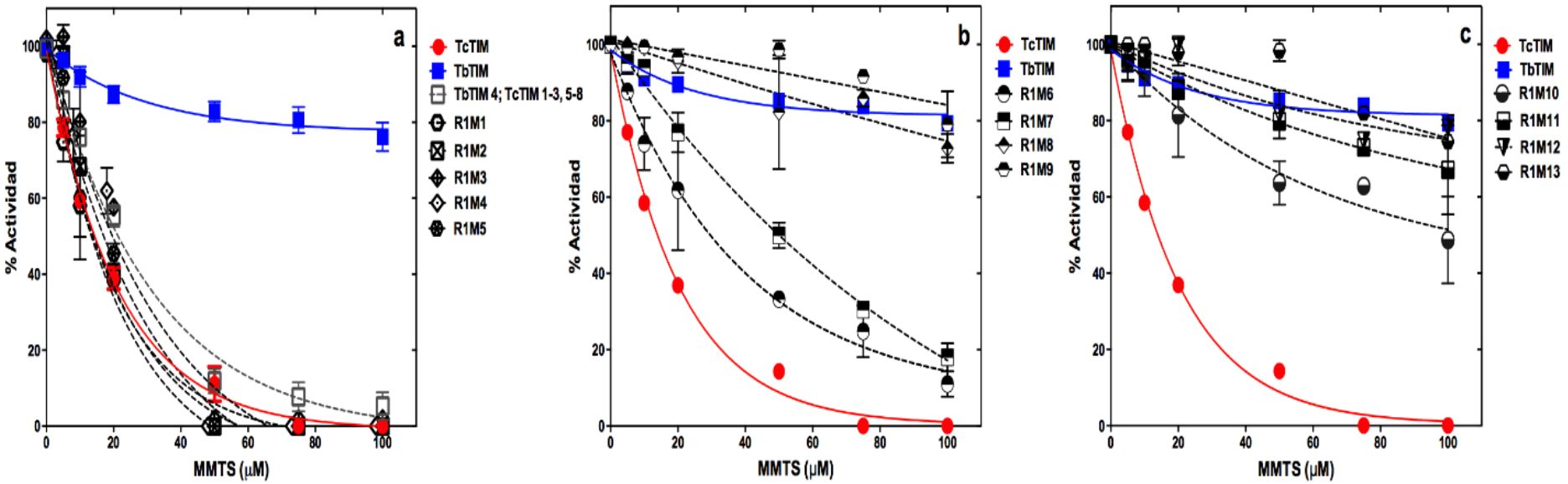

Figura 6.1. **Efecto del MMTS sobre mutantes aditivas de la región 1 y enzimas TcTIM y TbTIM silvestres**. Todas las enzimas se incubaron a 250 µg/mL con MMTS 5-100 µM trietanolamina 100 mM, EDTA 10 mM, pH 7.4 durante 2 horas a 25 °C. Los ensayos de MMTS para cada mutante se realizaron tres veces de forma independiente incluida una muestra sin MMTS para calcular el 100% de la actividad. Transcurrido el tiempo de incubación se determinó la actividad catalítica residual y se graficó en función de la concentración de MMTS. Panel a) R1M1, R1M2, R1M3, R1M4, R1M5, TcTIM y TbTIM. Panel b) R1M6, R1M7, R1M8, R1M9, TcTIM y TbTIM Panel c) R1M10, R1M11, R1M12, R1M13, TcTIM y TbTIM.

Por otra parte, la mutante R1M9 (con la mutación A30S) no mostró ningún cambio significativo en el comportamiento con respecto a la mutante aditiva R1M8 (fig. 6.1b), ya que la mutante R1M9 también presenta valores de actividad residual similares a TbTIM. La mutante aditiva R1M10 (con la mutación A31T) mostró mayor susceptibilidad al MMTS al disminuir su actividad residual al 48% en presencia de 100 μM de MMTS (fig. 6.1c). Esto indicó, claramente, que este aminoácido no fomenta la resistencia frente a la inactivación por el MMTS, y, por lo tanto, lo descartamos de formar parte del número mínimo de aminoácidos que son capaces de hacer que una TcTIM se comporte como TbTIM.

En esta etapa de la investigación se observó que las mutaciones aditivas producían efectos positivos, negativos o neutros en el patrón de susceptibilidad a la inactivación con MMTS en comparación con la mutante que la precedía. Más adelante se aclara que, en nuestra estrategia elegimos sólo considerar las mutaciones que exhibieron un efecto positivo, es decir, un incremento en la resistencia a la inactivación por MMTS. Tal fue el caso de la mutante aditiva R1M11 (con la mutación T32S) la cual mostró un incremento en la resistencia a la inactivación con MMTS (de 67% a una concentración de 100 μM de MMTS) (fig. 6.1c y tabla 9 del anexo).

Finalmente, las mutantes aditivas R1M12 y R1M13 (con las mutaciones F33I y D34N, respectivamente) presentaron patrones de inactivación neutros respecto a la mutante R1M11, que fue similar al patrón de inactivación de TbTIM silvestre (fig. 6.1c y tabla 9 del anexo).

Inactivación con MMTS de las mutantes aditivas de la región 4

Los cinco aminoácidos diferentes de la región 4 de TbTIM fueron introducidos de forma gradual en la quimera TbTIM 1-3,5-8; TcTIM4. Esta proteína tiene un 98% de la secuencia de TbTIM y su inactivación con MMTS se asemeja más a TcTIM ya que su actividad residual al ser tratada con 100 μM de MMTS es únicamente del 15% (véase la fig. 2c en [17] y fig. 6.2a). Por lo tanto, en las mutaciones aditivas esperábamos un aumento en la resistencia a la inactivación.

En la curva de inactivación de la mutante aditiva R4M1 (con la mutación L100A) a una concentración de 100 μM de MMTS, se obtuvo una actividad residual de 62%, lo que representa aproximadamente un 20% menos que la de TbTIM en las mismas condiciones. Sin embargo, la resistencia a la inactivación de la mutante R4M1 a MMTS 50 μM, o a una concentración menor, es incluso mayor que en la TbTIM (fig. 6.2a y tabla 10 en el anexo). Por lo tanto, parece que la alanina en la posición 100 tiene un efecto importante para conferir resistencia a esta proteína a bajas concentraciones de MMTS. La importancia de este residuo se detallará más adelante en el segmento donde se describe la inactivación de mutantes sitio-dirigidas con aminoácidos de las regiones 1 y 4 en TcTIM.

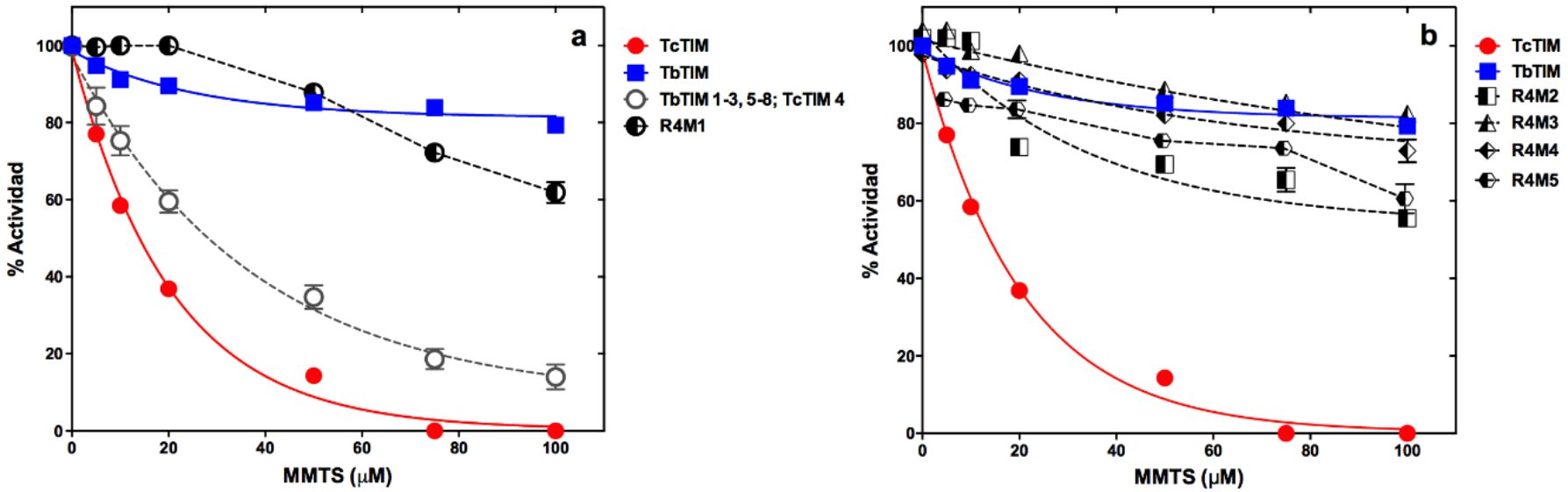

Figura 6.2. **Efecto del MMTS sobre mutantes aditivas de la región 4 y enzimas TcTIM y TbTIM silvestres**. Todas las enzimas se incubaron a 250 μg/mL con MMTS 5-100 μM trietanolamina 100 mM, EDTA 10 mM, pH 7.4 durante 2 horas a 25 °C. Los ensayos de MMTS para cada mutante se realizaron tres veces de forma independiente incluida una muestra sin MMTS para calcular el 100% de la actividad. Transcurrido el tiempo de incubación se determinó la actividad catalítica residual y se graficó en función de la concentración de MMTS. Panel a) R4M1, TcTIM y TbTIM; Panel b) R4M2, R4M3, R4M4, R4M5, TcTIM y TbTIM.

El papel del aspártico 111 de TbTIM se estudió mediante la mutante R4M2 que contiene la mutación E111D. Este residuo no incrementa la resistencia a la inactivación por MMTS, al contrario, a bajas concentraciones, la enzima R4M2 presenta un decremento en su actividad residual comparada con la mutante R4M1. A altas concentraciones de MMTS mantiene una actividad residual del 60.2% (tabla 10 del anexo y fig. 6.2b). Este resultado nos permitió descartar dicho aminoácido como uno de los responsables de fomentar resistencia frente a la inactivación por MMTS.

La importancia de la alanina 115 se estudió con la mutante R4M3, la cual tiene la mutación Q115A. Esta mutación tuvo otro efecto positivo en el aumento de la resistencia de la enzima a la inactivación con MMTS con un patrón que es ligeramente más susceptible que TbTIM en todas las concentraciones estudiadas (tabla 10 del anexo y fig. 6.2b). El papel que juega este aminoácido se describirá en una sección posterior, cuando se hagan las mutaciones sitio-dirigidas Q115A y A115Q sobre las enzimas TcTIM y TbTIM silvestres, respectivamente.

El efecto de la valina 117 se estudió con la mutante R4M4 (con la mutación C117V). Este residuo no parece alterar los resultados obtenidos con la mutante R4M3. El comportamiento de R4M4 fue neutral respecto a la mutación precedente. Lo mismo ocurrió con la mutante R4M5, en la cual se estudió la mutación A119S. Su reactividad frente a la inactivación por MMTS tuvo un efecto ligeramente negativo, con un patrón de susceptibilidad similar al de la mutante R4M1 (fig. 6.2b y tabla 10 del anexo).

La actividad específica de estas mutantes aditivas se muestra en la tabla 11 del anexo. Es importante resaltar que las actividades específicas de estas mutantes, al igual que los obtenidos en las mutantes aditivas de la región 1, son comparables con las obtenidas y reportadas para las enzimas silvestres.

Inactivación con MMTS de mutantes con aminoácidos de las regiones 1 y 4 en TcTIM

De acuerdo a los resultados previos con las mutantes aditivas de la región 1 y 4, concluimos que los aminoácidos en las posiciones 26, 27, 28, 30 y 32 de la región 1 y los aminoacidos en las posiciones 100 y 115 de la región 4 tienen un efecto positivo en conferir resistencia a la inactivación por MMTS. Por consiguiente, para cumplir nuestro objetivo de encontrar la mínima cantidad de aminoácidos que son responsables de la diferente susceptibilidad a la inactivación con MMTS de TbTIM y TcTIM, inicialmente construimos una serie de mutantes sitio-dirigidas con aminoácidos seleccionados sobre TcTIM.

En una serie de mutantes conservamos los aminoácidos de TbTIM de la región 4 (100 y 115) e introdujimos los aminoácidos 26, 27, 28, 30 y 32 de la región 1 en la secuencia de TcTIM. Podemos ver en la figura 6.3a (tabla 12 del anexo), que esta enzima con siete mutaciones mostró un patrón de resistencia similar, e incluso mayor, que TbTIM a la inactivación con MMTS.

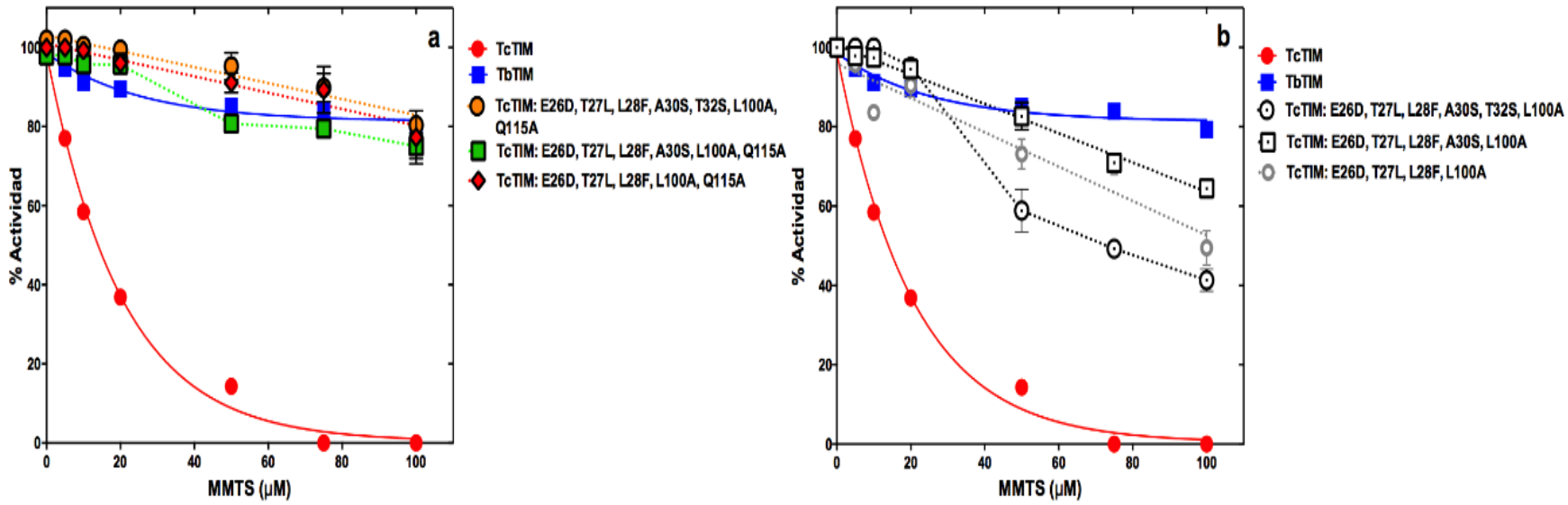

Figura 6.3. **Efecto del MMTS sobre mutantes sitio-dirigidas de aminoácidos selecionados de las regiones 1 y 4 en las secuencia de TcTIM silvestre y las enzimas TcTIM y TbTIM silvestres**. Todas las enzimas se incubaron a 250 µg/mL con MMTS 5-100 µM trietanolamina 100 mM, EDTA 10 mM, pH 7.4 durante 2 horas a 25 °C. Los ensayos de MMTS para cada mutante se realizaron tres veces de forma independiente incluida una muestra sin MMTS para calcular el 100% de la actividad. Transcurrido el tiempo de incubación se determinó la actividad catalítica residual y se graficó en función de la concentración de MMTS. Panel a) TcTIM: E26D, T27L, L28F, A30S, T32S, 100A, 115A; TcTIM: E26D, T27L, L28F, A30S, L100A, Q115A; TcTIM: E26D, T27L, L28F, L100A, Q115A; TcTIM y TbTIM. Panel b) TcTIM: E26D, T27L, L28F, A30S, T32S, L100A; TcTIM: E26D, T27L, L28F, A30S, L100A; TcTIM: E26D, T27L, L28F, L100A; TcTIM y TbTIM.

A continuación, preparamos mutantes con cuatro y tres cambios en la región 1 (y conservando la región 4) que fueron: TcTIM: E26D, T27L, L28F, A30S, L100A, Q115A y TcTIM: E26D, T27L, L28F, L100A, Q115A, para explorar cuales aminoácidos de la región 1 eran necesarios y suficientes para cambiar susceptibilidad de la mutante que contenía siete mutaciones. La figura 6.3a (tabla 12 del anexo) muestra que las enzimas con seis y cinco mutaciones todavía muestran un patrón de susceptibilidad similar a TbTIM. La curva de la mutante con seis cambios fue muy similar a la curva de la TbTIM silvestre, mientras que la curva de la mutante con cinco variaciones fue similar a la curva de la mutante con siete cambios, con un patrón de resistencia ligeramente incrementado a bajas concentraciones del reactivo sulfhidrilo.

Estas mutantes fueron importantes para concluir que los aminoácidos en las posiciones 30 y 32 en las mutantes aditivas (R1M9 y R1M11) que causan efectos positivos relativamente pequeños, no contribuían mucho a la resistencia. De hecho, la enzima con cinco mutaciones todavía muestra un comportamiento similar a TbTIM en presencia de MMTS.

Para la siguiente mutante volvimos nuestra atención al residuo en la posición 115 de la región 4. Consideramos el resultado obtenido con la mutante R4M3 que tenía la mutación Q115A, con un efecto positivo, pero no tan grande como el de la mutante R4M1 con la mutación (L100A). Por ello produjimos las mutantes: TcTIM: E26D, T27L, L28F, A30S, T32S, L100A; TcTIM: E26D, T27L, L28F, A30S, L100A y TcTIM: E26D, T27L, L28F, L100A en las cuales, deliberadamente, no se mutó el aminoácido en la posición 115.

Como puede observarse en la figura 6.3b, todas estas enzimas fueron más susceptibles que TbTIM a la inactivación por MMTS, particularmente a concentraciones de MMTS superiores a 50 μM. No obstante, no hubo una correlación evidente entre el número de aminoácidos mutados y la forma de la curva de inactivación. Concluimos que la A115 de TbTIM es importante para la resistencia a la inactivación a altas concentraciones de MMTS, ya que su ausencia en estas mutantes disminuyó la actividad residual a aproximadamente a la mitad.

Análisis más extenso

Investigamos si podíamos reducir aún más el número de aminoácidos de TbTIM y mantener el comportamiento con mayor resistencia a la inactivación con MMTS. Partiendo del resultado obtenido del patrón de inactivación de la quíntuple mutante (TcTIM: E26D, T27L, L28F, L100A, Q115A) se diseñó una serie de mutantes que nos ayudaron a determinar si la importancia de los tres residuos de la región 1 encontrados hasta ahora (E26D, T27L, L28F) se debía a un efecto aditivo entre ellos o a un efecto individual.

En esta serie, los aminoácidos A100 y A115 de la región 4 se mantuvieron constantes y se introdujeron mutaciones en los residuos 26, 27 y 28 de la región 1. Las curvas de inactivación de éstas cuádruples mutantes: TcTIM: T27L, L28F, L100A, Q115A; TcTIM: E26D, L28F, L100A, Q115A y TcTIM: E26D, T27L, L100A, Q115A se pueden ver en la figura 6.4a.

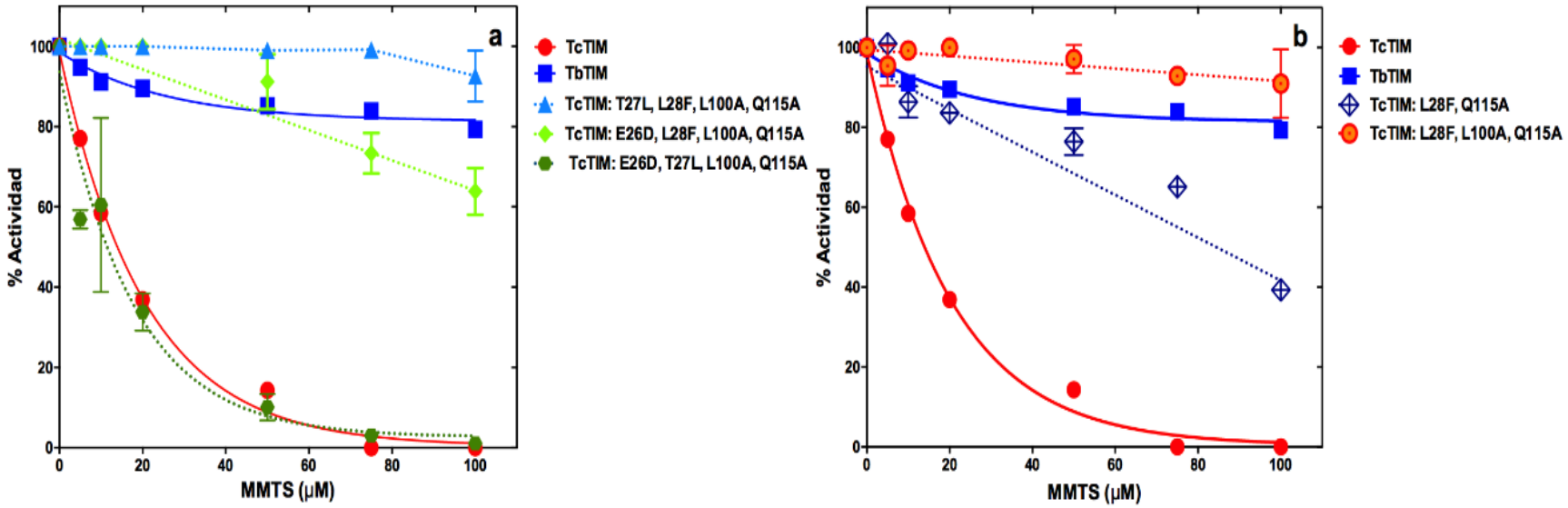

Figura 6.4**. Efecto del MMTS sobre mutantes sitio-dirigidas de aminoácidos selecionados de las regiones 1 y 4 en las secuencia de TcTIM silvestre y las enzimas TcTIM y TbTIM silvestres**. Todas las enzimas se incubaron a 250 µg/mL con MMTS 5-100 µM trietanolamina 100 mM, EDTA 10 mM, pH 7.4 durante 2 horas a 25 °C. Los ensayos de MMTS para cada mutante se realizaron tres veces de forma independiente incluida una muestra sin MMTS para calcular el 100% de la actividad. Transcurrido el tiempo de incubación se determinó la actividad catalítica residual y se graficó en función de la concentración de MMTS. Panel a) TcTIM: T27L, L28F, L100A, Q115A ; TcTIM: E26D, L28F, L100A, Q115A; TcTIM: E26D, T27L, L100A, Q115A; TcTIM y TbTIM. Panel b) TcTIM: T27L, L28F, L100A; TcTIM: L28F, L100A, Q115A; TcTIM: T27L, L100A, Q115A; TcTIM y TbTIM.

La curva de inactivación de la mutante TcTIM: E26D, L28F, L100A, Q115A, pese a que a altas concentraciones de MMTS disminuye ligeramente su actividad residual, presenta un comportamiento muy similar a la quíntuple mutante (TcTIM: E26D, T27L, L28F, L100A, Q115A) y a la TbTIM silvestre. Algo similar ocurre con la mutante TcTIM: T27L, L28F, L100A, Q115A. Sin embargo, la mutante TcTIM: E26D, T27L, L100A, Q115A pierde su actividad residual dramáticamente al ser incubada con MMTS.

A partir de estos resultados, es evidente que la F28 es fundamental para determinar el perfil de inactivación de una enzima mutante, ya que al estar ausente en la mutante TcTIM: E26D, T27L, L100A, Q115A, la proteína se vuelve tan susceptible como la TcTIM silvestre. Además, esta mutante indica que el D26 no es crucial para la resistencia a la inactivación con MMTS, por lo cual seguimos analizando cuidadosamete la L27 en las mutantes TcTIM: T27L, L100A, Q115A y TcTIM: T27L, L28F, L100A, Q115A. De su comportamiento se concluyó que la L27 no es un aminoácido que promueva resistencia a la inactivación por el MMTS (fig. 1 del anexo).

La importancia del aminoácido A100 se había observado en las mutantes aditivas de la región 4 (tabla 10 del anexo y fig. 6.2a). Para estudiar mejor su papel, decidimos construir la mutante doble TcTIM: L28F, Q115A. Como puede notarse en la figura 6.4b, a una concentración de MMTS 100 μM la actividad residual de esta proteína fue de 39% y la curva de inactivación de esta mutante muestra un comportamiento intermedio entre TbTIM y TcTIM. Con esta evidencia concluimos

que las mutaciones L28F y Q115A no bastaron para transformar a TcTIM en una enzima resistente al MMTS como TbTIM, por lo que se hizo la mutante TcTIM: L28F, L100A, Q115A, que resultó tener una resistencia mayor al MMTS que TbTIM (fig.6.4b).

Para cerciorarnos de que no existía otra combinación de aminoácidos de las regiones 1 y 4 que provocaran el mismo efecto de resistencia al MMTS, se produjeron mutantes dobles de los aminoácidos en las posiciones 28, 100 y 115. Las mutantes dobles fueron TcTIM: L28F, L100A y TcTIM: L100A, Q115A, las cuales demostraron no ser suficientes para mantener la resistencia al MMTS (fig. 6.5a).

Por otro lado, se produjeron mutantes simples para averiguar la contribución de cada uno de los tres aminoácidos en la mutante triple resistente. Estas mutantes fueron TcTIM: L28F; TcTIM: L100A y TcTIM: Q115A. Los resultados de inactivar estas mutantes con MMTS puede verse en la figura 6.5b. La mutante TcTIM:L100A mostró un comportamiento bastante similar al de la TcTIM silvestre a todas las concentraciones de MMTS estudiadas, por lo que la importancia de la alanina 100 parece ser únicamente un fenómeno concertado en presencia de los otros dos aminoácidos.

Por otra parte, la mutante TcTIM: L28F sí presenta una resistencia intermedia entre TcTIM y TbTIM, a bajas concentraciones de MMTS. Sin embargo, a una concentración de MMTS 100 μM, esta enzima sólo mantiene el 8% de su actividad

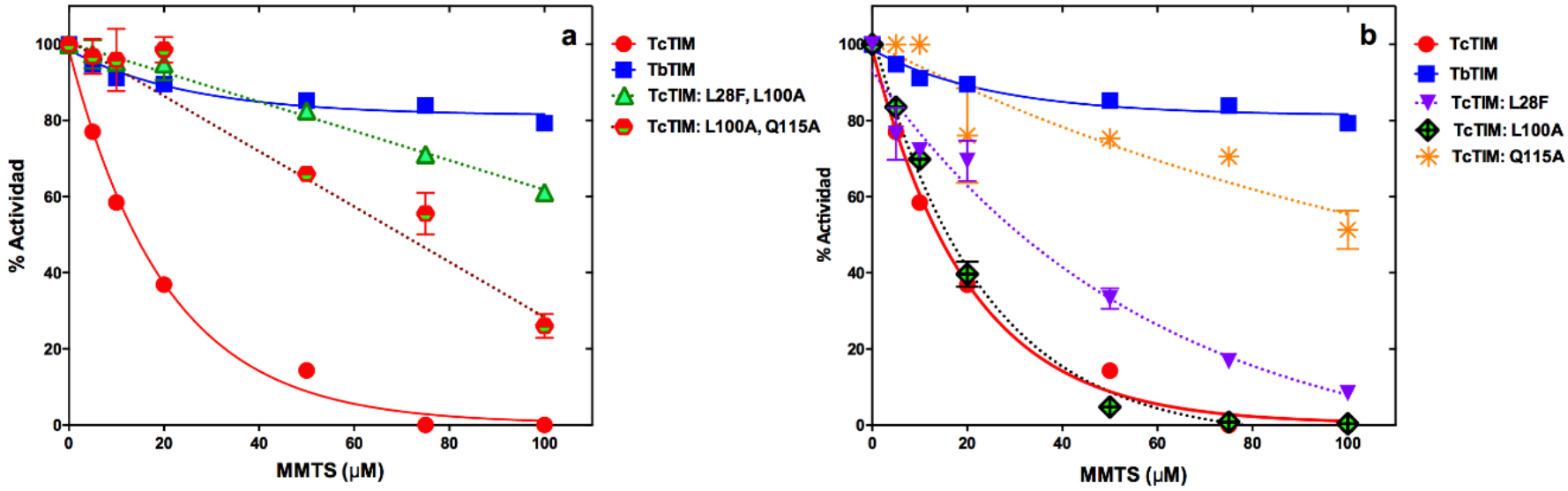

Figura 6.5. **Efecto del MMTS sobre mutantes sitio-dirigidas de aminoácidos selecionados de las regiones 1 y 4 en las secuencia de TcTIM silvestre y las enzimas TcTIM y TbTIM silvestres**. Todas las enzimas se incubaron a 250 µg/mL con MMTS 5-100 µM trietanolamina 100 mM, EDTA 10 mM, pH 7.4 durante 2 horas a 25 °C. Los ensayos de MMTS para cada mutante se realizaron tres veces de forma independiente incluida una muestra sin MMTS para calcular el 100% de la actividad. Transcurrido el tiempo de incubación se determinó la actividad catalítica residual y se graficó en función de la concentración de MMTS. Panel a) TcTIM: L28F, L100A; TcTIM: L100A, Q115A; TcTIM y TbTIM. Panel b) TcTIM: L28F, TcTIM: L100A, TcTIM: Q115A, TcTIM y TbTIM.

residual (fig. 6.5b). Este resultado sugirió que F28 contribuye a aumentar la resistencia ante el MMTS. Sin embargo, el residuo que más contribuyó a aumentar la resistencia al MMTS fue la alanina 115, ya que la mutante TcTIM:Q115A presentó una actividad residual del 61% a una concentración de MMTS 100 μM (fig. 6.5b).

En conjunto, los resultados presentados aquí indican que no existe otro número menor u otra combinación de aminoácidos que tres para obtener una mutante de TcTIM con una resistencia similar a la inactivación por MMTS a la TbTIM silvestre.

Inactivación con MMTS de mutantes en la secuencia de TbTIM

Hasta esta etapa de la investigación se encontró que la F28, la A100 y la A115 de TbTIM eran capaces de provocar en la TcTIM un incremento de resistencia a la inactivación con MMTS similar a la de TbTIM, por lo que nos preguntamos que le ocurriría a TbTIM si le sustituíamos los aminoácidos equivalentes de TcTIM en esas posiciones.

La respuesta la obtuvimos con la mutante TbTIM: F28L, A100L, A115Q. La curva de inactivación obtenida exhibió un patrón de inactivación que se asemeja al de TcTIM, como puede verse en la fig. 6.6a y la tabla 13 del anexo. Además, es tan susceptible como TcTIM a concentraciones de MMTS de 10 μM, o menores, y ligeramente más resistente a concentraciones superiores a 20 μM.

También se investigó la contribución individual o aditiva de estos tres aminoácidos. Para ello se realizaron mutantes simples y dobles en la secuencia de TbTIM. Como puede verse en la figura 6.6b, las mutantes dobles TbTIM: F28L, A100L, y TbTIM: F28L, A115Q presentaron un comportamiento intermedio entre TcTIM y TbTIM, indicando que la L28 y la Q115 contribuyen de igual manera a disminuir la resistencia frente al MMTS. En cambio, la mutante TbTIM: A100L, A115Q presentó una resistencia mayor a las dos mutantes anteriores, lo que indicó que esta combinación de aminoácidos es la que menos contribuye a la susceptibilidad a la inactivación por el MMTS (fig. 6.6b).

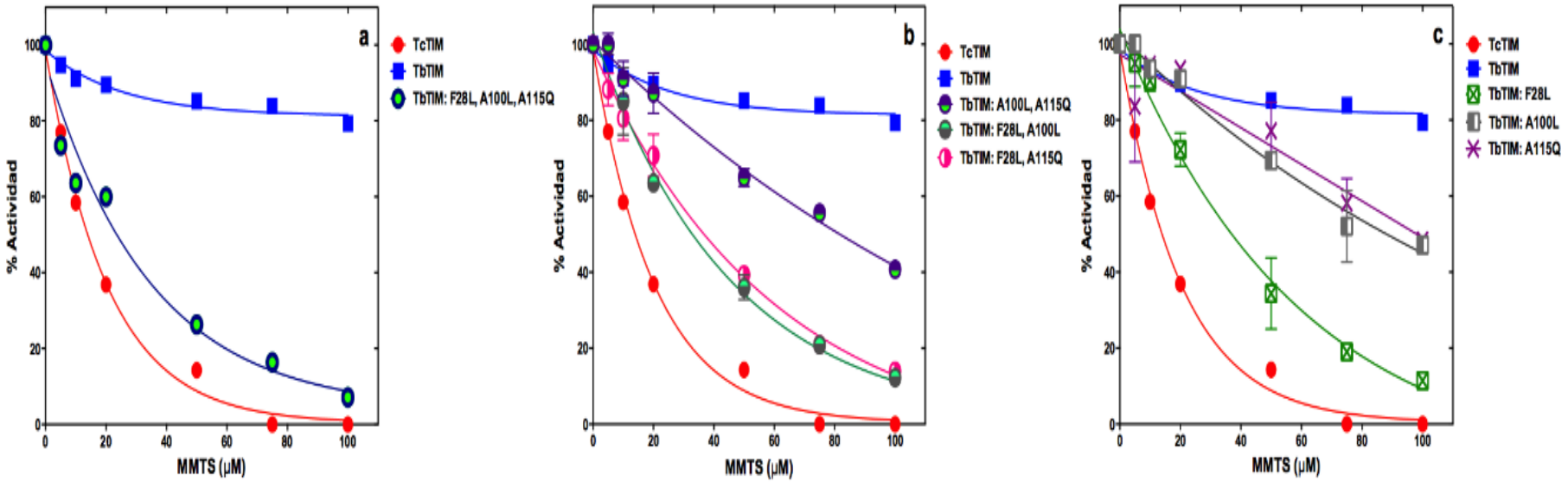

Figura 6.6. **Efecto del MMTS sobre mutantes sitio-dirigidas de aminoácidos selecionados de las regiones 1 y 4 en las secuencia de TbTIM silvestre y las enzimas TcTIM y TbTIM silvestres**. Todas las enzimas se incubaron a 250 µg/mL con MMTS 5-100 µM trietanolamina 100 mM, EDTA 10 mM, pH 7.4 durante 2 horas a 25 °C. Los ensayos de MMTS para cada mutante se realizaron tres veces de forma independiente incluida una muestra sin MMTS para calcular el 100% de la actividad. Transcurrido el tiempo de incubación se determinó la actividad catalítica residual y se graficó en función de la concentración de MMTS. Panel a) TbTIM: F28L, A100L, A115Q. Panel b) TbTIM: A100L, A115Q, TbTIM: F28L, A100L y TbTIM: F28L, A115Q. Panel c) TbTIM: F28L, TbTIM: A100L, TbTIM: A115Q, TcTIM y TbTIM.

También se evaluó la contribución individual de estos tres residuos con mutantes simples. En el caso de la L28 de TcTIM, la mutante TbTIM: F28L mostró un incremento de susceptibilidad ante el MMTS, dejando una actividad residual del 11.4% a una concentración de MMTS 100 μM (fig. 6.6c). Por otro lado, la L100 y la Q115 de TcTIM provocaron en las mutantes TbTIM: A100L y TbTIM: A115Q una susceptibilidad intermedia entre TcTIM y TbTIM, ya que mantuvieron el 50% de su actividad residual (fig. 6.6c). Las tres mutantes nos indican que esos aminoácidos de TcTIM provocan en TbTIM un incremento en la susceptibilidad a la inactivación por MMTS en diferentes grados. Particularmente, la L28 incrementa la susceptibilidad en mayor grado, mientras que la L100 y la Q115 la incrementan en igual magnitud.

El *pKa* de la cisteína 14 de interfaz y su correlación con la susceptibilidad al MMTS.

Anteriormente, Reyes-Vivas y colaboradores [11] reportaron que la reactividad de la TbTIM y la TcTIM a la inactivación por el MMTS depende del *pKa* de la cisteína 14 de interfaz. Aunque el mecanismo por el cual la diferencia en la susceptibilidad ocurre no está claro, entre más básico sea el *pKa* de esta cisteína, su susceptibilidad al MMTS será menor. El *pKa* de la cisteína de interfaz tiene un valor de 10.53 en TbTIM y de 9.2 en TcTIM [11]. En la tabla 6.1 se muestra cómo el grupo tiol de la cisteína de interfaz de la mutante TcTIM: L28F, L100A, Q115A tiene un *pKa* muy similar al de TbTIM (10.69) y que el *pKa* de la cisteína de interfaz de la mutante triple de TbTIM: F28L, A100L, A115Q es muy similar al de la TcTIM (9.23).

Además, se determinó el *pKa* de las cisteínas de interfaz de otras mutantes analizadas en este trabajo en las cuales observamos el mismo fenómeno. De tal forma que las mutantes TcTIM: E26D, T27L, L28F, L100A, Q115A; TcTIM: T27L, L28F, L100A, Q115A y TcTIM: E26D, L28F, L100A, Q115A que tienen una susceptibilidad baja a la inactivación con MMTS y sus cisteínas de interfaz tienen un *pKa* similar al de la TbTIM. Al contrario, la mutante TcTIM: E26D, T27L, L100A, Q115A que tiene una gran susceptibilidad a la inactivación por MMTS tiene una cisteina de interfaz con un *pKa* de 9.5, similar al de TcTIM, que es de 9.27.

Tabla 6.1. Valores de *pKa* de la cisteína 14 de interfaz

Enzima o mutante	*pKa* de la cisteína de interfaz
TbTIM	10.53 ± 0.06
TcTIM	9.27 ± 0,16
TcTIM: L28, L100A, Q115A	10.69 ± 0.01
TbTIM: F28L, A100L, A115Q	9.23 ± 0.03
TcTIM: E26D, T27L, L28F, L100A, Q115A	10.61 ± 0.39
TcTIM: T27L, L28F, L100A, Q115A	10.53 ± 0.47
TcTIM: E26D, L28F, L100A, Q115A	10.52 ± 0.017
TcTIM: E26D, T27L, L100A, Q115A	9.5± 0.042

6. Discusión

Nuestro trabajo muestra que es posible identificar sistemáticamente aminoácidos que rigen las características de una propiedad especifica dentro de una secuencia total de una proteína. Aquí hemos ampliado y afinado nuestro método experimental de utilizar una proteína homóloga en dos organismos relacionados para identificar los aminoácidos responsables de causar las diferencias en la susceptibilidad de inactivación con el reactivo sulfhidrilo MMTS. Al igual que nuestro enfoque inicial, el nuevo método no puede predecir cuales mutaciones afectarían las propiedades catalíticas y la susceptibilidad de la cisteína de interfaz a la acción del MMTS. Los resultados obtenidos en este trabajo no estuvieron sesgados por consideraciones estructurales, evolutivas o hipotéticas de importancia teórica de ciertos aminoácidos para la función, estabilidad u otras propiedades de la proteína. Los resultados experimentales de este trabajo dan una respuesta directa a la pregunta planteada.

Además, creemos que hay varios puntos que aún podemos aprender con nuestros resultados. Como puede verse en las tablas 11 y 14 del anexo, básicamente todas las proteínas quiméricas, tanto las mutantes aditivas como las mutantes puntuales, tenían propiedades catalíticas que son comparables a las de las enzimas silvestres. Como ya se señaló anteriormente, este es un resultado esperado en donde las mutaciones no afectaron propiedades generales de las TIMs, ni a residuos que son importantes para su función catalítica, a pesar de que dos de los tres aminoácidos catalíticos se encontraban en las regiones que trabajamos (1 y 4): la lisina 13 se ubica en la región 1 y la histidina 95 en la región 4; el último aminoácido catalítico

(ácido glutámico 167) se encuentra en la región 6, que está muy alejada de las regiones donde se produjeron las mutaciones, por lo que no se esperaba ninguna influencia sobre este residuo.

En nuestro trabajo publicado en el 2011 anticipamos que las propiedades de la cisteína 14 de interfaz no cambiarían en forma gradual o continua, sino que se alterarían en forma discontinua. Efectivamente esto resultó ser así (tabla 6.1).

En este trabajo obtuvimos la respuesta a la pregunta de cuál es el número mínimo de residuos implicados en la susceptibilidad a la inactivación con MMTS. El resultado fue que un mínimo de tres residuos (en la posición 28 de la región 1 y las posiciones 100 y 115 de la región 4) son suficientes para que una TcTIM cambie su susceptibilidad a la acción del MMTS a un patrón de resistencia similar a TbTIM (fig. 6.4b). Por otro lado, estos residuos también cambian la resistencia al MMTS de una TbTIM a un patrón de susceptibilidad similar al de la TcTIM (fig. 6.6a). Por lo tanto, estos son los residuos importantes, ya que ninguna mutante doble o simple pudieron cambiar completamente el patrón de susceptibilidad (fig. 6.6 b y c). Por otro lado, nuestros resultados también muestran que otras mutantes cuádruples, quíntuples, séxtuples y séptuples de TcTIM silvestre muestran el patrón resistente al MMTS igual o muy parecido al TbTIM silvestre. ¿Qué significa esto?

Generalmente los métodos de mutagénesis aleatoria se basan en encontrar una proteína que muestre alteraciones en una propiedad específica. Entonces se analizan él o los aminoácidos mutados que lo produjeron y se buscan las razones

que lo expliquen, si es posible. Pero con estas metodologías, la mutante analizada, pudiera ser sólo una de múltiples mutantes que produzcan ese efecto. En nuestro trabajo los ejemplos de las múltiples de mutantes que presentaron el comportamiento alterado frente al MMTS fueron: TcTIM: E26D, T27L, L28F, A30S, T32S, L100A, Q115A; TcTIM: E26D, T27L, L28F, A30S, L100A, Q115A; TcTIM: E26D, T27L, L28F, L100A, Q115A; TcTIM: T27L, L28F, L100A, Q115A y TcTIM: L28F, L100A, Q115A. Dependiendo de si ya se tiene el número mínimo de cambios, o un número mayor (que todavía produce las diferencias), la validación de que uno tiene el número mínimo de mutaciones para producir el comportamiento alterado, va a ser diferente.

En cualquier caso, un enfoque sistemático como el que se muestra en este trabajo debería ser útil para demostrar y comprender que en muchos casos el cambio de comportamiento no se debe a una sola mutación, también muestra la importancia de cada aminoácido individual, así como la cooperación sinérgica que produce las características alteradas y/o un cambio de función en una proteína.

En nuestra opinión, para comprender mejor el papel de cada aminoácido en características fisicoquímicas particulares o en la función de una proteína, un análisis sistemático utilizando mutagénesis como la descrita en García-Torres, et al. [17] y que se completó en este trabajo, identificará todos los residuos responsables, particularmente cuando no pueden ser deducidos o predichos por otros métodos de análisis de proteínas.

7. Conclusiones

Los aminoácidos de las posiciones 28 fenilalanina/leucina, 100 alanina/leucina y 115 alanina/glutamina en la secuencia de aminoácidos de las triosafosfato isomerasas de *T. cruzi* y *T. brucei* son los responsables de la distinta susceptibilidad que tienen dichas enzimas a la inactivación con el reactivo sulfhidrilo MMTS.

8. Otros trabajos publicados durante los estudios de Doctorado

García Torres I., Cabrera, N., Torres-Larios, A., Rodriguez-Bolaños, M., Díaz Mazariegos, S., Gómez-Puyou, A., Perez-Montfort, R.: Identification of amino acids that account for long-range interactions in two triosephosphate isomerases from pathogenic trypanosomes. PLoS ONE 6: e18791, 2011.

Identificación de aminoácidos que tienen interacciones a larga distancia en dos triosafosfato isomerasas de tripanosomas patógenos.

Resumen

Para comprender mejor la relación estructura-función en las proteínas es necesario identificar los aminoácidos que son relevantes para funciones importantes medibles de las proteínas. Debido a los numerosos contactos que los aminoácidos establecen en las proteínas, y la naturaleza cooperativa de sus interacciones, es difícil lograr este objetivo. Por lo tanto, el estudio de las interacciones proteína-ligando se centra generalmente en las diferencias estructurales en ambientes locales. En este trabajo, utilizando dos triosafosfato isomerasas con similitud extremadamente alta de dos tripanosomas patógenos diferentes, demostramos que el control de una diferencia de setenta veces en la reactividad de la cisteína de la interfaz se encuentra en varios aminoácidos de dos regiones estructuralmente no relacionadas y que no entran en contacto con la cisteína de interfaz susceptible al metilmetano tiosulfonato (un reactivo de sulhidrilo) ni tampoco tienen contacto con los residuos de su vecindad inmediata. El cambio en la reactividad se debe a un aumento del pKa aparente de la cisteína de la interfaz producida por los residuos mutados. Nuestro trabajo, que incluyó la sustitución sistemática de grandes segmentos de una proteína en la otra,

reveló interacciones insospechadas y multi-sitio de largo alcance, que modulan las propiedades de las cisteínas de la interfaz y tiene implicaciones generales para estudios futuros sobre las relaciones estructura-función de las proteínas.

Aguilera, E., Varela, J., Birriel, E., Serna, E., Torres, S., Yaluff, G., de Bilbao, N. V., Aguirre-López, B., Cabrera, N., Díaz Mazariegos, S., de Gómez-Puyou, M. T., Gómez-Puyou, A., Perez-Montfort, R., Minini, L., Merlino, A., Cerecetto, H., González, M., Alvarez, G.: Potent and selective inhibitors of *Trypanosoma cruzi* triosephosphate Isomerase with concomitant inhibition of Cruzipain: Inhibition of parasite growth through multitarget activity. Chem. Med. Chem. 11: 1328- 1338, 2016.

Inhibidores selectivos y potentes de la triosafosfato isomerasa de *Trypanosoma cruzi* con inhibición concomitante de cruzipaína: inhibición del crecimiento del parásito a través de la actividad contra múltiples blancos.

Resumen

La triosafosfato isomerasa (TIM) es una enzima esencial de *T.* cruzi y una de los pocos blancos de medicamentos validados contra la enfermedad de Chagas. Los inhibidores conocidos de esta enzima se comportan mal o tienen baja actividad en el parásito. En este trabajo se utilizaron diarilidenequitonas simétricas derivadas de estructuras con actividad tripanosomicida. Se obtuvo un inhibidor enzimático con un valor IC50 de 86 nm que no inhibe a la enzima de los mamíferos. Estas moléculas también afectaron la cruzipaina, otra enzima proteolítica esencial del parásito. Esta doble actividad es importante para evitar problemas de resistencia. Los compuestos fueron estudiados *in vitro* contra la forma epimastigote del parásito, y también se evaluó la toxicidad inespecífica contra las células de mamífero. Como prueba de concepto, también se analizaron, *in vivo*, tres de los mejores derivados. Algunos de

estos derivados mostraron una mayor actividad tripanosomicida *in vitro* que los fármacos de referencia y fueron eficaces para proteger a los ratones infectados. Además, estas moléculas podrían obtenerse por una vía sintética ecológicamente responsable, simple y económica, que es una característica importante en la investigación y el desarrollo de futuros fármacos para enfermedades olvidadas.

Quezada, A.G., Cabrera, N., Piñeiro, Á., Díaz-Salazar, A.J., Díaz-Mazariegos, S., Romero-Romero, S., Perez-Montfort, R., Costas, M. A strategy based on thermal flexibility to design triosephosphate isomerase proteins with increased or decreased kinetic stability. Biochem. Biophys. Res. Com. 503: 3017-3022, 2018.

Una estrategia basada en la flexibilidad térmica para diseñar proteínas de triosafosfato isomerasa con estabilidad cinética aumentada o disminuida

Resumen

La estabilidad cinética de las proteínas determina su susceptibilidad a desplegarse irreversiblemente, que es un proceso dependiente del tiempo y, por lo tanto, de su vida media. Recientemente se empleó un análisis de desplazamiento de residuos de simulaciones de dinámica molecular inducidas por temperatura para definir la flexibilidad térmica de las proteínas. Esta propiedad se encontró correlacionada con la barrera de energía de activación (Eact) que separa al estado nativo del estado de transición en el proceso de desnaturalización. La Eact se determinó a partir de la aplicación de un modelo irreversible de dos estados en experimentos de despliegue de temperatura utilizando calorimetría de barrido diferencial (DSC). La contribución de cada residuo a la flexibilidad térmica de las proteínas se utilizó aquí para proponer múltiples mutaciones en las triosafosfato isomerasas (TIM) de *T. brucei* (TbTIM) y *T. cruzi* (TcTIM), dos parásitos estrechamente relacionados evolutivamente. Estas dos enzimas, fueron utilizadas como sistemas modelo, tienen una estructura prácticamente idéntica, pero grandes diferencias en su estabilidad cinética. Construimos dos variantes funcionales de TIM con más de dos veces y menos de la mitad de la energía de activación de sus respectivas estructuras de referencia, las enzimas silvestres. Los resultados muestran que la estrategia propuesta es capaz de identificar los residuos cruciales para la estabilidad cinética de estas enzimas. Como ocurre con otras propiedades proteicas, que reflejan su comportamiento complejo, la estabilidad cinética parece ser la consecuencia de una extensa red de interacciones entre residuos, actuando de forma concertada. La

estrategia propuesta para diseñar variantes puede utilizarse con otras proteínas, para aumentar o disminuir su vida media funcional.

Anexo

Tabla 1**. Templado de DNA empleado para distintas mutantes aditivas**

Secuencia de DNA utilizada como templado	Mutante aditiva
TbTIM4	R1M1, R1M2, R1M3, R1M4, R1M5
R1M5	R1M6, R1M7, R1M8, R1M9, R1M10, R1M11, R1M12 y R1M13
TcTIM4	R4M1
R4M1	R4M2
R4M2	R4M3, R4M4 y R4M5

Tabla 2. **Oligonucleótidos utilizados para construir las mutantes aditivas de la región 1 en la quimera TbTIM4**

Mutante	Fw primer	Rv primer
R1M1	5'AAGTGCAACGGCTCCCAGAGTTTGCTTGTACCACTC3'	5'GAGTGGTACAAGCAAACTCTGGGAGCCGTTGCACTT3'
R1M2	5'TGGAAGTGCAACGGCTCCCAGCAGTTGCTTGTACCACTC3'	5'GAGTGGTACAAGCAACTGCTGGGAGCCGTTGCACTTCCA3'
R1M3	5'GCAAACTGGAAGTGCAACGGCTCCCAGCAGAGCCTTGTACCA3'	5'TGGTACAAGGCTCTGCTGGGAGCCGTTGCACTTCCAGTTTGC3'
R1M4	5'AAGTGCAACGGCTCCCAGCAGAGCCTTAGCCCACTCATCGAGACGCTC3'	5'GAGCGTCTCGATGAGTGGGCTAAGGCTCTGCTGGGAGCCGTTGCACTT3'
R1M5	5'CTGGAAGTGCAACGGCTCCCAGCAGAGCCTTAGCGAACTCATCGAGACGCT3'	5'AGCGTCTCGATGAGTTCGCTAAGGCTCTGCTGGGAGCCGTTGCACTTCCAG3'
R1M6	5'GAACTCATCGATACGCTCAATGCAGCGACTTTT3'	5'AAAAGTCGCTGCATTGAGCGTATCGATGAGTTC3'
R1M7	5'GAACTCATCGATCTGCTCAATGCAGCGACTTTTGAT3'	5'ATCAAAAGTCGCTGCATTGAGCAGATCGATGAGTTC3'
R1M8	5'GAACTCATCGATCTGTTTAATGCAGCGACT3'	5'AGTCGCTGCATTAAACAGATCGATGAGTTC3'
R1M9	5'ATCGATCTGTTTAATAGCGCGACTTTTGAT3'	5'ATCAAAAGTCGCGCTATTAAACAGATCGAT3'
R1M10	5'AGCCTTAGCGAACTCATCGATCTGTTTAATAGCACCACTTTTGATCAC3'	5'GTGATCAAAAGTGGTGCTATTAAACAGATCGATGAGTTCGCTAAGGCT3'
R1M11	5'AGCCTTAGCGAACTCATCGATCTGTTTAATAGCACCAGCTTTGATCACGATGTGCAA3'	5'TTGCACATCGTGATCAAAGCTGGTGCTATTAAACAGATCGATGAGTTCGCTAAGGCT3'
R1M12	5'AGCCTTAGCGAACTCATCGATCTGTTTAATAGCACCAGCATCGATCACGATGTGCAATGC3'	5'GCATTGCACATCGTGATCGATGCTGGTGCTATTAAACAGATCGATGAGTTCGCTAAGGCT3'
R1M13	5'AGCCTTAGCGAACTCATCGATCTGTTTAATAGCACCAGCATCAACCACGATGTGCAATGCGTGGTT3'	5'AACCACGCATTGCACATCGTGGTTGATGCTGGTGCTATTAAACAGATCGATGAGTTCGCTAAGGCT3'

Tabla 3. **Oligonucleótidos utilizados para construir las mutantes aditivas de la región 4 en la quimera TcTIM4**

Mutante	Fw primer	Rv primer
R4M1	5'GGTCACTCCGAGCGCCGCGCGTACTACGGCGAAACGAACGAAATCGTT3'	5'AACGATTTCGTTCGTTTCGCCGTAGTACGCGCGGCGCTCGGAGTGACC3'
R4M2	5'TCCGAGCGCCGCGCGTACTACGGCGAAACGAACGAAATCGTTGCGGATAAGGTGGCGCAGGCC3'	5'GGCCTGCGCCACCTTATCCGCAACGATTTCGTTCGTTTCGCCGTAGTACGCGCGGCGCTCGGA3'
R4M3	5'GAAACGAACGAAATCGTTGCGGATAAGGTGGCGGCGGCCTGCGCTGCC3'	5'GGCAGCGCAGGCCGCCGCCACCTTATCCGCAACGATTTCGTTCGTTTC3'
R4M4	5'AACGAAATCGTTGCGGATAAGGTGGCGGCGGCCGTGGCTGCCGGCTTCATGGT3'	5'ACCATGAAGCCGGCAGCCACGGCCGCCGCCACCTTATCCGCAACGATTTCGTT3'
R4M5	5'GCGGATAAGGTGGCGGCGGCCGTGGCTAGCGGCTTCATGGTTATTGCTTGCATC3'	5'GATGCAAGCAATAACCATGAAGCCGCTAGCCACGGCCGCCGCCACCTTATCCGC3'

Tabla 4. **Oligonucleótidos utilizados para construir las mutantes sitio-dirigidas de las regiones 1 y 4 en la secuencia de TcTIM**

Mutante	Fw primer	Rv primer
TcTIM: E26D, T27L, L28F, A30S, T32S, L100A, Q115A	5'CTGTTTAATAGCGCGAGCTTTGATCACGATGTGCAATGCGTG3'	5'CACGCATTGCACATCGTGATCAAAGCTCGCGCTATTAAACAG3'
TcTIM: E26D, T27L, L28F, A30S, T32S, L100A	5'CTGTTTAATAGCGCGAGCTTTGATCACGATGTGCAATGCGTG3'	5'CACGCATTGCACATCGTGATCAAAGCTCGCGCTATTAAACAG3'
TcTIM: E26D, T27L, L28F, A30S, L100A, Q115A	5'TTGCTTGTACCACTCATCGATCTGTTTAATAGCGCGACTTTTGATCAC3'	5'GTGATCAAAAGTCGCGCTATTAAACAGATCGATGAGTGGTACAAGCAA3'
TcTIM: E26D, T27L, L28F, A30S, L100A	5'TTGCTTGTACCACTCATCGATCTGTTTAATAGCGCGACTTTTGATCAC3'	5'GTGATCAAAAGTCGCGCTATTAAACAGATCGATGAGTGGTACAAGCAA3'
TcTIM: E26D, T27L, L28F, L100A, Q115A	5'TTGCTTGTACCACTCATCGATCTGTTTAATGCAGCGACTTTTGAT3'	5'ATCAAAAGTCGCTGCATTAAACAGATCGATGAGTGGTACAAGCAA3'
TcTIM: E26D, T27L, L28F, L100A	5'TTGCTTGTACCACTCATCGATCTGTTTAATGCAGCGACTTTTGAT3'	5'ATCAAAAGTCGCTGCATTAAACAGATCGATGAGTGGTACAAGCAA3'
TcTIM: T27L, L28F, L100A, Q115A	5'CTTGTACCACTCATCGAACTGTTTAATGCAGCGACT3'	5'AGTCGCTGCATTAAACAGTTCGATGAGTGGTACAAG3'
TcTIM: E26D, L28F, L100A, Q115A	5'CTTGTACCACTCATCGATACCTTTAATGCAGCGACT3'	5'AGTCGCTGCATTAAAGGTATCGATGAGTGGTACAAG3'
TcTIM: E26D, T27L, L100A, Q115A	5'CTTGTACCACTCATCGATCTGCTGAATGCAGCGACT3'	5'AGTCGCTGCATTCAGCAGATCGATGAGTGGTACAAG3'
TcTIM: T27L, L28F, L100A	5'GCGGAAAAGGTGGCGCAGGCCTGCGCTGCCGGC3'	5'GCCGGCAGCGCAGGCCTGCGCCACCTTTTCCGC3'
TcTIM: L28F, L100A, Q115A	5'GTACCACTCATCGAGACGTTTAATGCAGCGACTTTTGAT3'	5'ATCAAAAGTCGCTGCATTAAACGTCTCGATGAGTGGTAC3'
TcTIM: T27L, L100A, Q115A	5'CCACTCATCGAGCTGCTCAATGCAGCGACTTTT3'	5'AAAAGTCGCTGCATTGAGCAGCTCGATGAGTGG3'
TcTIM: L28F, Q115A	5'CCACTCATCGAGACGTTTAATGCAGCGACTTTT3'	5'AAAAGTCGCTGCATTAAACGTCTCGATGAGTGG3'
TcTIM: L28F, L100A	5'CGTTTCGCCGTAGTACGCACGCCGTTCCGA3'	5'TCGGAACGGCGTGCGTACTACGGCGAAACG3'
TcTIM: L100A, Q115A	5'GTTGCGGAAAAGGTGGCGGCGGCCTGCGCTGCCGGCTTC3'	5'GAAGCCGGCAGCGCAGGCCGCCGCCACCTTTTCCGCAAC3'
TcTIM: L28F	5'CCACTCATCGAGACGTTTAATGCAGCGACTTTT3'	5'AAAAGTCGCTGCATTAAACGTCTCGATGAGTGG3'
TcTIM: L100A	5'CGTTTCGCCGTAGTACGCACGCCGTTCCGA3'	5'TCGGAACGGCGTGCGTACTACGGCGAAACG3'
TcTIM: Q115A	5'GTTGCGGAAAAGGTGGCGGCGGCCTGCGCTGCCGGCTTC3'	5'GAAGCCGGCAGCGCAGGCCGCCGCCACCTTTTCCGCAAC3'

Tabla 5. **Oligonucleótidos utilizados para construir las mutantes sitio-dirigidas en la secuencia de TbTIM**

Mutante	Fw primer	Rv primer
TbTIM: F28L, A100L, A115Q	5'CACTCCGAGCGCCGCCTGTACTATGGTGAGACA3'	5'TGTCTCACCATAGTACAGGCGGCGCTCGGAGTG3'
TbTIM: A100L, A115Q	5'GCGGACAAGGTTGCCCAGGCCGTTGCTTCTGGT3'	5'ACCAGAAGCAACGGCCTGGGCAACCTTGTCCGC3'
TbTIM: F28L, A115Q	5'GCGGACAAGGTTGCCCAGGCCGTTGCTTCTGGT3'	5'ACCAGAAGCAACGGCCTGGGCAACCTTGTCCGC3'
TbTIM: F28L, A100L	5'CACTCCGAGCGCCGCCTGTACTATGGTGAGACA3'	5'TGTCTCACCATAGTACAGGCGGCGCTCGGAGTG3'
TbTIM: A115Q	5'GCGGACAAGGTTGCCCAGGCCGTTGCTTCTGGT3'	5'ACCAGAAGCAACGGCCTGGGCAACCTTGTCCGC3'
TbTIM: A100L	5'CACTCCGAGCGCCGCCTGTACTATGGTGAGACA3'	5'TGTCTCACCATAGTACAGGCGGCGCTCGGAGTG3'
TbTIM: F28L	5'GAGCTTATTGATCTGCTGAACTCCACAAGCATC3'	5'GATGCTTGTGGAGTTCAGCAGATCAATAAGCTC3'

Tabla 6. **Secuencia de DNA usado para obtener las mutantes sitio-dirigidas de las regiones R1 y R4 en TcTIM**

Secuencia de DNA utilizada como templado	Mutante sitio-dirigida
TcTIM: L100A	TcTIM: E26D, T27L, L28F, L100A; TcTIM: E26D, T27L, L28F, A30S, L100A; TcTIM: L100A, Q115A
TcTIM: E26D, T27L, L28F, A30S, L100A	TcTIM: E26D, T27L, L28F, A30S, T32S, L100A
TcTIM: L100A, Q115A	TcTIM: E26D, T27L, L28F, A30S, L100A, Q115A; TcTIM: E26D, T27L, L28F, L100A, Q115A; TcTIM: T27L, L28F, L100A, Q115A; TcTIM: E26D, L28F, L100A, Q115A; TcTIM: E26D, T27L, L100A, Q115A; TcTIM: L28F, L100A, Q115A; TcTIM: T28L, L100A, Q115A;
TcTIM: E26D, T27L, L28F, A30S, L100A, Q115A	TcTIM: E26D, T27L, L28F, A30S, T32S, L100A, Q115A
TcTIM: T27L, L28F, L100A, Q115A	TcTIM: T27L, L28F, L100A
TcTIM: Q115A	TcTIM: L28F, Q115A
TcTIM: L28F	TcTIM: L28F, L100A
TcTIM	TcTIM: L28F TcTIM: L100A TcTIM: Q115A

Tabla 7. **Secuencia de DNA utilizado para obtener las mutantes sitio-dirigidas de las regiones R1 y R4 en TbTIM**

Secuencia de DNA utilizada como templado	Mutante sitio-dirigida
TbTIM	TbTIM: F28L TbTIM: A100L TbTIM: A115Q
TbTIM: F28L	TbTIM: F28L, A100L TbTIM: F28L, A115Q
TbTIM: A100L	TbTIM: A100L, A115Q
TbTIM: F28L, A115Q	TbTIM: F28L, A100L, A115Q

Tabla 8. **Regiones del monómero de la triosafosfato isomerasa**

Región	aminoácidos
1	1-35
2	36-60
3	61-91
4	92-119
5	120-161
6	162-206
7	207-227
8	228-250

Tabla 9. **Mutaciones sobre la quimera TbTIM4**

mutante	Región 1													%Actividad a 100uM MMTS
TcTIM	--------													0
TbTIM4														0
R1M1	E18Q													0
R1M2	E18Q	S19Q												0
R1M3	E18Q	S19Q	L20S											0
R1M4	E18Q	S19Q	L20S	V22S										0
R1M5	E18Q	S19Q	L20S	V22S	P23E									0
R1M6	E18Q	S19Q	L20S	V22S	P23E	E26D								11.01
R1M7	E18Q	S19Q	L20S	V22S	P23E	E26D	T27L							18.02
R1M8	E18Q	S19Q	L20S	V22S	P23E	E26D	T27L	L28F						72.81
R1M9	E18Q	S19Q	L20S	V22S	P23E	E26D	T27L	L28F	A30S					79.06
R1M10	E18Q	S19Q	L20S	V22S	P23E	E26D	T27L	L28F	A30S	A31T				48.68
R1M11	E18Q	S19Q	L20S	V22S	P23E	E26D	T27L	L28F	A30S	A31T	T32S			67.09
R1M12	E18Q	S19Q	L20S	V22S	P23E	E26D	T27L	L28F	A30S	A31T	T32S	F33I		74.78
R1M13	E18Q	S19Q	L20S	V22S	P23E	E26D	T27L	L28F	A30S	A31T	T32S	F33I	D34N	78.18
TbTIM	----------													79.3

Tabla 10. **Mutaciones aditivas sobre la quimera TcTIM4**

	Región 4					% Actividad residual a 100uM MMTS
TcTIM	----------					0
TcTIM4						15
R4M1	L100A					61.85
R4M2	L100A	E111D				53.53
R4M3	L100A	E111D	Q115A			78.47
R4M4	L100A	E111D	Q115A	C117V		75.11
R4M5	L100A	E111D	Q115A	C117V	A119S	60.59
TbTIM	----------					79.3

Tabla 11**. Actividades específicas de las mutantes aditivas sobre TbTIM4 comparadas con los valores de TbTIM y TcTIM**

Mutante	Actividad especifica µmol/min.mg
TcTIM	4041.8 ±1.51
TbTIM	5508.03 ±1.85
R1M1	2539.12±3.03
R1M2	3796.94±4.54
R1M3	3825.29±2.69
R1M4	3274.38±1.15
R1M5	3729.90±6.06
R1M6	4329.04±3.65
R1M7	5310.82±3.56
R1M8	3832.79±3.41
R1M9	3705.25±3.01
R1M10	4539.12±1.51
R1M11	3425.50±3.03
R1M12	4396.57±2.73
R1M13	4805.39±6.71

Mutante	Actividad especifica µmol/min.mg
TcTIM	4041.80±1.51
TbTIM	5508.03±1.85
R4M1	4659.57±1.74
R4M2	3920.36±2.36
R4M3	3789.91±1.81
R4M4	3477.16±4.54
R4M5	4226.58±1.51

Tabla 12. **Mutaciones sitio-dirigidas de las regiones 1 y 4 sobre TcTIM**

Región 1						Región 4		%Actividad residual a 100uM MMTS
TcTIM	------					------		0
Primera serie de mutantes								
TcTIM	E26D	T27L	L28F	A30S	T32S	L100A	Q115A	78.35
TcTIM	E26D	T27L	L28F	A30S		L100A	Q115A	77.05
TcTIM	E26D	T27L	L28F			L100A	Q115A	79.28
Segunda serie de mutantes								
TcTIM	E26D	T27L	L28F	A30S	T32S	L100A		41.32
TcTIM	E26D	T27L	L28F	A30S		L100A		64.65
TcTIM	E26D	T27L	L28F			L100A		49.49
Tercera serie de mutantes								
TcTIM		T27L	L28F			L100A	Q115A	92.61
TcTIM	E26D		L28F			L100A	Q115A	63.85
TcTIM	E26D	T27L				L100A	Q115A	1.06
Cuarta serie de mutantes								
TcTIM			L28F				Q115A	39.32
TcTIM			L28F			L100A	Q115A	90.96
Quinta serie de mutantes								
TcTIM			L28F					8.42
TcTIM						L100A		0.37
TcTIM							Q115A	51.29
TbTIM	------					------		79.3

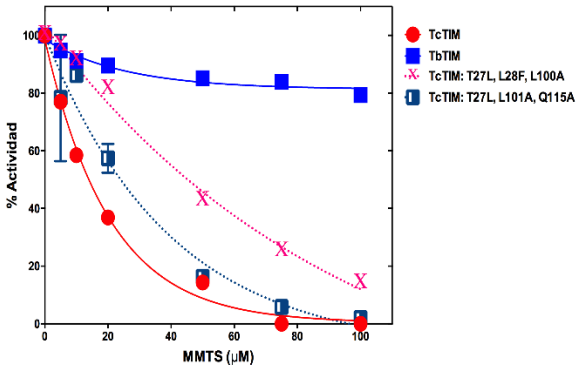

Figura 1. **Inactivación con MMTS de la mutante TcTIM: T27L, A100L, A115Q y TcTIM: T27L, L28F, A100L.** Efecto de MMTS en mutantes TcTIM: T27L, A100L, A115Q y TcTIM: T27L, L28F, A100L. Las enzimas se incubaron a 250 µg/mL con 5-100 µM de MMTS, 100 mM de trietanolamina, 10 mM de EDTA a pH 7.4 durante 2 horas a 25 °C. Trascurrido el tiempo de incubación, la actividad catalítica residual se determinó (%), incluida una muestra sin MMTS para calcular el 100% de la actividad y se graficó vs las diferentes concentraciones de MMTS. Los ensayos de MMTS para cada mutante se realizaron tres veces de forma independiente.

Tabla 13. **Mutaciones sitio-dirigidas de las regiones 1 y 4 sobre TbTIM**

	Región 1	Región 4		%Actividad residual a 100uM MMTS
TbTIM	------	------		79.3
Mutantes simples				
TbTIM	L28F			11.44
TbTIM		L100A		47.10
TbTIM			Q115A	48.40
Mutantes dobles				
TbTIM		L100A	Q115A	40.74
TbTIM	L28F	L100A		12.24
TbTIM	L28F		Q115A	13.97
Mutante triple				
TbTIM	L28F	L100A	Q115A	7.15
TcTIM	------	------		0

Tabla 14. **Parámetros cinéticos**

Enzima	Vmax	Km(mM)	k_{cat} (Min^{-1})	k_{cat}/Km ($M^{-1}S^{-1}$)
TbTIM	5666	0.1511	$3.09x10^5$	$3.4x10^7$
TcTIM	4829	0.1988	$2.72x10^5$	$2.2x10^7$
TcTIM: L28F, L100A, Q115A	5002	0.4475	$2.73x10^5$	$1.0x10^7$
TbTIM: F28L, A100L, A115Q	4692	0.6674	$2.56x10^5$	$6.0x10^6$

Referencias

1. Pearson WR. An Introduction to Sequence Similarity ("Homology") Searching. Curr Protoc Bioinforma. 2013;42: 3.1.1-3.1.8. doi:10.1002/0471250953.bi0301s42
2. Kosloff M, Kolodny R. Sequence-similar, structure-dissimilar protein pairs in the PDB. Proteins Struct Funct Bioinforma. 2008;71: 891–902. doi:10.1002/prot.21770
3. Kaczanowski S, Zielenkiewicz P. Why similar protein sequences encode similar three-dimensional structures? Theor Chem Acc. 2010;125: 643–650. doi:10.1007/s00214-009-0656-3
4. Chothia C, Lesk AM. The relation between the divergence of sequence and structure in proteins. EMBO J. 1986;5: 823–826.
5. Nagano et al. - 2002 - One Fold with Many Functions The Evolutionary Rel.pdf.
6. Goldman AD, Beatty JT, Landweber LF. The TIM Barrel Architecture Facilitated the Early Evolution of Protein-Mediated Metabolism. J Mol Evol. 2016;82: 17–26. doi:10.1007/s00239-015-9722-8
7. Wierenga RK. The TIM-barrel fold: a versatile framework for e¤cient enzymes. FEBS Lett. 2001; 6.
8. Maldonado E, Soriano-García M, Moreno A, Cabrera N, Garza-Ramos G, Tuena de Gómez-Puyou M, et al. Differences in the intersubunit contacts in triosephosphate isomerase from two closely related pathogenic trypanosomes. J Mol Biol. 1998;283: 193–203. doi:10.1006/jmbi.1998.2094
9. Wierenga RK, Kapetaniou EG, Venkatesan R. Triosephosphate isomerase: a highly evolved biocatalyst. Cell Mol Life Sci. 2010;67: 3961–3982. doi:10.1007/s00018-010-0473-9
10. Katebi AR, Jernigan RL. The critical role of the loops of triosephosphate isomerase for its oligomerization, dynamics, and functionality: Role of TIM in Catalytic Activity. Protein Sci. 2014;23: 213–228. doi:10.1002/pro.2407
11. Reyes-Vivas H, Hernández-Alcantara G, López-Velazquez G, Cabrera N, Pérez-Montfort R, Tuena de Gómez-Puyou M, et al. Factors That Control the Reactivity of the Interface Cysteine of Triosephosphate Isomerase from *Trypanosoma brucei* and *Trypanosoma cruzi* †. Biochemistry. 2001;40: 3134–3140. doi:10.1021/bi002619j
12. Zomosa-Signoret V, Hernández-Alcántara G, Reyes-Vivas H, Martínez-Martínez E, Garza-Ramos G, Pérez-Montfort R, et al. Control of the Reactivation Kinetics of Homodimeric Triosephosphate Isomerase from Unfolded Monomers †. Biochemistry. 2003;42: 3311–3318. doi:10.1021/bi0206560
13. Costas M, Rodríguez-Larrea D, De Maria L, Borchert TV, Gómez-Puyou A, Sanchez-Ruiz JM. Between-Species Variation in the Kinetic Stability of TIM Proteins Linked to Solvation-Barrier Free Energies. J Mol Biol. 2009;385: 924–937. doi:10.1016/j.jmb.2008.10.056
14. Ostoa-Saloma P, Garza-Ramos G, Ramírez J, Becker I, Berzunza M, Landa A, et al. Cloning, expression, purification and characterization of triosephosphate isomerase from Trypanosoma cruzi. Eur J Biochem. 1997;244: 700–705.
15. Garza-Ramos G, Pérez-Montfort R, Rojo-Domínguez A, de Gómez-Puyou

MT, Gómez-Puyou A. Species-specific inhibition of homologous enzymes by modification of nonconserved amino acids residues. The cysteine residues of triosephosphate isomerase. Eur J Biochem. 1996;241: 114–120.
16. Garza-Ramos G, Cabrera N, Saavedra-Lira E, Tuena de Gómez-Puyou M, Ostoa-Saloma P, Pérez-Montfort R, et al. Sulfhydryl reagent susceptibility in proteins with high sequence similarity--triosephosphate isomerase from Trypanosoma brucei, Trypanosoma cruzi and Leishmania mexicana. Eur J Biochem. 1998;253: 684–691.
17. García-Torres I, Cabrera N, Torres-Larios A, Rodríguez-Bolaños M, Díaz-Mazariegos S, Gómez-Puyou A, et al. Identification of Amino Acids that Account for Long-Range Interactions in Two Triosephosphate Isomerases from Pathogenic Trypanosomes. Wong NS, editor. PLoS ONE. 2011;6: e18791. doi:10.1371/journal.pone.0018791
18. Pérez-Montfort R, Garza-Ramos G, Alcántara GH, Reyes-Vivas H, Gao X, Maldonado E, et al. Derivatization of the Interface Cysteine of Triosephosphate Isomerase from *Trypanosoma brucei* and *Trypanosoma cruzi* as Probe of the Interrelationship between the Catalytic Sites and the Dimer Interface †. Biochemistry. 1999;38: 4114–4120. doi:10.1021/bi982425s
19. Téllez-Valencia A, Olivares-Illana V, Hernández-Santoyo A, Pérez-Montfort R, Costas M, Rodríguez-Romero A, et al. Inactivation of triosephosphate isomerase from Trypanosoma cruzi by an agent that perturbs its dimer interface. J Mol Biol. 2004;341: 1355–1365. doi:10.1016/j.jmb.2004.06.056
20. Hernández-Alcántara G, Garza-Ramos G, Hernández GM, Gómez-Puyou A, Pérez-Montfort R. Catalysis and stability of triosephosphate isomerase from Trypanosoma brucei with different residues at position 14 of the dimer interface. Characterization of a catalytically competent monomeric enzyme. Biochemistry. 2002;41: 4230–4238.
21. Wierenga RK, Noble ME, Vriend G, Nauche S, Hol WG. Refined 1.83 A structure of trypanosomal triosephosphate isomerase crystallized in the presence of 2.4 M-ammonium sulphate. A comparison with the structure of the trypanosomal triosephosphate isomerase-glycerol-3-phosphate complex. J Mol Biol. 1991;220: 995–1015.
22. Garza-Ramos G, Tuena de Gómez-Puyou M, Gómez-Puyou A, Gracy RW. Dimerization and reactivation of triosephosphate isomerase in reverse micelles. Eur J Biochem. 1992;208: 389–395.
23. Casal JI, Ahern TJ, Davenport RC, Petsko GA, Klibanov AM. Subunit interface of triosephosphate isomerase: site-directed mutagenesis and characterization of the altered enzyme. Biochemistry. 1987;26: 1258–1264.
24. Zabori S, Rudolph R, Jaenicke R. Folding and association of triose phosphate isomerase from rabbit muscle. Z Naturforsch [C]. 1980;35: 999–1004.
25. García Torres, Itzhel. Produccion y caracterizacion de una triosafosfato isomerasa de Trypanosoma brucei con la interfase de la triosafosfato isomerasa de Trypanosoma cruzi. TESIUNAM; 2006.
26. Borchert TV, Abagyan R, Jaenicke R, Wierenga RK. Design, creation, and characterization of a stable, monomeric triosephosphate isomerase. Proc Natl Acad Sci. 1994;91: 1515–1518. doi:10.1073/pnas.91.4.1515
27. Olivares-Illana V, Rodríguez-Romero A, Becker I, Berzunza M, García J,

Pérez-Montfort R, et al. Perturbation of the Dimer Interface of Triosephosphate Isomerase and its Effect on Trypanosoma cruzi. Dalton J, editor. PLoS Negl Trop Dis. 2007;1: e1. doi:10.1371/journal.pntd.0000001

28. Gómez-Puyou A, Saavedra-Lira E, Becker I, Zubillaga RA, Rojo-Domlnguez A, Perez-Montfort R. Using evolutionary changes to achieve species-specific inhibition of enzyme action — studies with triosephosphate isomerase. Chem Biol. 1995;2: 847–855. doi:10.1016/1074-5521(95)90091-8

PLOS ONE

RESEARCH ARTICLE

Three unrelated and unexpected amino acids determine the susceptibility of the interface cysteine to a sulfhydryl reagent in the triosephosphate isomerases of two trypanosomes

Selma Díaz-Mazariegos, Nallely Cabrera, Ruy Perez-Montfort*

Departamento de Bioquímica y Biología Estructural, Instituto de Fisiología Celular, Universidad Nacional Autónoma de México, Ciudad de México, México

* ruy@ifc.unam.mx

Check for updates

OPEN ACCESS

Citation: Díaz-Mazariegos S, Cabrera N, Perez-Montfort R (2018) Three unrelated and unexpected amino acids determine the susceptibility of the interface cysteine to a sulfhydryl reagent in the triosephosphate isomerases of two trypanosomes. PLoS ONE 13(1): e0189525. https://doi.org/10.1371/journal.pone.0189525

Editor: Claudio M. Soares, Universidade Nova de Lisboa Instituto de Tecnologia Quimica e Biologica, PORTUGAL

Received: August 27, 2017

Accepted: November 27, 2017

Published: January 17, 2018

Copyright: © 2018 Díaz-Mazariegos et al. This is an open access article distributed under the terms of the Creative Commons Attribution License, which permits unrestricted use, distribution, and reproduction in any medium, provided the original author and source are credited.

Data Availability Statement: All relevant data are within the paper and its Supporting Information files.

Funding: This work was supported by grant no. 254694 from the Consejo Nacional de Ciencia y Tecnologia and grant no. IN206816 from the Direccion General de Asuntos del Personal Academico Universidad Nacional Autonoma de Mexico (to RP-M). SD-M was the recipient of a

Abstract

Proteins with great sequence similarity usually have similar structure, function and other physicochemical properties. But in many cases, one or more of the physicochemical or functional characteristics differ, sometimes very considerably, among these homologous proteins. To better understand how critical amino acids determine quantitative properties of function in proteins, the responsible residues must be located and identified. This can be difficult to achieve, particularly in cases where multiple amino acids are involved. In this work, two triosephosphate isomerases with very high similarity from two related human parasites were used to address one such problem. We demonstrate that a seventy-fold difference in the reactivity of an interface cysteine to the sulfhydryl reagent methylmethane sulfonate in these two enzymes depends on three amino acids located far away from this critical residue and which could not have been predicted using other current methods. Starting from previous observations with chimeric proteins involving these two triosephosphate isomerases, we developed a strategy involving additive mutant enzymes and selected site directed mutants to locate and identify the three amino acids. These three residues seem to induce changes in the interface cysteine in reactivity by increasing (or decreasing) its apparent pKa. Some enzymes with four to seven mutations also exhibited altered reactivity. This study completes a strategy for identifying key residues in the sequences of proteins that can have applications in future protein structure-function studies.

Introduction

Sequence similarity searching is the most common method to identify homologous sequences. It is generally assumed that proteins with similar sequences will usually be homologous (share a common ancestry) and also have a similar function [1]. This is particularly so when the sequence identity is very high [2–4]. One would expect two nearly identical enzyme sequences

fellowship from CONACyT (no. 263707). The funders had no role in study design, data collection and analysis, decision to publish, or preparation of the manuscript.

Competing interests: The authors have declared that no competing interests exist.

to be very similar in their three dimensional structures, their catalytic functions and also in their physicochemical characteristics, as well as their susceptibility to chemical and physical inactivating agents. Yet, although in general terms this is true in many cases, very frequently there also exist great differences in the magnitude of the efficiency of the function, the stability of the proteins to physical and chemical denaturants, or in their susceptibility to different types of inactivating agents. These can vary in ranges of orders of magnitude, thus permitting, with the appropriate manipulation, the transformation of specific properties of the proteins within the bounds of these differences and perhaps, sometimes, extending them to greater extremes. An example of this phenomenon are the triosephosphate isomerases (TIMs) from *Trypanosoma brucei* and *T*. *cruzi*. These TIMs have 73.9% identity and a sequence similarity of 92.4%. As expected, their three-dimensional structures superimpose with an RMSD of 0.96 Å and both have an identical catalytic site in each monomer formed by residues K13, H95 and E167 (based on the numbering for the sequence of TIM from *T*. *brucei* (TbTIM) which will be used throughout this article). TIM is the prototype of the $(\beta/\alpha)_8$ barrel fold family of proteins and is active only as a homodimer. However, these extremely similar proteins have some outstanding differences in several functional properties and their behavior to physico-chemical agents and inactivating molecules. For example, their velocity and extent of reactivation from guanidine chloride unfolded monomers [5,6], their susceptibility to digestion with subtilisin [7], and quantitative differences in their susceptibility to several low molecular weight agents [8], and in particular to sulfhydryl reagents [9–13].

A question that arises from observing these large differences is: which amino acid(s) in the sequence is (are) responsible for fine-tuning these differences in behavior?

Some time ago, we started developing a strategy that would help us find an answer to this question. In the work of Garcia-Torres et al. [14] we divided the sequence of TIM into eight interchangeable modular regions. We then progressively grafted different portions of TIM from one trypanosome (*T*. *brucei*) (TbTIM) into the equivalent region of the TIM of the other trypanosome (*T*. *cruzi*) (TcTIM), with the different trait. Following this procedure, we found out which part of the enzyme participated in the expression of the feature that interested us, namely the 70-fold difference in susceptibility to inactivation of the enzymatic activity with the thiol reagent methylmethane thiosulfonate (MMTS). Here it is important to point out that previous work has established that the reaction of MMTS with both enzymes is the unique interface cysteine (Cys) which is in position 14 or 15 of the sequences of TbTIM and TcTIM, respectively [9–13,15–17]. We found that the change in susceptibility to MMTS was due to two regions (regions 1 and 4) of the enzyme that are not in contact with the interface cysteines, which react initially with the thiol reagent, destabilizing and monomerizing the homo-oligomeric protein and causing its inactivation. These two regions are not connected to each other, neither in their primary or tertiary structure. Comparing the sequences of TbTIM and TcTIM, region 1 has thirteen different residues and region 4 has five different residues, respectively. Our conclusion in that work was that, of a total of sixty-five differences between the sequences of the two trypanosomes, we could assign the high or low susceptibility to inactivation in the presence of MMTS to the eighteen different amino acids located in regions 1 and 4. But at that time, the question remained if those eighteen residues were all necessary to produce TbTIM-like or TcTIM-like behaviors.

This work answers the question by refining the strategy, introducing first "additive mutations" [6] and then multiple site directed mutagenesis of the wild type (WT) TIMs.

Our whole general approach to find the key amino acids is ordered and systematic. It initially involves progressive grafting of different large portions of one of these two proteins to an equivalent region of the other protein. This allows the identification of the region, or regions, that contribute to the quantitative differences under investigation. Once these have been

established the participation of all the different amino acids contained in the region, or regions responsible for the difference, is explored by "additive" mutants. As in the initial identification of regions with chimeric enzymes, only the residues identified by "additive" mutagenesis that have a positive effect are taken into account. Finally, systematic site-directed mutagenesis of the identified amino acids reveals their role in the occurrence, control and extent of the differences in the behavior that is being studied. Although our scheme involves the testing and analysis of numerous mutant enzymes, we prefer it to random mutagenesis approaches. With this procedure, a comparatively small and limited number of enzymes are monitored by direct experimental results and no other considerations need to be taken into account.

It is important to point out, that this same strategy has also worked in identifying the residues which are responsible for the differences in reactivation velocity and efficiency of TbTIM and TcTIM [6], thus broadening the scope of its application.

Results

The amino acids in regions 1 and 4 of TbTIM confer resistance to the inactivation of chimeric enzyme TbTIM 1, 4; TcTIM 2–3, 5–8, using the sulfhydryl reagent MMTS

In our previous work, we showed that the chimeric enzyme TbTIM 1, 4; TcTIM 2–3, 5–8, which has a sequence containing 92.8% of the amino acids of WT TcTIM, has an inactivation profile that is comparable, and even slightly more resistant, than WT TbTIM when exposed to the sulfhydryl reagent MMTS [14]. This implies that within the 18 amino acids that are different in these two regions, either all, or a subset of them, account for the differences in the susceptibility to MMTS in TcTIM and TbTIM. What is clear from that work is that one or more amino acids from both regions 1 and 4 are necessary to change the behavior of the enzymes to inactivation by MMTS.

The strategy we devised to find out which, and how many, amino acids are involved conferring MMTS-susceptibility to these enzymes, consisted in constructing additive mutants from previously reported chimeric proteins (see Materials and Methods) and also site-directed mutagenesis of selected amino acids from regions 1 and 4 in enzymes with the sequences of WT TbTIM and WT TcTIM, respectively.

The sequences of WT TbTIM and WT TcTIM have 13 differences in region 1 and 5 differences in region 4 (Fig 1).

Susceptibility to inactivation with MMTS of the additive mutants of region 1

To identify which amino acids in region 1 are important in determining the susceptibility of TbTIM and TcTIM to inactivation by MMTS, chimeric enzyme TbTIM 4; TcTIM 1–3, 5–8 was chosen as the starting point, since this protein inactivates almost like WT TcTIM (see Fig 2C in [14] and Fig 2A), and an increase in resistance to inactivation was to be expected. In the inactivation curves of the thirteen additive mutants of region 1 (Fig 2) we observed that the amino acids in positions 18, 19, 20, 22 and 23 (which are Q, Q, S, S and E in the sequence of TbTIM, and include additive mutants R1M1, R1M2, R1M3, R1M4 and R1M5, respectively) have practically no effect on the inactivation pattern of chimeric enzyme TbTIM 4; TcTIM 1–3, 5–8 (see Fig 2A).

When additive mutant R1M6 (which has the additional mutation of E26D) was tested, the resistance to inactivation to 100 μM MMTS was increased to 11% and the form of the curve showed increased resistance to inactivation in all other concentrations of MMTS studied (Fig

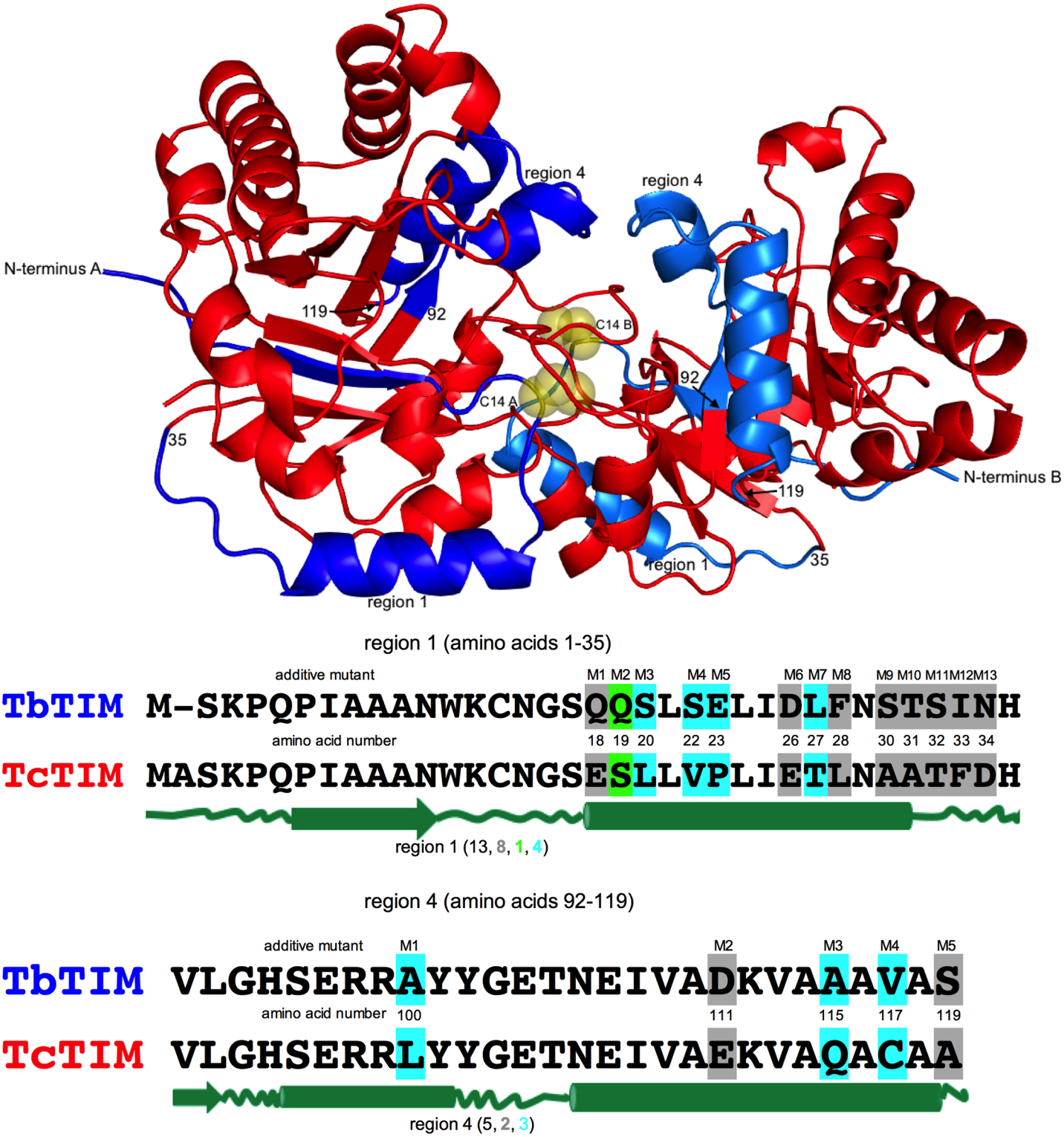

Fig 1. Location of regions 1 and 4 in a ribbon diagram of the structure of WT TbTIM and aligned sequences of regions 1 and 4 of WT TbTIM and WT TcTIM. The ribbon diagram of the structure of 5TIM in the PDB database, corresponding to a dimer of WT TbTIM, is shown in red. Regions 1 and 4 are shown in blue and marine blue for monomers A and B, respectively. The n-terminus of each monomer and the position of amino acids 35, 92 and 119 are indicated by the corresponding text or number, sometimes using an arrow, on the diagram. The interface cysteines of both monomers are shown as yellow spheres. In the alignments, the differences in the amino acids are highlighted as conservative (similar size and polarity) in grey, semiconservative (similar polarity) in green, and without similarity in cyan. Secondary structure elements are shown below as dark green lines (loops), arrows (beta sheets) and barrels (alpha helixes).

https://doi.org/10.1371/journal.pone.0189525.g001

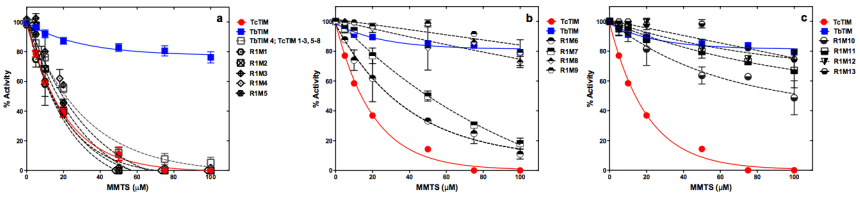

Fig 2. Effect of MMTS on WT TbTIM, WT TcTIM and on different additive mutants of region 1. Enzymes were incubated at a concentration of 250 μg/mL in 100 mM TEA, 10 mM EDTA pH 7.4 and 5–100 μM MMTS for 2 h at 25˚C. At that time, the activity of the samples was determined, including a sample without MMTS to calculate the percentage of remaining activity. Panel a) effect of MMTS on WT TcTIM, WT TbTIM and R1M1, R1M2, R1M3, R1M4, R1M5 and TbTIM 4; TcTIM 1–3, 5–8. Panel b) effect of MMTS on WT TcTIM, WT TbTIM and R1M6, R1M7, R1M8 and R1M9. Panel c) effect of MMTS on WT TcTIM, WT TbTIM and R1M10, R1M11, R1M12 and R1M13. Assays were performed independently three times.

https://doi.org/10.1371/journal.pone.0189525.g002

2B). Additive mutant R1M7, which introduces mutation T27L, yields an enzyme that is somewhat more resistant than the preceding one (Fig 2B). At this point, the importance of the amino acids in positions 26 and 27 is not apparent yet, but it will be made clear in the section of further analysis of site-directed mutagenesis of selected amino acids from regions 1 and 4 in enzymes with the sequences of WT TbTIM and WT TcTIM.

The importance of the amino acid in position 28 was immediately evident observing the behavior of additive mutant R1M8 (with mutation L28F), since this enzyme resists inactivation with 100 μM MMTS, resembling WT TbTIM with an activity of 72.8% (Fig 2B). The effect of the substitution of a L for a F and of a F for a L in position 28 of the sequence of TcTIM and TbTIM, respectively, will also be described in the section of further analysis of site-directed mutagenesis of selected amino acids from regions 1 and 4 in enzymes with the sequences of WT TbTIM and WT TcTIM.

Additive mutant R1M9 (A30S) did not show any significant change of behavior, with respect to the previous additive mutant (Fig 2B), and additive mutant R1M10 (A31T) even increased the susceptibility of the resulting enzyme to inactivation with MMTS (decreasing the activity to 48% in the presence of 100 μM MMTS) (Fig 2C).

Here it is important to point out that additive mutations could produce positive, negative or neutral effects on the susceptibility pattern, when compared with the additive mutant that preceded it. As will become clear further on for the development of our strategy, we only chose to consider and use the mutations that exhibited a positive effect in causing resistance to the inactivating effects of MMTS.

Additive mutant R1M11 with mutation T32S did show an increased resistance to inactivation with MMTS with respect to the preceding mutant (67% in the presence of 100 μM MMTS) (Fig 2C).

Finally, additive mutants R1M12 and R1M13, with mutations F33I and D34N respectively, were neutral with respect to additive mutant R1M11 and exhibited essentially the same inactivation pattern in the presence of MMTS seen for WT TbTIM (Fig 2C).

Susceptibility to inactivation with MMTS of the additive mutants of region 4

The five amino acids in region 4 were tested by using the chimeric enzyme TbTIM 1–3, 5–8; TcTIM 4 as the starting point, since this protein, which has 98% of the sequence of TbTIM, inactivates following a similar pattern to WT TcTIM (see Fig 2C in [14] and Fig 3A). So, once again, an increase in resistance to inactivation was to be expected. In the inactivation curves of the five additive mutants of region 4 (Fig 3) we observed that the amino acid in position 100

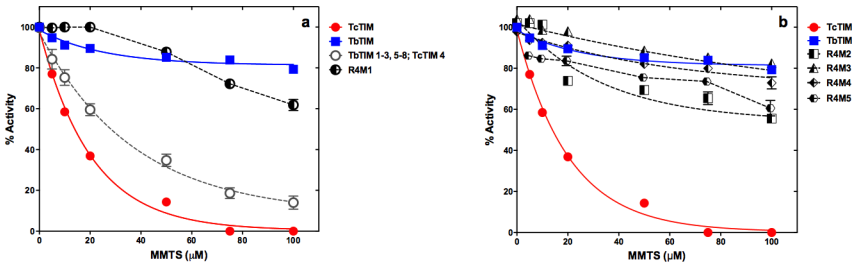

Fig 3. Effect of MMTS on WT TbTIM, WT TcTIM and on different additive mutants of region 4. Enzymes were incubated at a concentration of 250 μg/mL in 100 mM TEA, 10 mM EDTA pH 7.4 and 5–100 μM MMTS for 2 h at 25˚C. At that time, the activity of the samples was determined, including a sample without MMTS to calculate the percentage of remaining activity. Panel a) effect of MMTS on WT TcTIM, WT TbTIM, R4M1 and TbTIM 1–3, 5–8; TcTIM 4. Panel b) effect of MMTS on WT TcTIM, WT TbTIM and R4M2, R4M3, R4M4 and R4M5. Assays were performed independently three times.

https://doi.org/10.1371/journal.pone.0189525.g003

has a very important effect in conferring resistance to MMTS. This additive mutant is R4M1, which has the mutation L100A. The residual activity shown by additive mutant R4M1 at a concentration of 100 μM MMTS is 62%, which is approximately 20% lower than that of WT TbTIM under the same conditions, but, the resistance to inactivation of additive mutant R4M1 at concentrations of MMTS of 50 μM or lower is even higher than that of WT TbTIM (Fig 3A). So, it seems that the alanine at position 100 in the sequence of TbTIM has an important role in the resistance of this protein to inactivation by low concentrations of MMTS. In contrast, additive mutant R4M2 showed an increase in susceptibility to inactivation with MMTS, producing a negative effect with respect to the previous mutant (Fig 3B).

The next additive mutant R4M3, with mutation Q115A, which again introduces an alanine, had another positive effect in increasing the resistance of the enzyme to inactivation with MMTS with a pattern that is slightly more susceptible to the reagent than WT TbTIM at all the concentrations of MMTS studied (Fig 3B).

Additive mutation R4M4 was neutral in its effect to the preceding mutation and the last additive mutation R4M5 had a slightly negative effect, returning to a susceptibility pattern that is very similar to that of the first additive mutant R4M1 (Fig 3B).

Site directed mutagenesis of selected amino acids of regions 1 and 4 from the sequence of TbTIM onto TcTIM

Judging from our previous results with the additive mutants of regions 1 and 4, we could conclude that the amino acids that have a positive effect of conferring resistance to inactivation with MMTS are five in positions 26, 27, 28, 30 and 32, of region 1, and two in positions 100 and 115, of region 4. Thus, to produce a TcTIM with the inactivation susceptibility pattern of TbTIM, we initially constructed the site directed mutant TcTIM: E26D, T27L, L28F, A30S, T32S, L100A, Q115A. As expected, and can be seen in Fig 4A, the enzyme with seven mutations showed a similar and even slightly better resistance pattern to the inactivation with MMTS than WT TbTIM, particularly at concentrations lower than 100 μM.

Since the positive effect of mutations A30S and T32S, which corresponded to additive mutants R1M9 and R1M11, respectively, had not been too great compared with their individual previous mutants, we decided to prepare the following site directed mutants, to explore if all five amino acids of region 1 were necessary to change the susceptibility response of the first mutant that contained seven mutations. Thus, site directed mutants TcTIM: E26D, T27L, L28F, A30S, L100A, Q115A and TcTIM: E26D, T27L, L28F, L100A, Q115A were prepared and subjected to inactivation with MMTS. Fig 4A shows that both enzymes, with six and five

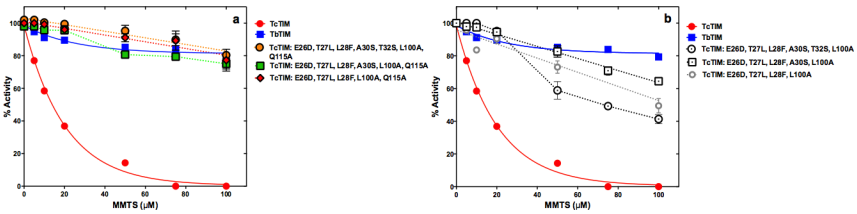

Fig 4. Effect of MMTS on WT TbTIM, WT TcTIM and on different site directed mutants of selected amino acids of regions 1 and 4 of the sequence of WT TbTIM onto WT TcTIM. Enzymes were incubated at a concentration of 250 μg/mL in 100 mM TEA, 10 mM EDTA pH 7.4 and 5–100 μM MMTS for 2 h at 25˚C. At that time, the activity of the samples was determined, including a sample without MMTS to calculate the percentage of remaining activity. Panel a) effect of MMTS on WT TcTIM, WT TbTIM and TcTIM: E26D, T27L, L28F, A30S, T32S, L100A, Q115A, TcTIM: E26D, T27L, L28F, A30S, L100A, Q115A and TcTIM: E26D, T27L, L28F, L100A, Q115A. Panel b) effect of MMTS on WT TcTIM, WT TbTIM and TcTIM: E26D, T27L, L28F, A30S, T32S, L100A; TcTIM: E26D, T27L, L28F, A30S, L100A and TcTIM: E26D, T27L, L28F, L100A. Assays were performed independently three times.

https://doi.org/10.1371/journal.pone.0189525.g004

mutations, still show a susceptibility pattern that is essentially the same as that of WT TbTIM. The curve of the six-fold mutant was almost completely superimposable to the curve of WT TbTIM, while the curve of the five-fold mutant was superimposable to the seven-fold mutant, again, with a slightly increased resistance pattern at low concentrations of the sulfhydryl reagent.

Once it was established that two mutations in region 1 with relatively small positive effects on the susceptibility pattern could be omitted and the resulting enzyme still shows a behavior like that of WT TbTIM being inactivated with MMTS, we turned our attention to the residue in position 115 of region 4. This was because the change of Q for A in additive mutant R4M3 had been positive but not as great as that for the change of L for A in additive mutant R4M1.

Nevertheless, we decided to produce three site directed mutants with six, five and four mutations, deliberately omitting to change the amino acid in position 115.

These site directed mutants were: TcTIM: E26D, T27L, L28F, A30S, T32S, L100A; TcTIM: E26D, T27L, L28F, A30S, L100A and TcTIM: E26D, T27L, L28F, L100A, respectively.

As can be seen in Fig 4B, all these mutant enzymes were more susceptible than WT TbTIM to inactivation by MMTS, particularly at concentrations of 50 μM and above. There was no evident correlation between the number of mutants and the shape of the inactivation curve. Thus, the alanine in position 115 of the sequence of TbTIM was important for the resistance to inactivation by higher concentrations of MMTS.

Further analysis

Starting from the five-fold mutant TcTIM: E26D, T27L, L28F, L100A, Q115A, with the susceptibility pattern comparable to WT TbTIM, we decided to establish if we could further reduce the number of changes in the sequence of TcTIM, and still retain the behavior with increased resistance to inactivation by MMTS. Knowing the importance of an alanine in position 115 of region 4 to achieve TbTIM-like resistance at higher concentrations of MMTS, this residue was always included in subsequent experiments. We therefore prepared three site directed mutants with four mutations which were: TcTIM: T27L, L28F, L100A, Q115A; TcTIM: E26D, L28F, L100A, Q115A and TcTIM: E26D, T27L, L100A, Q115A.

The inactivation curves at different concentrations of MMTS can be seen in Fig 5A. From the results, it is evident that the amino acid in position 28 is fundamental in determining the inactivation profile of the corresponding site directed mutant enzyme. A phenylalanine will give an enzyme that resists inactivation in a manner similar to WT TbTIM, and a leucine will increase susceptibility to the levels of WT TcTIM.

To explore the influence of residues in positions 26 and 27, a triple site directed mutant was prepared: TcTIM: L28F, L100A, Q115A. The inactivation curve, seen in Fig 5B, shows a profile that indicates more resistance of the mutant enzyme to inactivation with all concentrations of MMTS than WT TbTIM.

So, we now had a mutant of TcTIM with 98.8% of its sequence, which had an inactivation profile like that of TbTIM. The only amino acid, whose role had not been tested, was that in position 100 of region 4. Consequently, we produced double site directed mutant TcTIM: L28F, Q115A. As can be seen in Fig 5B the inactivation curve of this mutant shows an intermediate behavior between WT TbTIM and WT TcTIM.

These experiments suggested that a minimum of three mutations, one in region 1 and two in region 4, are sufficient and necessary to change the inactivation profile of WT TcTIM to that of WT TbTIM.

Confirmation with site directed mutants of TbTIM

Complete or partial confirmation of the results shown previously could be obtained if site directed mutants of WT TbTIM in residues in positions 28, 100 and 115 showed and increased susceptibility to inactivation by MMTS, resembling, or equal to, that of WT TcTIM. Thus, the site directed mutant TbTIM: F28L, A100L, A115Q was prepared and tested. The corresponding results can be seen in Fig 6A where the mutant, with 98.8% of the sequence of WT TbTIM, exhibited an inactivation pattern that resembles that of WT TcTIM, being just as susceptible at concentrations of MMTS of 10 μM or lower and slightly more resistant at concentrations above 20 μM.

The contribution of the individual or the three combinations of pairs of mutated amino acids was also investigated. As can be seen in Fig 6B and 6C the observation made previously with TcTIM that the phenylalanine in position 28 is fundamental to confer resistance to inactivation with MMTS is confirmed in the single and double site directed mutants of TbTIM.

Thus, our results show that the inactivation profiles of WT TbTIM and WT TcTIM depend mainly on three residues: one located in position 28 (of region 1) and two located in positions 100 and 115 (of region 4), completely confirming our previous results with the chimeric enzyme TbTIM 1, 4; TcTIM 2–3, 5–8 [14].

The pKa of the interface Cys14 is regulated by amino acid in position 28 of region 1 and amino acids in positions 100 and 115 of region 4

Although the mechanism by which the difference in susceptibility to inactivation with MMTS occurs is not clear, we have previously reported that the reactivity of the interface Cys14 in

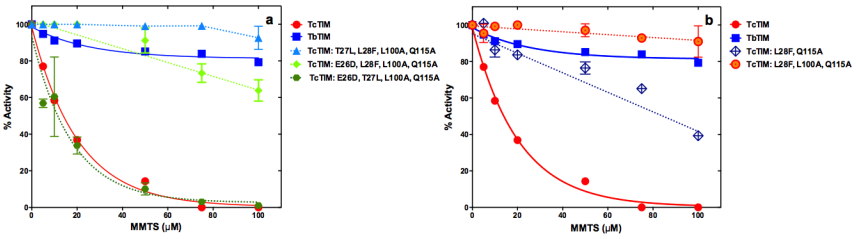

Fig 5. Effect of MMTS on WT TbTIM, WT TcTIM and on different site directed mutants of selected amino acids of regions 1 and 4 of the sequence of WT TbTIM onto WT TcTIM. Enzymes were incubated at a concentration of 250 μg/mL in 100 mM TEA, 10 mM EDTA pH 7.4 and 5–100 μM MMTS for 2 h at 25˚C. At that time, the activity of the samples was determined, including a sample without MMTS to calculate the percentage of remaining activity. Panel a) effect of MMTS on WT TcTIM, WT TbTIM and TcTIM: T27L, L28F, L100A, Q115A; TcTIM: E26D, L28F, L100A, Q115A and TcTIM: E26D, T27L, L100A, Q115A. Panel b) effect of MMTS on WT TcTIM, WT TbTIM, TcTIM: L28F, L100A, Q115A and TcTIM: L28F, Q115A. Assays were performed independently three times.

https://doi.org/10.1371/journal.pone.0189525.g005

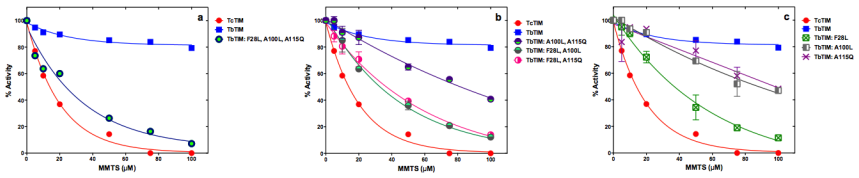

Fig 6. Effect of MMTS on WT TbTIM, WT TcTIM and on different site directed mutants of selected amino acids of regions 1 and 4 on the sequence of WT TbTIM. Enzymes were incubated at a concentration of 250 μg/mL in 100 mM TEA, 10 mM EDTA pH 7.4 and 5–100 μM MMTS for 2 h at 25˚C. At that time, the activity of the samples was determined, including a sample without MMTS to calculate the percentage of remaining activity. Panel a) effect of MMTS on WT TcTIM, WT TbTIM and TbTIM: F28L, A100L, A115Q. Panel b) effect of MMTS on WT TcTIM, WT TbTIM and TbTIM: A100L, A115Q, TbTIM: F28L, A100L and TbTIM: F28L, A115Q. Panel c) effect of MMTS on WT TcTIM, WT TbTIM and TbTIM: F28L, TbTIM: A100L and TbTIM: A115Q. Assays were performed independently three times.

https://doi.org/10.1371/journal.pone.0189525.g006

TbTIM and TcTIM depends on the pKa of its thiol group [18]. In our most recent determination it was 10.53 for WT TbTIM and 9.27 for WT TcTIM [14]. Table 1 shows that the thiol group of Cys14 of the triple site directed mutant TcTIM: L28F, L100A, Q115A has a very similar pKa to that of WT TbTIM (10.69) and that the pKa of Cys14 of triple mutant TbTIM: F28L, A100L, A115Q is very similar to that of WT TcTIM (9.23).

Based on these results, the predicted ratio of protonated/deprotonated sulfhydryl groups at pH 7.4 are 1445, 69, 1950, and 67.6 for WT TbTIM, WT TcTIM, TcTIM: L28F, L100A, Q115A and TbTIM: F28L, A100L, A115Q, respectively. It can be calculated that there are over 20 times more predicted protonated sulfhydryl groups in the proteins with a Cys with low reactivity to MMTS than in the more susceptible ones. Thus, part of the explanation for a greater susceptibility of Cys 14 in WT TcTIM and TbTIM: F28L, A100L, A115Q is due to this higher ratio because the reactivity of MMTS with the protonated thiol group is immensely lower than with the thiolate anion [19].

Discussion

Our work shows that it is possible to systematically identify the amino acids in a sequence that are responsible for a given property of a protein. Here, we have extended and refined our experimental method of using the same protein from two evolutionarily closely related organisms to identify the regions relevant for a given function [14]. Like our initial approach, the new method again cannot, and does not predict, which mutations would affect the catalytic properties and the susceptibility of the interface Cys to MMTS. It is not biased by structural, evolutionary or hypothetical considerations of the possible, or theoretical, importance of certain amino acids for the function, stability or other properties of the protein, but gives the answer directly from the experimental results.

We think there are several noteworthy insights to be learned from our results. As can be seen in S1 Table (in the supplementary material) basically all chimeric proteins, additive mutants, and site directed mutants had catalytic properties that are comparable to those of the

Table 1. pKa values of Cys 14/15 in WT TbTIM and WT TcTIM and some mutant enzymes.

Enzyme or mutant	pKa of Cys14
WT TbTIM	10.56 ± 0.22
WT TcTIM	9.24 ± 0.04
TcTIM: L28F, L100A, Q115A	10.69 ± 0.01
TbTIM: F28L, A100L, A115Q	9.23 ± 0.03

https://doi.org/10.1371/journal.pone.0189525.t001

WT enzymes. As already pointed out previously, this is an expected result since, although of the three catalytic amino acids, K13 is in region 1 and H95 is in region 4, the mutations did not affect their properties nor those of other residues that are important for their function. E167 is in region 6, which is far removed from the regions where the mutations were made, thus, no influence of this residue was expected.

From our previous work, we already anticipated that the properties of the interface Cys would not change gradually or continuously, but would respond in a more discontinuous manner. This turned out to be the case. But the answer to the question of the minimum number of residues involved in MMTS susceptibility yielded an interesting answer. On the one hand, our results clearly suggest that a minimum of three residues (in position 28 of region 1 and positions 100 and 115 of region 4) are necessary for a WT TcTIM to change its susceptibility to MMTS inactivation to one like WT TbTIM (Fig 5B), and that these same residues will change the susceptibility of WT TbTIM almost to that of a TcTIM (Fig 6A). Thus, these are the crucial residues, because no double or single mutant can change completely the susceptibility pattern (Fig 6B and 6C). On the other hand, our results also show that other fourfold, fivefold, sixfold and sevenfold mutants of WT TcTIM (Figs 4A and 5A) also have the decreased susceptibility to MMTS shown by WT TbTIM. What is the significance of this?

Random mutagenesis methods usually rely on (rapidly) finding one protein, which shows the altered function or stability characteristics, and then analyze the mutated amino acid or amino acids that produced the change, and, if possible, what the reasons were for it. But, this might be just one of multiple possible mutants that have the altered behavior. In this case these would be mutants TcTIM: E26D, T27L, L28F, A30S, T32S, L100A, Q115A; TcTIM: E26D, T27L, L28F, A30S, L100A, Q115A; TcTIM: E26D, T27L, L28F, L100A, Q115A; TcTIM: T27L, L28F, L100A, Q115A and TcTIM: L28F, L100A, Q115A. Depending on whether it is the minimal number of changes, or some larger number, which still produces the differences, the validation that one has the minimum of mutations to produce the altered behavior will be different. In any case, a systematic approach like the one shown in this work, should be useful to prove and understand that, in many cases, the change in behavior is not due to only one mutation, and also what the importance of each individual amino acid is, when there is a synergic cooperation to produce the altered characteristics and/or a change of function in a protein.

In our opinion, to better understand the role of each amino acid for either, particular physicochemical characteristics, or the function of a protein, a systematic analysis using mutagenesis like the one described in Garcia-Torres et al. [14] and in this work, will identify all the responsible residues even if, and particularly when, they cannot be inferred or predicted by other methods of analysis of the protein.

Materials and methods

Design of the genes of different mutant enzymes

This work is a continuation of the work of García-Torres et al. [14], and thus, we used some of the chimeric proteins produced for that investigation. In that article a central conclusion was that the chimeric enzyme TbTIM 1,4;TcTIM 2,3, 5–8 (called TcTIM 2,3, 5–8 in that publication) had an equal or slightly less pronounced susceptibility pattern to inactivation with MMTS than WT TbTIM. The sequence of TbTIM 1,4;TcTIM 2,3,5–8 has eighteen different amino acids from that of WT TcTIM.

To find out which of the thirteen different residues of region 1 or the five different residues of region 4 were involved, we designed the strategy of the "additive mutants". For the additive mutants of region 1 we started out with chimeric protein TbTIM 4;TcTIM 1–3, 5–8 as the template, and progressively mutated the first different amino acid in region 1, and then the first

and second different amino acids in region 1, and then the first, second and third, and so on, until all thirteen different amino acids were "additively" mutated. In this work, the nomenclature for the additive mutants has the form RXMX, where R is the region in which the mutation occurs and M is the number of additive mutants it contains. Therefore, mutant R1M12 has twelve mutations in region 1 and mutant R4M1 has one mutation in region 4 (see S2 Table).

Besides the additive mutants, a series of single and multiple site directed mutant enzymes were produced, to test the importance of individual or combinations of amino acids in the susceptibility or resistance to inactivation in both, the sequences of WT TbTIM and WT TcTIM to the inactivation with MMTS. For this, DNA sequences X03921 and U53867 for TbTIM and TcTIM, respectively, were used to produce all site directed mutant enzymes. From TcTIM a total of eighteen and for TbTIM a total of eight site-directed mutants were produced. Their names are as follows: the sequence on which the site directed mutant was made (either TbTIM or TcTIM) and then the original amino acid, then the position in the sequence and then the mutant amino acid. Thus, TcTIM: E26D, T27L, L28F, A30S, L100A, Q115A is a site directed mutant of WT TcTIM with four mutations in region 1 and two mutations in region 4 in positions 26, 27, 28 and 30 and 100 and 115, respectively.

The site directed mutants, the templates and the oligonucleotides used to produce them are shown in S3 Table in the Supplementary Material.

Expression and purification of the proteins

All genes were cloned into the pET- 3a expression plasmid using the *Nde*-I and *Bam*HI restriction sites. Every gene was completely sequenced and transformed into BL21(DE3)pLysS cells (Novagen, Madison WI).

Bacteria containing the plasmids with each of the genes were grown in one liter of Luria Bertani medium supplemented with 100 μg/mL ampicillin and were incubated at 37˚C. Once the cell cultures reached an A600 nm = 0.8, a final concentration of 1 mM isopropyl -b-D thiogalactopyranoside was used for induction and the bacteria were incubated 12 h more at 30˚C before harvesting them.

Harvested bacteria were centrifuged for 20 min at 6400 × *g* and resuspended in 40 ml of lysis buffer (100 mM MES, 1 mM DTT, 0.5 mM EDTA, 0.2 mM PMSF, 300 mM NaCl, pH 6.3) [20]. Each suspension was sonicated at a potency of 5 W for 5 times 40 sec with 1 min rest between each cycle. The sonicated suspensions were centrifuged at 110 660 × *g* for 40 min. The supernatant of each chimeric enzyme or mutant was diluted until the final concentration of NaCl was 20 mM and was then applied to a SP Sepharose Fast flow column that had been previously equilibrated with 50 mM MES pH 6.3. The protein was eluted using a NaCl linear gradient 50 mM MES, NaCl 0–500 mM pH 6.3. Crystalline ammonium sulfate was gradually added up to 70% (w/v) saturation at 4˚C under agitation to the fractions containing TIM. This suspension was further agitated for 12 h and then centrifuged for 20 min at 23 000 × *g*. The precipitate was resuspended into 10 ml of 100 mM triethanolamine (TEA), 10 mM EDTA, pH 7.4. Enough ammonium sulfate was added to have a final concentration of 2.2 M.

The protein was then applied to a hydrophobic interaction column of butyl toyopearl that had been previously been equilibrated with 100 mM TEA, 10 mM EDTA and 2.2 M ammonium sulfate. The protein was eluted with a linear gradient of 2.2 to 0 M of ammonium sulfate. The fractions containing TIM were pooled and concentrated. Protein concentration was determined at 280 nm, using an extinction coefficient $\varepsilon = 34\,950\ M^{-1}\ cm^{-1}$. The extinction coefficients for all the mutants were calculated from their amino acid sequence and the online program ProtParam from Expasy. Also, SDS-PAGE with 16% acrylamide gels was used as a control of the purification procedure for all mutants.

Determination of catalytic activity

Enzyme activity was measured at 25˚C following the conversion of DL-glyceraldehyde 3-phosphate (D,L-GAP) to dihydroxyacetone phosphate using a-glycerolphosphate dehydrogenase (α-GDH) as coupling enzyme [14]. The oxidation of NADH was monitored at 340 nm, and the reaction mixture had 10 mM TEA, 10 mM EDTA, 1 mM GAP, 0.2 mM NADH and 20 μg/mL α-GDH. The reaction was started by adding 5 ng/mL of the corresponding protein [21].

Calculation of the kinetic parameters

To calculate kinetic parameters, GAP concentration was varied between 0.04 and 3 mM, and the data were adjusted to the Michaelis–Menten model using non-linear regression to calculate K_m and V_{max}. The catalytic constant k_{cat} and the catalytic efficiency k_{cat}/K_m were also calculated from these data [15].

Inactivation assays with MMTS

WT enzymes, as well as all mutants, at a concentration of 250 mg/mL were incubated with concentrations of 5–100 μM of MMTS in a buffer containing 100 mM TEA, 10 mM EDTA, pH 7.4 for 2 h at 25˚C. At this time, the mixtures were diluted and an aliquot of the dilution was withdrawn to measure activity at a concentration of 5 ng/mL of reaction mixture in a Cary 60 spectrophotometer from Agilent Technologies (Santa Clara, CA, USA). The activity data are reported as percentage of residual activity, taking the activity of each corresponding enzyme in the absence of MMTS as 100% [14]. Graphs with the data were made using Prism GraphPad version 6.0. Whenever possible, the data of the graphs was adjusted using nonlinear regression. On those curves that did not adjust, lines were drawn joining the points to guide the eye.

Determination of the pKa of the interface Cys. The pKa of the interface Cys of WT TbTIM, WT Tc TIM and of site directed mutants TcTIM: L28F, L100A, Q115A; and TbTIM: F28L, A100L, A115Q, was determined as described in reference [18] with some modifications. Briefly, the enzymes were incubated for 1 min at a concentration of 250 μg/mL in 100 mM TEA and 10 mM EDTA adjusted to the desired pH (7.0, 7.4, 7.8, 8.0, 8.4, 8.8, 9.0, 9.2 and 9.5); MMTS at a concentration of 80 μM was also added. The residual catalytic activity was measured at 340 nm in the spectrophotometer as described before. The apparent pKa of the interface Cys was determined from plots of ln of percent remaining activity versus pH. The data were fitted to a model derived from the Henderson-Hasselbach equation:

$$\ln(\%\ \text{activity}) = (Y_i + Y_h \times 10^{pKa-pH})/(1 + 10^{pKa-pH})$$

where Y_i and Y_h represent the initial and final activities, respectively.

Supporting information

S1 Table. Kinetic parameters of WT TbTIM, WT Tc TIM and additive mutants and mutants obtained by site directed mutagenesis. All data shown are the means of three independent determinations.
(DOCX)

S2 Table. Strategy for the production of the additive mutants of regions 1 and 4. The amino acids highlighted in grey, green or cyan were changed from the amino acid present in the sequence of WT TcTIM to the one present in the sequence of WT TbTIM.
(DOCX)

S3 Table. Oligonucleotides used for the additive mutagenesis of regions 1 and 4 and the production of selected site directed mutants WT TbTIM and WT TcTIM.
(DOCX)

Acknowledgments

This work was performed by SDM as part of the fulfillment of her doctoral dissertation in the Programa de Doctorado en Ciencias Biomedicas, Universidad Nacional Autónoma de México (UNAM). The authors acknowledge Dr. Armando Gomez-Puyou for the helpful discussions during the initial stages of the research and Dr. Diego Gonzalez-Halphen for helpful discussions and careful revision of the manuscript.

Author Contributions

Conceptualization: Selma Díaz-Mazariegos, Ruy Perez-Montfort.

Formal analysis: Ruy Perez-Montfort.

Funding acquisition: Ruy Perez-Montfort.

Investigation: Selma Díaz-Mazariegos, Nallely Cabrera.

Methodology: Selma Díaz-Mazariegos, Nallely Cabrera.

Project administration: Ruy Perez-Montfort.

Supervision: Ruy Perez-Montfort.

Validation: Ruy Perez-Montfort.

Visualization: Selma Díaz-Mazariegos.

Writing – original draft: Selma Díaz-Mazariegos, Ruy Perez-Montfort.

Writing – review & editing: Ruy Perez-Montfort.

References

1. Pearson WR, (2013) An introduction to sequence similarity ("homology") searching. Curr Protoc Bioinformatics Chapter 3: Unit 3.1. https://doi.org/10.1002/0471250953.bi0301s42 PMID: 23749753
2. Kaczanowski S, Zielenliewicz P (2010) Why similar protein sequences encode similar three-dimensional structures? Theor Chem Acc 125: 643–650.
3. Kosloff M, Kolodny R, (2008) Sequence-similar, structure-dissimilar protein pairs. Proteins 71: 891–902. https://doi.org/10.1002/prot.21770 PMID: 18004789
4. Chothia C, Lesk AM (1986) The relation between the divergence of sequence and structure in proteins. EMBO J 5: 823–826. PMID: 3709526
5. Zomosa-Signoret V, Hernandez-Alcantara G, Reyes-Vivas H, Martinez-Martinez E, Garza-Ramos G, Perez-Montfort R, et al. (2003) Control of the reactivation of homodimeric triosephosphate isomerase from unfolded monomers. Biochemistry 42: 3311–3318. https://doi.org/10.1021/bi0206560 PMID: 12641463
6. Rodriguez-Bolaños M, Cabrera N, Perez-Montfort R. (2016) Identification of the critical residues responsible for differential reactivation of the triosephosphate isomerases of two trypanosomes. Open Biol. 6: 160161. http://dx.doi.org/10.1098/rsob.160161 PMID: 27733588
7. Reyes-Vivas H, Martinez-Martinez E, Mendoza-Hernandez G, Lopez-Velazquez G, Perez-Montfort R, Tuena de Gómez-Puyou M, et al. (2002) Susceptibility to proteolysis of triosephosphate isomerase from two pathogenic parasites. Characterization of an enzyme with an intact and a nicked monomer. Proteins 48: 580–590. https://doi.org/10.1002/prot.10179 PMID: 12112681
8. Tellez-Valencia A, Avila-Rios S, Perez-Montfort R, Rodriguez-Romero A, Tuena de Gomez-Puyou M, López-Calahorra F, et al. (2002) Highly specific inactivation of triosephosphate isomerase from

Trypanosoma cruzi by agents that act on the dimer interface. Biochem Biophys Res Com 295: 958–963. PMID: 12127988

9. Maldonado E, Moreno A, Panneerselvam K, Ostoa-Saloma P, Garza-Ramos G, Soriano-García M, et al. (1997) Crystallization and preliminary X-Ray analysis of triosephosphate isomerase from *Trypanosoma cruzi*. Prot Pept Lett 4: 139–144.
10. Maldonado E, Soriano-Garcia M, Moreno A, Cabrera N, Garza-Ramos G, de Gómez-Puyou M, et al. (1998) Differences in the intersubunit contacts in triosephosphate isomerase from two closely related pathogenic trypanosomes. J Mol Biol 283: 193–203. PMID: 9761683
11. Ostoa-Saloma P, Garza-Ramos G, Ramirez J, Becker I, Berzunza M, Landa A, et al. (1997) Cloning, expression and characterization of triosephosphate isomerase from *Trypanosoma cruzi*. Eur J Biochem 244: 700–705. PMID: 9108237
12. Garza-Ramos G, Cabrera N, Saavedra-Lira E, Tuena de Gomez-Puyou M, Ostoa-Saloma P, Perez-Montfort R, et al. (1998) Sulfhydryl reagent susceptibility in proteins with high sequence similarity: triosephosphate isomerase from *Trypanosoma brucei*, *T. cruzi*, and *Leishmania mexicana*. Eur J Biochem 253: 684–691. PMID: 9654066
13. Perez-Montfort R, Garza-Ramos G, Hernandez-Alcantara G, Reyes-Vivas H, Gao XG, Maldonado E, et al. (1999) Derivatization of the interface cysteine of triosephosphate isomerase from *Trypanosoma brucei* and *Trypanosoma cruzi* as probe of the interrelationship between the catalytic sites and the dimer interface. Biochemistry 38: 4114–4120. https://doi.org/10.1021/bi982425s PMID: 10194326
14. García-Torres I, Cabrera N, Torres-Larios A, Rodríguez-Bolaños M, Díaz-Mazariegos S, Gómez-Puyou A, et al. (2011) Identification of amino acids that account for long- range interactions in two triosephosphate isomerases from pathogenic trypanosomes. PLoS ONE 6(4): e18791. https://doi.org/10.1371/journal.pone.0018791 PMID: 21533154
15. Gomez-Puyou A, Saavedra-Lira E, Becker I, Zubillaga R, Rojo-Dominguez A, Perez-Montfort R (1995) Using evolutionary changes to achieve species specific inhibition of enzyme action. Studies with triosephosphate isomerase. Chemistry and Biology 2: 847–855. PMID: 8807818
16. Garza-Ramos G, Perez-Montfort R, Rojo-Dominguez A, Tuena de Gomez- Puyou M, Gomez-Puyou A (1996) Species specific inhibition of homologous enzymes by modification of nonconserved amino acids. The cysteines of triosephosphate isomerase. Eur J Biochem 241: 114–120. PMID: 8898895
17. Cabrera N, Hernandez-Alcantara G, Mendoza-Hernandez G, Gomez-Puyou A, Perez-Montfort R (2008) Key residues of loop 3 in the interaction with the interface residue at position 14 in triosephosphate isomerase from *Trypanosoma brucei*. Biochemistry 47: 3499–3506. https://doi.org/10.1021/bi702439r PMID: 18298085
18. Reyes-Vivas H, Hernandez-Alcantara G, Lopez-Velazquez G, Cabrera N, Perez-Montfort R, Tuena de Gómez-Puyou M, et al. (2001) Factors that control the reactivity of the interface cysteine of triosephosphate isomerase from *Trypanosoma brucei and Trypano- soma cruzi*. Biochemistry 40: 3134–3140. PMID: 11258928
19. Roberts DD, Lewis SD, Ballou DP, Olson ST, Shafer JA (1986) Reactivity of small thiolate anions and cysteine-25 in papain toward methyl methanesulfonate. Biochemistry 25: 5595–5601. PMID: 3778876
20. Borchert TV, Pratt K, Zeelen JP, Callens M, Noble ME, Opperdoes FR, et al. (1993) Overexpression of trypanosomal triosephosphate isomerase in *Escherichia coli* and characterization of a dimer-interface mutant. Eur J Biochem 211: 703–710. PMID: 8436128
21. Olivares-Illana V, Rodríguez-Romero A, Becker I, Berzunza M, García J, Perez-Montfort R, et al. (2007) Perturbation of the dimer interface of triosephosphate isomerase and its effect on *Trypanosoma cruzi*. PLoS Negl Trop Dis 1: e1, https://doi.org/10.1371/journal.pntd.0000001 PMID: 17989778

OPEN ACCESS Freely available online

PLoS one

Identification of Amino Acids that Account for Long-Range Interactions in Two Triosephosphate Isomerases from Pathogenic Trypanosomes

Itzhel García-Torres, Nallely Cabrera, Alfredo Torres-Larios, Mónica Rodríguez-Bolaños, Selma Díaz-Mazariegos, Armando Gómez-Puyou, Ruy Perez-Montfort*

Departamento de Bioquímica y Biología Estructural, Instituto de Fisiología Celular, Universidad Nacional Autónoma de México, Circuito Exterior S/N, Ciudad Universitaria, México DF, Mexico

Abstract

For a better comprehension of the structure-function relationship in proteins it is necessary to identify the amino acids that are relevant for measurable protein functions. Because of the numerous contacts that amino acids establish within proteins and the cooperative nature of their interactions, it is difficult to achieve this goal. Thus, the study of protein-ligand interactions is usually focused on local environmental structural differences. Here, using a pair of triosephosphate isomerase enzymes with extremely high homology from two different organisms, we demonstrate that the control of a seventy-fold difference in reactivity of the interface cysteine is located in several amino acids from two structurally unrelated regions that do not contact the cysteine sensitive to the sulfhydryl reagent methylmethane sulfonate, nor the residues in its immediate vicinity. The change in reactivity is due to an increase in the apparent pKa of the interface cysteine produced by the mutated residues. Our work, which involved grafting systematically portions of one protein into the other protein, revealed unsuspected and multisite long-range interactions that modulate the properties of the interface cysteines and has general implications for future studies on protein structure-function relationships.

Citation: García-Torres I, Cabrera N, Torres-Larios A, Rodríguez-Bolaños M, Díaz-Mazariegos S, et al. (2011) Identification of Amino Acids that Account for Long-Range Interactions in Two Triosephosphate Isomerases from Pathogenic Trypanosomes. PLoS ONE 6(4): e18791. doi:10.1371/journal.pone.0018791

Editor: Nai Sum Wong, University of Hong Kong, Hong Kong

Received September 25, 2010; **Accepted** March 18, 2011; **Published** April 18, 2011

Copyright: © 2011 García-Torres et al. This is an open-access article distributed under the terms of the Creative Commons Attribution License, which permits unrestricted use, distribution, and reproduction in any medium, provided the original author and source are credited.

Funding: Dirección General de Asuntos del Personal Académico, Universidad Nacional Autónoma de México (IN200507 and IN202910) and by the Instituto de Ciencia y Tecnología del Distrito Federal (304/2009 and PIFUTP09-279) to RPM and ATL, respectively, and also by the Universidad Nacional Autónoma de México. IGT was the recipient of a fellowship from CONACyT (No. 177322). The funders had no role in study design, data collection and analysis, decision to publish, or preparation of the manuscript.

Competing Interests: The authors have declared that no competing interests exist.

* E-mail: ruy@ifc.unam.mx

Introduction

It is assumed that the structure-function relationship from similar protein sequences will usually yield similar physicochemical and functional properties. Take for example the glycolytic enzyme triosephosphate isomerase (TIM) from two evolutionarily related pathogenic parasites, Trypanosoma brucei and T. cruzi. These are two pathogenic protists of the order of the kinetoplastidae that cause sleeping sickness and Chagas disease in humans, respectively. Many of the proteins of these parasites have a high degree of sequence identity; in the case of the two trypanosomal TIMs it is 73.9%, with a sequence similarity of 92.4%. Both enzymes are homodimers whose three dimensional structures superpose with an RMS of 0.96 Å and both have an identical catalytic site in each monomer formed by residues K13, H95 and E167 (based on the numbering for the sequence of TIM from *T. brucei* (TbTIM)).

However, even though the two enzymes are markedly similar, there are several striking differences in several functional properties of the two proteins. For example, their susceptibility to digestion with subtilisin [1], their velocity and extent of reactivation from guanidine chloride unfolded monomers [2], and their susceptibility to inactivation by several low molecular weight agents [3]. Of particular relevance to this work is their remarkably different susceptibility to sulfhydryl reagents like methylmethane thiosulfonate (MMTS): the enzyme from T. cruzi is 70 times more sensitive than the enzyme from T. brucei [4–8]. The initial site of action of the thiol reagent in both enzymes is their only interface cysteine (Cys), which is at position 14 or 15 of TbTIM and TIM from T. cruzi (TcTIM), respectively; it is surrounded by residues of loop 3 of the other subunit [4–11]. Since the three dimensional arrangements of the interface Cys relative to the other monomer are nearly identical in the two enzymes, the question arose as to which residues or parts of the enzymes are responsible for the different susceptibility to the thiol reagent.

The question of finding the amino acids in a protein sequence that have an influence on certain measurable protein functions has occupied protein chemists for many decades and, in consequence, numerous methods have been used to solve the problem [12–17]. Among the approaches to understand the relation between the structure and function of proteins, the use of chimeras has been rather frequent. Indeed, chimeras formed with different protein domains have been successfully used to ascertain the interplay between different portions of the protein and how each domain contributes to the overall function of the protein [18–20].

In this work, we show that by progressive grafting of different portions of a protein into equivalent regions of a homologous protein with a different trait, it is possible to ascertain the parts (and the amino acids) of the protein that participate in the expression of that feature.

A priori, we expected to find the determinants responsible for the susceptibility/resistance of the enzymes to MMTS either among the residues surrounding the interface Cys, or in residues that form the dimer interface, or in residues distributed throughout the whole protein. Instead, we found that the change in susceptibility to MMTS was due to residues that are not in contact with the interface Cys, and most are not part of the dimer interface, but belong to two specific regions of the protein that are not connected to each other either in a sequential or a structural basis. Our findings show that the assignment of a function or property to a few, or even a single amino acid, in functional and structural studies of proteins, should often be reconsidered and extended beyond the identification and definition of simple cavities or local interaction sites.

Results

Triosephosphate isomerase was divided into eight interchangeable modular regions

Because of its octamerous β/α barrel fold, the sequence of both TIMs was divided into eight regions that approximately correspond to a beta sheet, the corresponding beta-alpha loop and the alpha helix (Figure 1). In order to determine the amino acids that account for the different susceptibility of the two

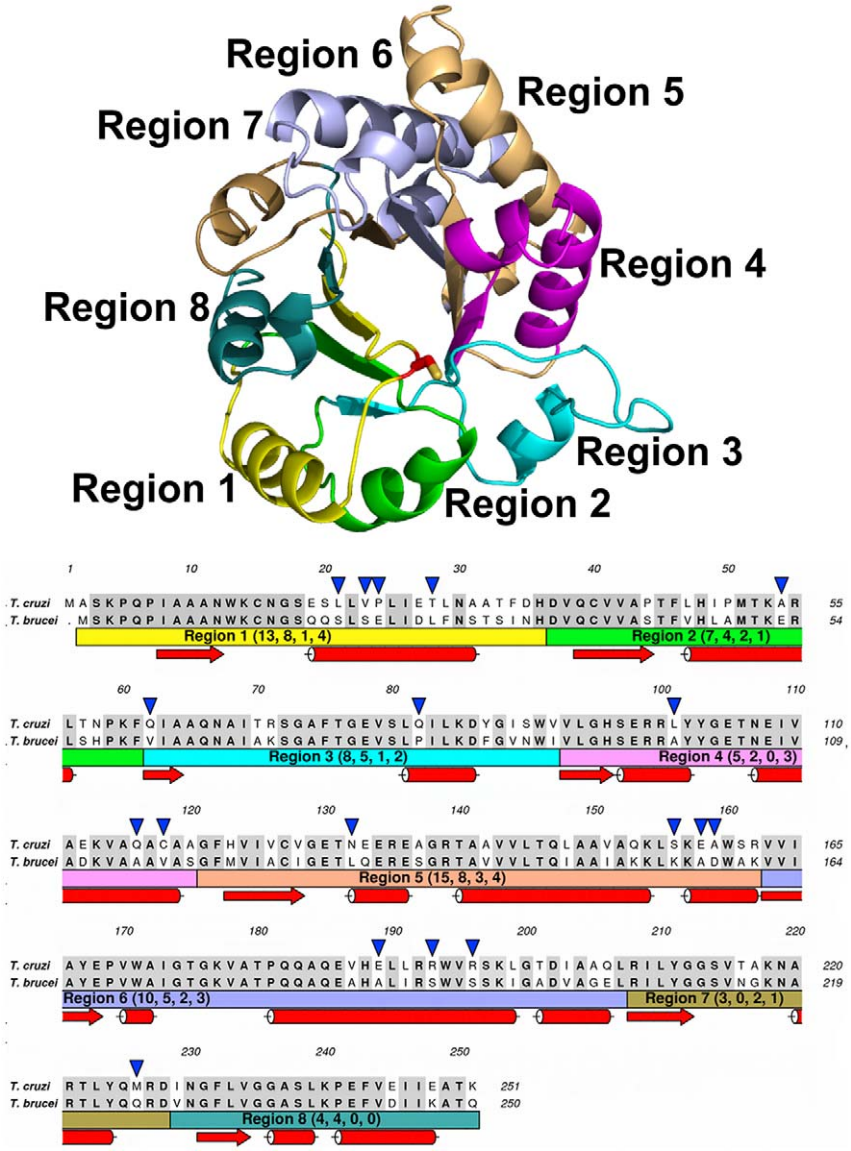

Figure 1. Position of the regions in the structure and aligned sequences of TbTIM and TcTIM. The ribbon diagram shows a monomer of TbTIM with each region in a different color and the interface Cys represented as sticks. The alignment of both sequences shows the identical amino acids shaded in grey. The color bars below indicate the region with the corresponding number of total differences, conserved substitutions, semiconserved substitutions and substitutions without homology in parenthesis, respectively. The blue arrowheads point to all substitutions without homology. Secondary structure elements of the sequences are also shown as red arrows (beta sheets) or cylinders (alpha helixes). The numbering of the amino acid sequence of TcTIM was used and the number and type of substitutions was taken from an alignment made using the Clustal W algorithm.
doi:10.1371/journal.pone.0018791.g001

enzymes to MMTS, we gradually transformed TcTIM into TbTIM by creating chimeras that had an increasing number of TbTIM regions and examined their susceptibility to the action of MMTS. Figure 1 depicts the amino acids that comprise each region and the differences in their amino acid sequence. There are 65 different residues in the two enzymes, the majority of them being in regions 1–6. We initially constructed six chimeras that contained a progressive number of TbTIM regions and a diminishing number of TcTIM regions; they were named according to their content of TcTIM regions. For example, the first chimera that was constructed is termed TcTIM 1–6 (it contains regions 1 to 6 of TcTIM and regions 7 and 8 of TbTIM), as a further example, we also constructed TcTIM 1 (it contains region 1 of TcTIM and regions 2–8 of TbTIM). Table 1 shows the chimeras used in this work.

Purification of the chimerical proteins

All the chimerical proteins were cloned and expressed in Escherichia coli. Different purification methods are used for wild type (WT) TbTIM and WT TcTIM, this is because after disruption of the cells and centrifugation, WT TcTIM partitions to the soluble fraction, whereas TbTIM localizes in the precipitate. Therefore, TbTIM was purified by treating the cell lysate with a 300 mM NaCl solution to solubilize the enzyme (see Methods). Due to these differences, in all the chimeras, the supernatant and precipitate obtained after cell disruption were analyzed by SDS-PAGE in order to ascertain whether the enzyme distributed in the soluble or insoluble fraction. According to the data, the corresponding chimera was purified by the procedures described for either TcTIM or TbTIM. Table 1 shows the purification method used for each chimera; in general, the chimeras that contained a majority of regions from TcTIM were purified from the soluble fraction, while those with more regions of TbTIM were purified by adding 300 mM NaCl to the lysis buffer (see Materials and Methods). The yield of pure protein for the chimeras was similar to that of the WT enzymes (60–80 mg/L of culture). Only chimera TcTIM 1 yielded lower quantities of purified protein (approximately 25 mg/L of culture).

The catalytic properties of the chimerical proteins are similar to those of the wild-type enzymes

The steady state kinetics of all chimerical enzymes were determined in the direction of glyceraldehyde 3-phosphate to dihydroxyacetone-phosphate. The Km and kcat values of the chimeras and WT enzymes were within the same range (Table 1). The kinetic parameters of chimera TcTIM 1–6 were lower when compared with the WT enzymes; nevertheless, its catalytic efficiency (kcat/Km) was similar to that of the WT enzymes. The catalytic efficiency of TcTIM 1–5 was approximately one half of that of the WT TIMs, mainly due to a lower kcat.

The non-identical amino acids of regions 5 to 8 (49%) are not involved in MMTS susceptibility

The sulfhydryl reagent methylmethane thiosulfonate (MMTS) inactivates TbTIM and TcTIM by reacting initially with their only interface Cys 14 or Cys 15, respectively [4–11]. Confirming previous results [21], we observed that the exposure of WT TcTIM and WT TbTIM to MMTS induced abolition of catalysis and that TcTIM was about 70 times more sensitive to the sulfhydryl reagent than TbTIM (Figure 2). Because the two enzymes are markedly similar in amino sequences and crystal structures, we sought to find which region or regions are responsible for the difference in susceptibility of TbTIM and TcTIM to the inactivating action of MMTS. Thus, we determined the effect of different concentrations of MMTS on the catalytic activity of the chimeras. The three chimeras TcTIM 1–6, TcTIM 1–5 and TcTIM 1–4 exhibited an inactivation pattern similar to that of WT TcTIM (Figure 2 Panel a). It is noteworthy that the susceptibility to MMTS of chimera TcTIM 1–4 that has one half the sequence of each of the two enzymes and a difference of 33 amino acids with TbTIM (87% identity) is similar to that of WT TcTIM.

Region 4 is involved in the susceptibility of TcTIM and TbTIM to low MMTS concentrations

When region 4 of TbTIM was subsequently incorporated in chimera TcTIM 1–4 to produce chimera TcTIM 1–3, an important change in the inactivation pattern with MMTS was observed (Figure 2 Panel b). This chimerical enzyme was the first in which we observed a pattern of inactivation by MMTS that resembled that of TbTIM. A salient feature of the MMTS inhibition curve of this chimera is that similarly to WT TbTIM, it retains 100% activity at concentrations below 10 μM MMTS. These findings indicated that the five differences in the amino acid sequences in region 4 (Figure 1) contribute to the susceptibility of WT TcTIM and WT TbTIM to MMTS. For this reason, we

Table 1. Method of purification used for wild type TbTIM, wild type TcTIM and each mutant enzyme and their kinetic constants.

Enzyme	Method of purification	*K*m (mM)	*k*cat $\cdot 10^5$ (min^{-1})	*k*cat/*K*m $\cdot$ 10^7(M^{-1} s^{-1})
TbTIM	**300 mM NaCl**	0.45	3.10	1.15
TcTIM	**No NaCl**	0.43	2.70	1.05
TcTIM 1–6	**No NaCl**	0.13	0.96	1.23
TcTIM 1–5	**No NaCl**	0.38	1.55	0.68
TcTIM 1–4	**300 mM NaCl**	0.63	3.32	0.87
TcTIM 1–3	**300 mM NaCl**	0.58	3.31	0.95
TcTIM 1–2	**300 mM NaCl**	0.57	3.28	0.95
TcTIM 1	**300 mM NaCl**	0.48	3.17	1.10
TcTIM 4	**300 mM NaCl**	0.37	2.38	1.07
TcTIM 1–3, 5–8	**No NaCl**	0.44	2.60	0.97
TcTIM 2,3, 5–8	**No NaCl**	0.26	3.59	2.29

doi:10.1371/journal.pone.0018791.t001

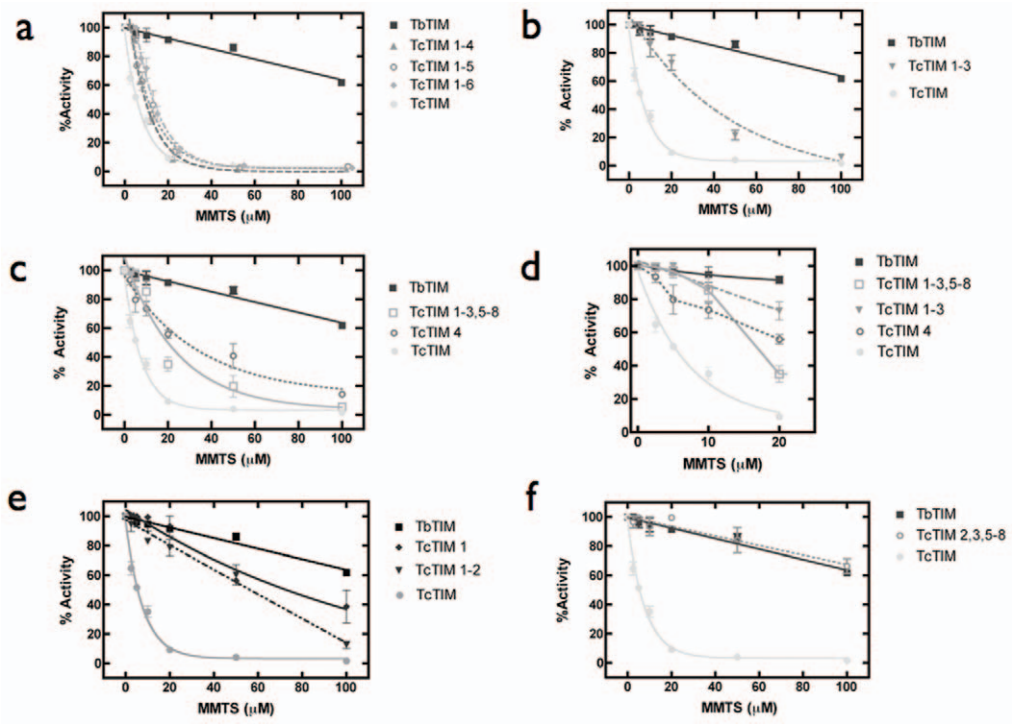

Figure 2. Effect of MMTS on WT TcTIM, WT TbTIM and on different chimeras. The enzymes were incubated at a concentration of 250 μg/mL in 100 mM TEA, 10 mM EDTA, and the indicated concentrations of MMTS (pH 7.4) for 2 h. At that time the activity of the samples was determined, including a sample without MMTS to calculate the percentage of remaining activity. Panel a) Effect of MMTS on WT TcTIM, WT TbTIM and chimeras TcTIM 1–6, TcTIM 1–5 and TcTIM 1–4. Panel b) Effect of MMTS on WT TcTIM, WT TbTIM and on chimera TcTIM 1–3. Panel c) Effect of MMTS on WT TcTIM, WT TbTIM and on two chimeras of region 4: TcTIM 1–3, 5–8 and TcTIM 4. Panel d) Close up of the first part of the curves shown in panel c, including the data for chimera TcTIM 1–3 shown on Panel b. Panel e) Effect of MMTS on WT TcTIM, WT TbTIM and on chimeras TcTIM 1–2 and TcTIM 1. Panel f) Effect of MMTS on WT TcTIM, WT TbTIM and on chimera TcTIM 2,3, 5–8.
doi:10.1371/journal.pone.0018791.g002

made two new chimeras: a TbTIM that had only region 4 of TcTIM (TcTIM 4) and a TcTIM that had only region 4 of TbTIM (TcTIM 1–3, 5–8). The susceptibility to the inactivating effect of MMTS of these two chimeras is shown in Figure 2 Panel c. Remarkably, the chimeras showed an overall intermediate response between the susceptible WT TcTIM and the resistant WT TbTIM. Nevertheless, there is an important difference between them (Figure 2 Panel d); chimera TcTIM 4, with only region 4 of TcTIM, started to loose activity with 2.5 μM MMTS, in the same way as WT TcTIM. Conversely, chimera TcTIM 1–3, 5–8 was hardly affected by low concentrations of MMTS, resembling WT TbTIM. Thus, the five different amino acids in the sequences of region 4 (Figure 1) are active participants in the overall response of the WT enzymes to MMTS.

Region 1 is instrumental in the susceptibility of TcTIM and TbTIM to high MMTS concentrations

Because chimeras with alternate regions 4 of TcTIM or TbTIM showed intermediate susceptibility to the inactivating action of MMTS, we tested two chimeras that contained additional regions of TbTIM: chimera TcTIM 1–2 and chimera TcTIM 1. The susceptibility of these chimeras to MMTS is shown in Figure 2 Panel e. TcTIM 1–2 retained most of its activity at concentrations below 20 μM MMTS; at higher concentrations, its activity was progressively inhibited and with 100 μM MMTS, inhibition was almost complete. A similar phenomenon occurred with chimera TcTIM 1, at low MMTS concentrations, it exhibited almost full activity; at higher concentrations, activity started to decrease, reaching 40% of its original activity with 100 μM MMTS. Thus, at high MMTS concentrations the behavior of TcTIM 1 approached, but still did not equal that of WT TbTIM.

The latter observations indicated that region 1 plays a central role in the susceptibility of the enzymes to MMTS; likewise the data of Figure 2 Panels c and d show that region 4 has a strong influence on the response to the thiol reagent. We therefore designed a chimera of TcTIM with regions 1 and 4 of TbTIM (TcTIM 2,3, 5–8). This chimera and WT TbTIM exhibited almost identical inactivation profiles at low and high concentrations of MMTS (Figure 2 Panel f). Thus, by using a region exchange method, we were able to build a chimera that had an MMTS inactivation profile undistinguishable from that of WT TbTIM. Taken together, the data with chimeras TcTIM 1 and TcTIM 2,3, 5–8 it may be concluded that, at most, the 13 different amino acids in region 1 of the two WT enzymes account for their different susceptibilities to MMTS at concentrations higher than 50 μM.

Initial experimental proof that these 13 different amino acids are involved in this difference of behavior was obtained by mutational analysis of some of the residues. Using TcTIM 2,3, 5–8 as the template, we prepared mutant TcTIM 2,3, 5–8:19E, 20S, 21L, 23V, 24P (reverting the first five different amino acids in region 1 of TbTIM to those found in the sequence of TcTIM). The susceptibility of this mutant to MMTS was determined in the same conditions as those of the other chimeras and the result showed that it had an intermediate susceptibility between WT TbTIM and WT TcTIM (Figure 3). Other double and single mutants namely: TcTIM 2,3, 5–8:19E, 20S; TcTIM 2,3, 5–8: 21L, 23V and TcTIM 2,3, 5–8: 24P tended to have a susceptibility

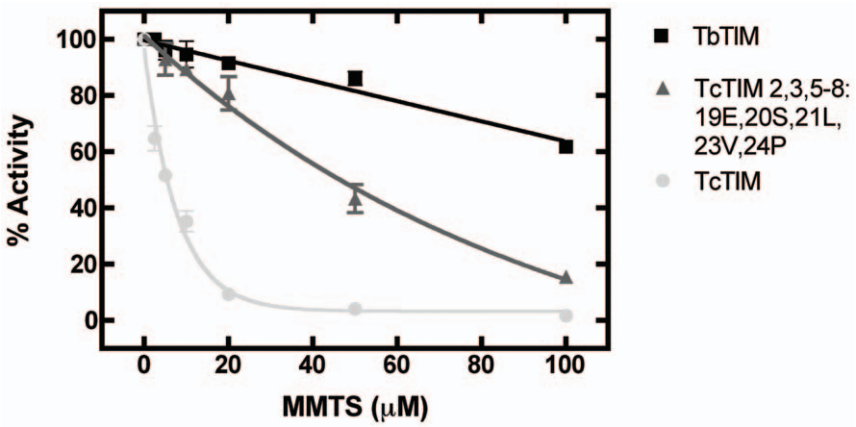

Figure 3. Effect of MMTS on WT TcTIM, WT TbTIM and on mutant TcTIM 2,3, 5–8: 19E, 20S, 21L 23V, 24P. The enzymes were incubated at a concentration of 250 μg/mL in 100 mM TEA, 10 mM EDTA, and the indicated concentrations of MMTS (pH 7.4) for 2 h. At that time the activity of the samples was determined, including a sample without MMTS to calculate the percentage of remaining activity.
doi:10.1371/journal.pone.0018791.g003

to MMTS which was more similar to the original template (supplementary Figure S1) indicating that these first five amino acids are largely responsible for the susceptibility of TcTIM to high concentrations of MMTS. The kinetic parameters of all these four mutants were very similar to those of TcTIM 2,3, 5–8 (supplementary Table S1).

Since TcTIM has a higher susceptibility than TbTIM towards other thiol reactive agents like 5,5-dithiobis(2-nitrobenzoate) (DTNB), 4,4 dithiopyridine, and n-ethylmaleimide [4], we also tested the inactivation of different chimeras with 1 mM DTNB. Table 2 shows that Cys14 of TbTIM needs 18 min to derivatize while Cys15 of TcTIM takes less than a minute. After twelve minutes, approximately 4 of the 8 Cys in a dimer of WT TcTIM are derivatized, while approximately one Cys per dimer from the 6 Cys in the dimer of TbTIM has reacted. As can be seen from the corresponding time at which the interface Cys was derivatized and the number of Cys derivatized in the dimers of the chimeras by DTNB at 12 minutes, the behavior of all proteins paralleled the inactivation scheme they had shown in the presence of MMTS, indicating that the susceptibility to this reagent is also affected by the amino acids in regions 1 and 4.

Table 2. Derivatization of Cys by DTNB in the dimers of wild type TbTIM, wild type TcTIM and nine mutant enzymes.

Enzyme	Cys per dimer	Time for derivatization of the first cysteine (Cys14 or 15)	Derivatized Cys per dimer after twelve minutes with DTNB
TbTIM	6	18 min	0.9
TcTIM	8	<1 min	3.8
TcTIM 1–6	8	<1 min	4.7
TcTIM 1–5	8	<1 min	4.7
TcTIM 1–4	8	<1 min	3.4
TcTIM 1–3	6	3 min	2.0
TcTIM 1–2	6	9 min	1.6
TcTIM 1	6	6 min	1.8
TcTIM 4	8	4 min	2.6
TcTIM 1–3,5–8	6	6 min	2.0
TcTIM 2,3, 5–8	6	>20 min	0.33

doi:10.1371/journal.pone.0018791.t002

The interface Cys does not contact the residues of regions 1 and 4 that confer different susceptibility to MMTS

The three dimensional location of the residues in regions 1 and 4 that account for the different susceptibility to MMTS in TcTIM and TbTIM shows several surprising features (Figure 4). None of the 18 residues that are relevant for the susceptibility of the interface Cys are in contact with this residue, nor with those that surround it. Also, according to an analysis of the structure of TbTIM (PDB code 5TIM) with the PISA server [22], only one of the 18 residues in regions 1 and 4 forms part of the dimer interface, albeit in the case of TcTIM (PDB code 1TCD), 18Q–19E may be considered part of the interface with a buried surface area of 64 $Å^2$. Finally, there are no contacts between the relevant residues of regions 1 and 4 (Figure 4). Thus, from the structural point of view, it would seem that the effects of region 1 are independent from those of region 4, and vice versa. Altogether, the data show that the relevant residues of regions 1 and 4 modulate the reactivity of the interface Cys through long-range interactions and that the interface residues do not play a role in the susceptibility to MMTS.

In order to check for the absence of major conformational differences due to the sequence perturbations on the chimeras, we solved the crystal structure at 1.65 Å resolution of chimera TcTIM 2,3, 5–8 (Figs. 5 and 6). The analysis of the structure shows that the chimera can be superposed on the crystal structures of TcTIM and TbTIM with a RMSD of 0.385 and 0.437 Å respectively, with a minor displacement on the loop of region 1 (Figure 7). A displacement in region 6 is also observed, which corresponds to the amino acids of the flexible loop involved in enzyme catalysis (Figure 7) [23]. Thus, it can be suggested that the disparities in susceptibility to thiol reactive agents between the different proteins produced by changes in regions 1 and 4 are due to the effect of their side chains and not to any major rearrangement of the main chain.

The pKa of the interface Cys is regulated by regions 1 and 4

In previous work, we reported that a factor that controlled the reactivity of the interface Cys in TIM from T. brucei and T. cruzi

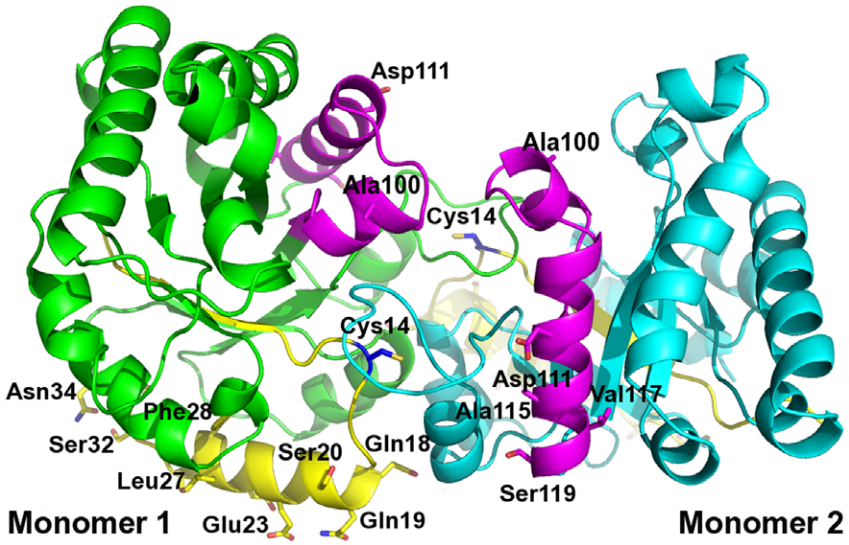

Figure 4. Three-dimensional localization of regions 1 and 4. Representation of the TIM dimer and the 18 residues that differ between region 1 and 4 of TbTIM and TcTIM. The color code used for regions 1 and 4 is the same as in Figure 1, and the two monomers are colored in green and turquoise. The altered residues are highlighted as sticks. Sequence numbers are according to TbTIM (PDB code 5TIM), and register as 1 amino acid less, when compared to TcTIM.
doi:10.1371/journal.pone.0018791.g004

is the pKa of its thiol group, which is 0.8 pH units lower in TcTIM than in TbTIM [24]; the respective values were 9.28±0.07 and 10.08±0.03. When the pKa of the thiol group for Cys 14/15 of the wild type enzymes and the chimerical enzyme TcTIM 2,3, 5–8 were determined anew, under the same conditions, the values turned out to be 9.27, 10.53 and 10.61 for TcTIM, TbTIM and

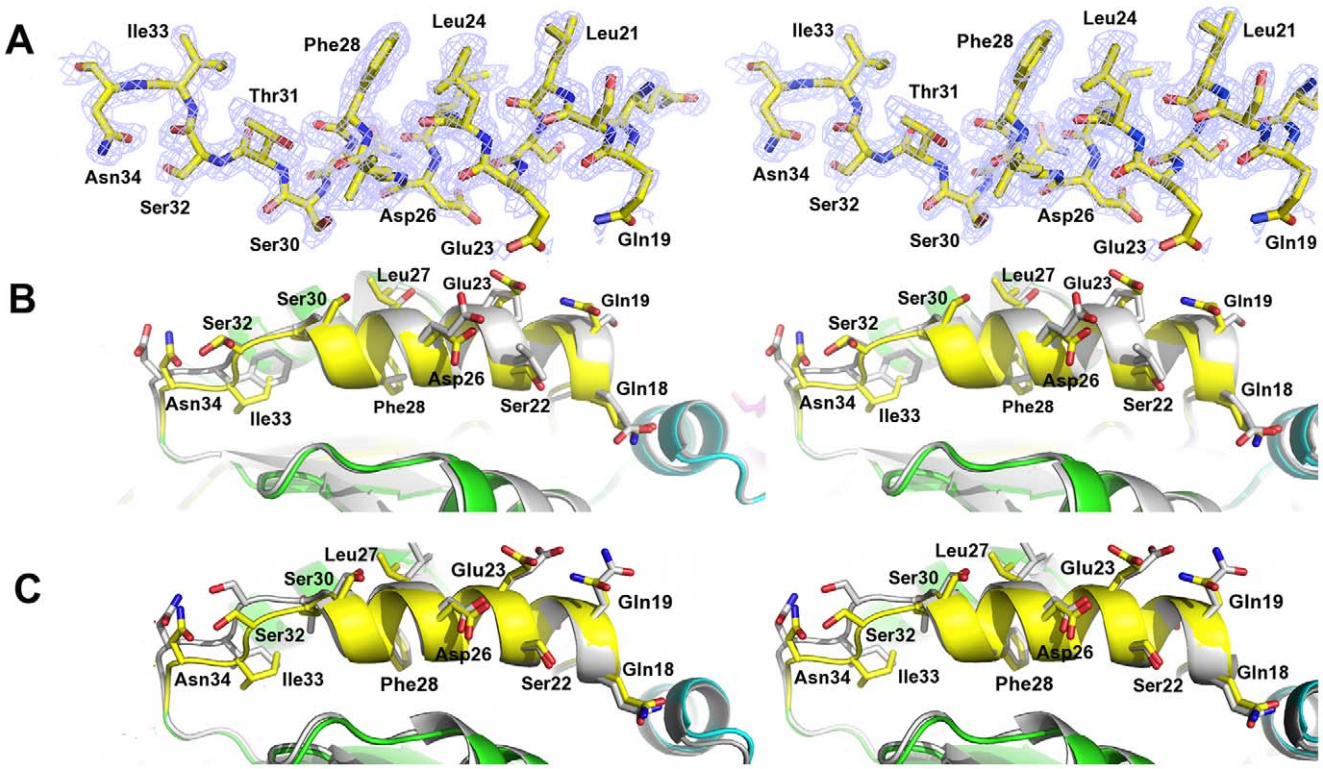

Figure 5. Region 1 of the crystal structure of chimera TcTIM 2,3, 5–8. A. Stereo view of sigma weighted, 2Fo-Fc simulated annealing omit map contoured at 1σ for region 1 in the final model of the crystal structure of chimera TcTIM 2,3, 5–8 (colored ribbon). B. Superposition on TcTIM (grey cartoon). The rmsd value for this region is 0.363 Å, for the Cα atoms. C. Superposition on TbTIM (grey cartoon). The rmsd value for this region is 0.237 Å. The sequence numbers are the same as in Figure 4.
doi:10.1371/journal.pone.0018791.g005

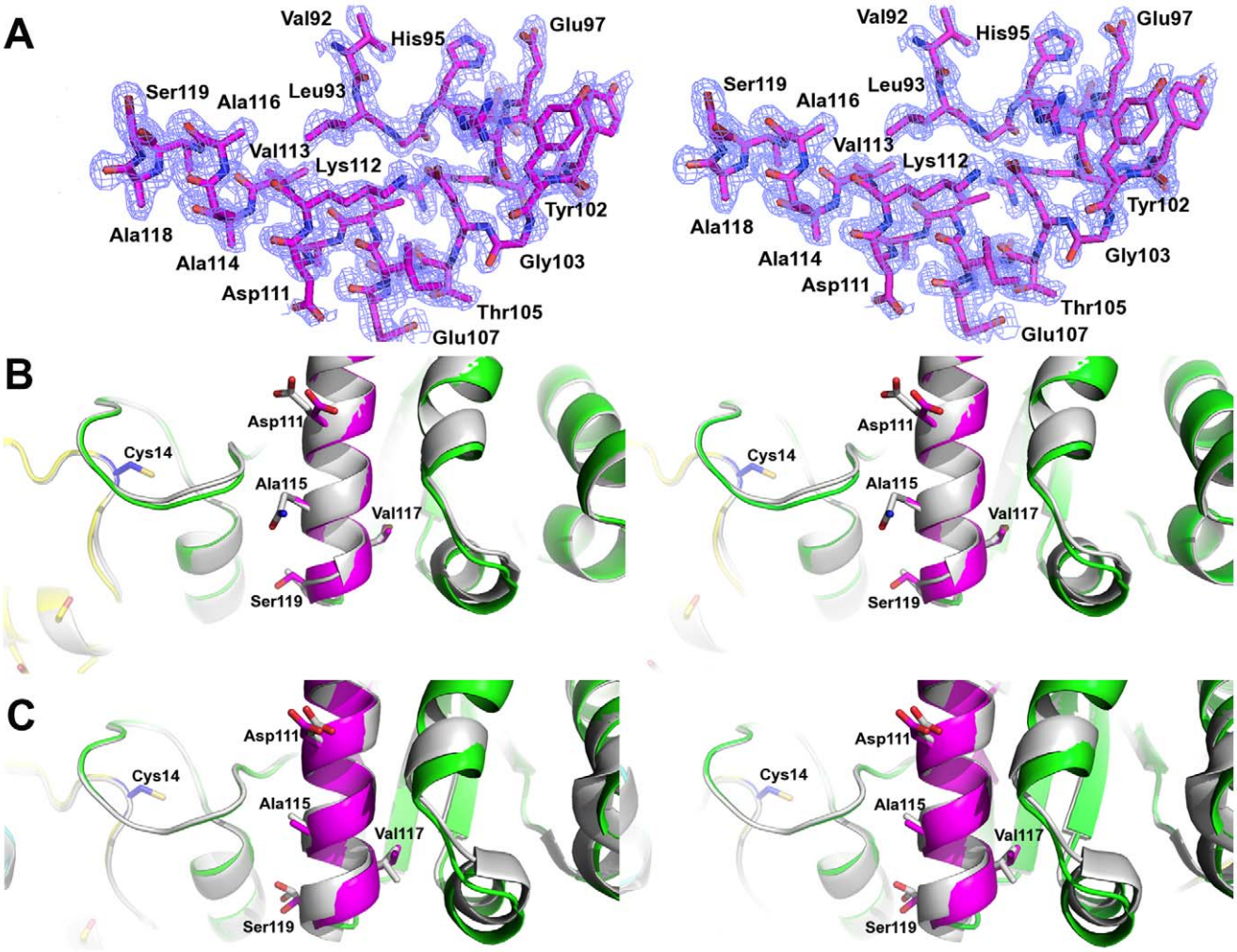

Figure 6. Region 4 of the crystal structure of chimera TcTIM 2,3, 5–8. A. Stereo view of sigma weighted, 2Fo-Fc simulated annealing omit map contoured at 1σ for region 4 in the final model of the crystal structure of chimera TcTIM 2,3, 5–8 (colored ribbon). B. Superposition on TcTIM (grey cartoon). The rmsd value for this region is 0.219 Å, for the Cα atoms. C. Superposition on TbTIM (grey cartoon). The rmsd value for this region is 0.150 Å. The sequence numbers are the same as in Figure 4. The interface Cys is shown as blue sticks.
doi:10.1371/journal.pone.0018791.g006

TcTIM 2,3, 5–8, respectively (Table 3). Interestingly the interface Cys of TcTIM 1–4 (with a susceptibility to thiol reactive agents like TcTIM) had a pKa of 9.17, and those of chimeras TcTIM 1–3, TcTIM 1 and TcTIM 1–3, 5–8 (with an intermediate susceptibility to thiol reactive reagents) had pKas of 9.86, 9.49 and 9.59, respectively.

Discussion

In this work, we have developed a method in which, by taking the same protein from two evolutionary closely related organisms, it is feasible to locate the amino acids responsible for a given property of a protein. It is noteworthy that the method is not biased by structural or hypothetical considerations; it is an experimental approach that indicates the protein region (or protein regions) relevant for a given function.

This strategy is probably best suited for proteins with a high level of homology. For example, our attempts to build chimeras of TcTIM and TIM from Homo sapiens (TcTIM 1–4: HsTIM 5–8 and HsTIM 1–4: TcTIM 5–8) yielded catalytic inert proteins. Most likely, the proteins did not fold correctly, since we observed that, upon expression, the proteins were predominantly found in inclusion bodies. Nonetheless, our experimental approach may be useful in the study of other pairs of proteins from the TIM barrel superfamily or other protein families, particularly if they have highly similar amino acids sequences.

Before beginning this study, it was not possible to predict which mutations would affect the catalytic properties and the susceptibility of the interface Cys to sulfhydryl reagents. However, by grafting different portions of the proteins, we identified two separate and discrete regions of the protein (regions 1 and 4) that establish the resistance/susceptibility of the interface Cys to thiol reagents. Taken as a whole, our data show several points that are noteworthy. First, although some of the chimeras exhibited relatively low kcat, the catalytic efficiency of all the chimeras was comparable to those of the WT enzymes. This is not surprising, since the catalytic amino acids K13, H95 and E167 are strictly conserved and, thus, the exchange of one region for another did not alter them; in consequence catalysis was not affected. Nevertheless, it is somewhat remarkable that the introduction of regions with a significant number of different residues did not affect the catalytic events, indicating that the

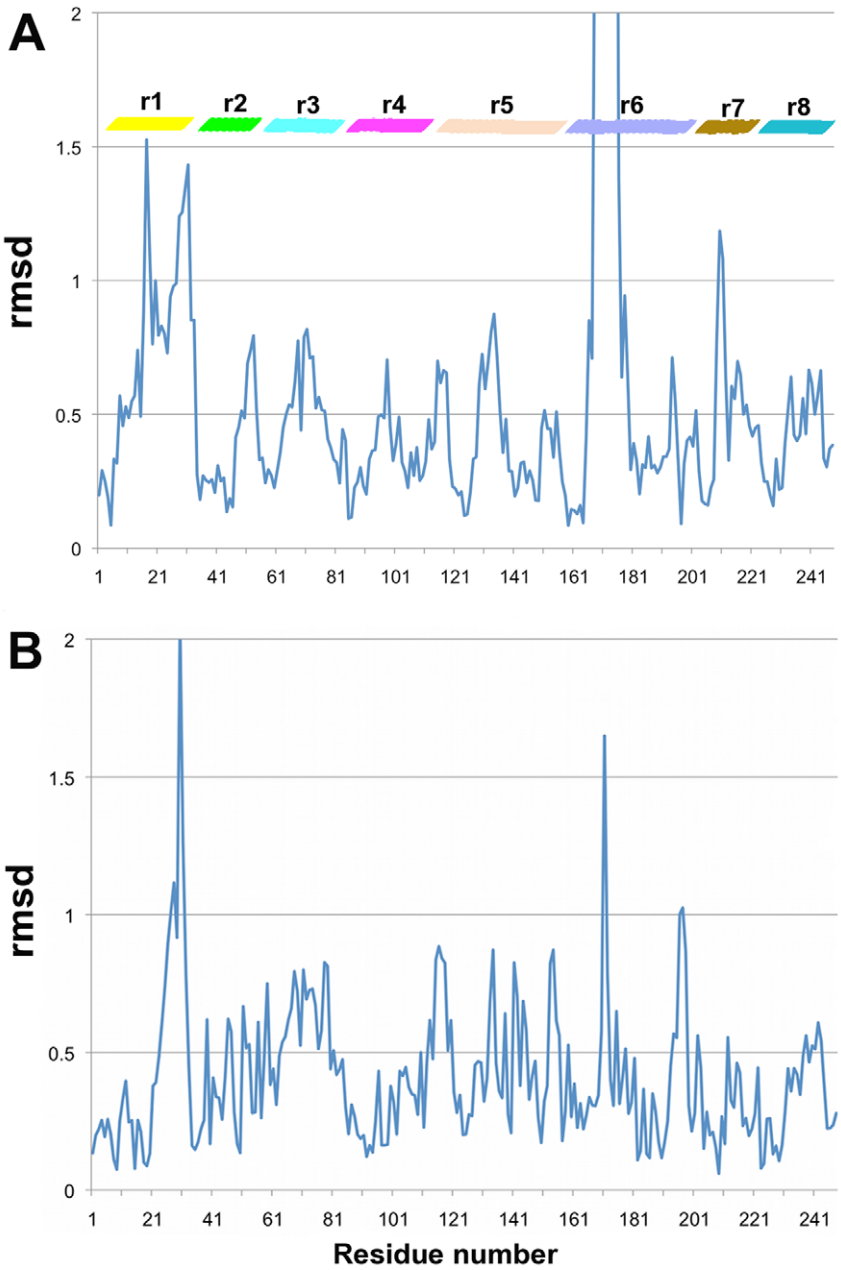

Figure 7. Root mean square deviations between the structures of chimera TcTIM 2,3,5–8, TcTIM and TbTIM. A. RMS deviations between chimera TcTIM 2,3, 5–8 and TcTIM (PDB code 1TCD), overall rmsd 0.385 Å. B. RMS deviations between chimera TcTIM 2,3, 5–8 and TbTIM (PDB code 5TIM), overall rmsd 0.437 Å. The relative location of the 8 TIM regions is indicated in color bars using the same color code as in Figure 1.
doi:10.1371/journal.pone.0018791.g007

exchange of regions with different amino acid composition is well tolerated. Second, the properties of the interface Cys are not the result of a gradual and continuous change, indicating that all parts of the protein do not contribute to the properties of the interface Cys and that instead, they are modulated by a small number of amino acids. In fact, substitution of region 5 to 8 which together comprise 32 of the total 65 amino acid differences between the two WT enzymes did not affect the reactivity of the interface Cys. This strongly suggests that a feature of a given residue, or at least that of the interface Cys, is not a global phenomenon, instead it appears to depend on the integrity and communication between a few residues. Third, of the 18 amino acid differences in regions 1 and 4 of WT TcTIM and WT TbTIM, only one of them may be considered part of the dimer interface. This is completely opposite to our original hypothesis, in which we thought that the susceptibility determinants of MMTS action were localized in the interface. In this regard, we note that mutants in which the interfacial residues of TbTIM were incorporated into TcTIM, and vice versa, did not significantly alter the susceptibility of the respective enzymes to MMTS. Fourth, none of the different residues in regions 1 and 4 contact the interface Cys or the residues surrounding it. Thus, the overall data indicate that amino acids of regions that are distant from the interface Cys determine its reactivity to the sulfhydryl reagent (Figure 4). Further studies will be needed to locate more precisely the minimum number of residues involved in MMTS susceptibility.

Table 3. pKa values of Cys 14/15 in TbTIM and TcTIM and some mutant enzymes.

Enzyme	MMTS concentration used (μM)	pKa
TbTIM	80	10.53±0.06
TcTIM	10	9.27±0.16
TcTIM 1–4	10	9.17±0.12
TcTIM 1–3	10 and 80	9.86±0.05
TcTIM 1	80	9.49±0.08
TcTIM 1–3, 5–8	10 and 80	9.59±0.06
TcTIM 2,3, 5–8	80	10.61±0.06

doi:10.1371/journal.pone.0018791.t003

Our study is an example of how long-range interactions, or perhaps evolutionary protein segments that apparently have no structural coherence [14], can determine the behavior and properties of different parts of the protein in a given milieu. Thus, we would like to point out that our experimental approach, using a modular, systematic approach, and not a random mutagenesis method, together with results that give new insights into the factors that control the properties of protein-inhibitor interactions, could be of value in studies that probe protein-function relationships.

Materials and Methods

Design of the genes of chimerical proteins

DNA sequences X03921 and U53867 at the NCBI database for TbTIM and TcTIM, respectively, were used for the design of the three chimerical proteins: TcTIM 1–6, TcTIM 1–5 and TcTIM 1–4. These genes were synthesized by GenScript (Piscataway NJ). The gene for chimera TcTIM 1–4 was planned in such a manner that it could serve as basis for the construction of other chimerical proteins. The sequence of TcTIM 1–4 was slightly altered so that it included a restriction site for HaeII between bases 292 and 300. Using this restriction enzyme, both, regions 4 from TbTIM or TcTIM could be obtained and the chimerical proteins TcTIM 1–3 and TcTIM 4 could be constructed. The gene for chimera TcTIM 1–3, 5–8 was also synthesized by GenScript. Three PCR reactions, using Accuzyme DNA polymerase (Bioline, Taunton MA), were necessary to obtain chimera TcTIM 1–2. The external T7 promoter oligonucleotide and the sequence 5′GCGTTCTGTGCGGCAATCTG3′ (Rv12) were used to amplify regions 1 and 2 of TcTIM using DNA from chimera TcTIM 1–4 as a template. The external T7 terminator oligonucleotide and the sequence 5′CAGAACGCCATTGCAAAGAGC3′(Fw38) were used to amplify regions 3 to 8 from TbTIM using WT TIM DNA as a template.

This same strategy was used to make chimera TcTIM 1 using the same external oligonucleotides and the sequences 5′GTGCAATGCGTAGTGGCCTCC3′(Fw28) and 5′TGATCACGATGTGCAATGCGT3′(Rv1). The template DNAs were from chimera TcTIM1–4 and from TbTIM for the first and second PCR reactions, respectively.

These same oligonucleotides were used to build chimera TcTIM 2,3, 5–8. The DNA of TbTIM was taken as a template with the T7 promoter and sequence Rv1 to amplify region 1 from TbTIM and join it to regions 2–8 from chimera TcTIM 1–3, 5–8 amplified with the T7 terminator and sequence Fw28 using the DNA of this same chimera as a template.

The mutant enzyme TcTIM 2,3, 5–8:19E, 20S, 21L, 23V, 24P was also built using three PCR reactions. The DNA of chimera TcTIM 2,3, 5–8 was used as a template together with the following mutagenic nucleotides: 5′GCTCCGAAAGCCTGTTGGTTCCGCTTATTGATCTGTTTAACTCC3′ (Fw) and 5′CGAGGCTTTCGGACAACCCAGGCGAATAACTAGACAAATTGAGG3′ (Rv).

The mutant enzymes TcTIM 2,3, 5–8:19E, 20S; TcTIM 2,3, 5–8: 21L, 23V and TcTIM 2,3, 5–8: 24P were prepared with the QuikChange site directed mutagenesis kit and the following sequences: for TcTIM 2,3, 5–8:19E, 20S 5′GCAACGGCTCCGAAAGCTCTTTGTCGG3′ (Fw) and 5′CGTTGCCGAGGCTTTCGAGAAACAGCC 3′ (Rv), for TcTIM 2,3, 5–8: 21L, 23V 5′AACGGCTCCCAACAGCTGTTGGTTGAG3′ (Fw) and 5′TTGCCGAGGGTTGTCGACAACCAACTCG3′(Rv), and for TcTIM 2,3, 5–8: 24P 5′GTCGCCGCTTATTGATCTGTTTAACTCC3′ (Fw) and 5′CAGCGGCGAATAACTAGACAAATTGAGG3′ (Rv), respectively.

All genes of the chimerical proteins were cloned into the pET-3a expression plasmid using the Nde-I and BamHI restriction sites. Every gene was completely sequenced and transformed into BL21(DE3)pLysS cells (Novagen, Madison WI).

Expression and purification of chimerical proteins

Bacteria containing the plasmids with each of the chimerical genes were grown in Luria Bertani medium supplemented with 100 μg/mL ampicillin and were incubated at 37°C. Once the cell cultures reached an $A_{600\ nm} = 0.6$, a final concentration of 0.4 mM isopropyl -β-D thiogalactopyranoside was used for induction and the bacteria were incubated 12 h more at 30°C before harvesting them.

Since TcTIM and TbTIM have different purification protocols described in references [6] and [25], respectively, some modifications had to be introduced to purify the chimerical proteins containing different regions of each sequence. TcTIM tends to distribute mainly in the soluble fraction of the bacterial extract, while TbTIM tends to be with the membrane fraction and has to be solubilized with 300 mM NaCl. Each chimerical enzyme was subjected to a preliminary test to determine if it was mainly localized in the soluble supernatant or the insoluble fraction. They were then treated accordingly as TcTIM or TbTIM, respectively (Table 1).

After the 12 h induction, bacteria were collected by centrifugation and the cells were resuspended in 40 mL of lysis buffer (100 mM MES, 1 mM DTT, 0.5 mM EDTA and 0.2 mM PMSF, pH 6.3). In the case of those chimerical enzymes that distributed mainly to the insoluble fraction the lysis buffer additionally contained 300 mM NaCl. Each suspension was sonicated 5 times for 40 seconds, with 1 min rest between each cycle. The sonicated suspensions were then centrifuged at 144000× g for one hour to separate the cellular debris from the soluble fraction.

The supernatants of the chimerical enzymes treated like TbTIM were diluted to have a final salt concentration of approximately 20 mM before application to the column. All supernatants were applied to a fast flow SP-sepharose column that had been equilibrated previously with 50 mM MES buffer pH 6.3, and the protein was eluted with a 0–500 mM NaCl gradient in the same buffer. The eluted protein was pooled and precipitated under agitation with 70% (w/v) ammonium sulfate for 12 h. The precipitate was centrifuged at 23000× for 15 min and dissolved in 3 mL of 100 mM triethanolamine (TEA), 1 mM EDTA pH 7.4. To this solution enough ammonium sulfate was added to have a final concentration of 2.2 M and was applied to a hydrophobic Toyopearl column, which had been previously equilibrated with 100 mM TEA, 1 mM EDTA, pH 7.4 and 2.2 M ammonium

sulfate. The chimerical proteins were eluted with a linear gradient of ammonium sulfate of 2.2 to 0 M. The fractions containing enzyme were pooled and concentrated to have 1 mg/mL or more of protein concentration. All steps of the different purifications were monitored with SDS-PAGE gels (16% acrylamide) stained with Coomassie Blue and by measuring catalytic activity. All proteins were stored at 4°C in 70% ammonium sulfate at concentrations greater than 1 mg/mL.

At intermediate stages of the purification process of all chimerical enzymes, protein concentrations were determined using the bicinchoninic acid method (BCA, protein assay reagent kit) at 562 nm and the molar extinction coefficients at 280 nm for purified proteins were 36440 M^{-1} cm^{-1} for WT TcTIM, TcTIM 1–6, TcTIM 1–5, TcTIM 1–4, TcTIM 1–3, TcTIM 1–3, 5–8 and TcTIM 2,3, 5–8 and 34950 M^{-1} cm^{-1} for WT TbTIM, TcTIM 4, TcTIM 1–2 and TcTIM 1, respectively.

Activity assays

Enzyme activity was measured at 25°C following the conversion of glyceraldehyde 3 –phosphate (GAP) to dihydroxyacetone phosphate using α-glycerolphosphate dehydrogenase (α- GDH) as coupling enzyme. NADH oxidation was monitored at 340 nm. The reaction mixture had 100 mM TEA, 10 mM EDTA, pH 7.4, 1 mM GAP, 0.2 mM NADH and 20 μg/mL α-GDH. The reaction was initiated by addition of 5 ng/mL of the corresponding TIM. To calculate the kinetic parameters, GAP concentration was varied between 0.05 and 2 mM. The data were adjusted to the model of Michaelis and Menten and the values of *K*im and Vmax were calculated by non-linear regression.

Inactivation assays with MMTS

Both, WT enzymes, as well as chimerical enzymes, at a concentration of 250 μg/mL were incubated with the indicated concentrations of MMTS in a buffer containing 100 mM TEA, 10 mM EDTA, pH 7.4 for 2 h at 25°C. At this time the mixtures were diluted and an aliquot of the dilution was withdrawn to measure activity at a concentration of 5 ng/ml of reaction mixture. The activity data are reported as percentage of residual activity, taking the activity of each corresponding enzyme in the absence of MMTS as 100%.

Number of Cys derivatized by DTNB as a function of time

The number of Cys derivatized by DTNB was determined for WT TbTIM, WT TcTIM and 9 chimeras (Table 2) essentially as described in reference [11]. In this case, all the enzymes (200 μg) were incubated in at 25°C in 1 mL of a buffer containing 100 mM TEA, 10 mM EDTA and 1 mM DTNB pH 7.4 for 20 min. The absorbance at 412 nm was recorded immediately after adding the enzymes. The value of a blank, with no enzyme, was subtracted from the experimental values. The number of derivatized Cys at 8 and 12 min was calculated with the equation

$$N = (A412/\varepsilon)/(\text{protein concentration in mg/MW of the protein})$$

where A is the absorbance and ε is the extinction coefficient of nitrobenzoic acid, 13,600 M^{-1} cm^{-1} .

Determination of the pKa of the interface Cys

The pKa of the interface Cys of WT TbTIM, WT Tc TIM and of 5 chimeras, including TcTIM 2,3, 5–8 (Table 3), was determined as described in reference [24] with some modifications. Briefly, the enzymes were incubated at a concentration of 5 μg/mL in 100 mM TEA and 10 mM EDTA adjusted to the desired pH; MMTS at a concentration of 10 or 80 μM was also added. For chimeras that had an MMTS-inactivation profile similar to TbTIM we used 80 μM MMTS and for those with a profile similar to TcTIM we used 10 μM MMTS. For chimeras with an intermediate MMTS-inactivation profile, both concentrations were used and the mean of the result of both experiments was taken as the pKa value. The apparent pKa of the interface Cys was determined from plots of ln of percent remaining activity versus pH. The data were fitted to a model derived from the Henderson-Hasselbach equation:

$$\ln(\%\text{activity}) = (Y_i + Y_h \times 10^{pKa-pH})/(1 + 10^{pKa-pH})$$

where Y_i and Y_h represent the initial and final activities, respectively.

Table 4. X-ray data collection and refinement statistics, Values in parentheses are for the last resolution shell.

Parameters	
Data collection statistics	
Space group	$P2_1$
Unit cell dimensions	
a, b, c (Å)	83.6, 77.2, 85.4
α, β, γ angles (degrees)	90.0, 116.6, 90.0
Resolution range (Å)	54.3-1.65 (1.74-1.65)
Number of reflections	336,767 (40,524)
Number of unique reflections	107,171 (13,903)
Data completeness (%)	91.9 (82.4)
R_{sym} (%)[a]	7.3 (27.5)
I/σ	6.9 (2.3)
Mn(I)/sd	10.5 (3.9)
Refinement statistics	
Resolution range (Å)	41.7-1.65 (1.70-1.65)
R_{cryst}/R_{free} (%)[b,c,d]	18.9 (25.4)/22.0 (30.7)
Number of atoms, protein/solvent	7540/991
Mean B value ($Å^2$)	13.2
B value from Wilson plot ($Å^2$)	13.6
Root mean square deviation bond lengths (Å)[e]	0.006
Root mean square deviation bond angles (degrees)[e]	1.005
Cross-validated σA coordinate error	0.21
Residues in Ramachandran plot (%)[f]	
Most allowed region	822 (94.2%)
Allowed region	49 (5.6%)
Generously allowed region	2 (0.2%)
Disallowed region	0 (0.0%)

[a]R_{sym} is defined as $\sum|(I-<I>)|/\sum I$, where I is the intensity individual reflection and <I> is the average intensity for this reflection; the summation is over all intensities.
[b]$R_{cryst} = |F_o| - ||F_c|/F_o$ for all reflections.
[c]R_{free} is the same as R_{cryst}, but calculated on the 5% of data excluded from refinement.
[d]No σ cut-offs used on the refinement (F>0σF).
[e]Engh RA, Huber R (1991) Acta Cryst A47: 392–400. Engh RA, Huber R (2001) International Tables for Crystallography, Vol. F, edited by M. G. Rossmann & E. Arnold, pp. 382–392. Dordrecht: Kluwer Academic Publishers.
[f]Kleywegt GJ, Jones TA (1996). Structure 15: 1395–1400.
doi:10.1371/journal.pone.0018791.t004

The rest of the procedure and the conditions and corrections applied were performed as previously described [24].

Crystallization of chimera TcTIM 2,3, 5–8 and data collection

Chimera TcTIM 2,3, 5–8 was crystallized via vapor diffusion using the sitting drop method. One µl of a solution of protein at 35 mg/ml was mixed with 1 µl of reservoir solution. Crystals were obtained in the H3 condition of the Index HT kit (Hampton Research) after 1 or 2 weeks of incubation. The best crystals were grown at 9°C and obtained with a reservoir solution of 200 mM sodium malonate and 20% polyethylene glycol 3350. The crystals were cryoprotected by increasing the concentration of polyethylene glycol 3350 in the crystal drop to 35% and they were immediately frozen in liquid nitrogen. Diffraction data were collected at the Life Sciences Collaborative Access Team (LS-CAT) 21-ID-F beamline in the Advanced Photon Source (Argonne National Laboratory), using a MarMosaic 225 detector. The data were processed with MOSFLM [26] and reduced with SCALA [27].

Structure Determination and Refinement

The structure was solved by the molecular replacement method with the program PHASER [28] using the coordinates of the native TcTIM at 1.8 Å resolution (Protein Data Bank code 1TCD) as the search model. Refinement was made with the programs Refmac [29] and Phenix [30], followed by model building with COOT [29]. The existence of the mutations in regions 1 and 4 was initially confirmed by difference Fourier maps calculated using the structure of TcTIM. On two of the four monomers in the asymmetric unit, residues 170–177 (loop 6 or flexible loop) are less clear on the electron density map. These regions are normally poorly defined in apo-TIMs. Five percent of the data were used to validate the refinement. σA-weighted, F_o - F_c simulated annealing omit maps were used to further validate the quality of the model. Data collection and refinement statistics are given in Table 4. Figures were generated with PyMOL (available on http://www.pymol.org/). The atomic coordinates and structure factors (code 3Q37) have been deposited in the Protein Data Bank, Research Collaboratory for Structural Bioinformatics, Rutgers University, New Brunswick, NJ (http://www.rcsb.org/).

Supporting Information

Figure S1 Effect of MMTS on WT TcTIM, WT TbTIM and on mutants TcTIM 2,3, 5–8: 19E, 20S; TcTIM 2,3, 5–8: 21L 23V and TcTIM 2,3, 5–8: 24P. The enzymes were incubated at a concentration of 250 µg/mL in 100 mM TEA, 10 mM EDTA, and the indicated concentrations of MMTS (pH 7.4) for 2 h. At that time the activity of the samples was determined, including a sample without MMTS to calculate the percentage of remaining activity.
(TIF)

Table S1 Kinetic constants of mutants TcTIM 2,3 5–8: 19E, 20S, 21L, 23V, 24P; TcTIM 2,3, 5–8: 19E, 20S; TcTIM 2,3, 5–8: 21L 23V and TcTIM 2,3, 5–8: 24P.
(DOC)

Author Contributions

Conceived and designed the experiments: ATL AGP RPM. Performed the experiments: IGT NC ATL MRB SDM. Analyzed the data: IGT ATL AGP RPM. Contributed reagents/materials/analysis tools: ATL AGP RPM. Wrote the paper: ATL AGP RPM.

References

1. Reyes-Vivas H, Martínez-Martínez E, Mendoza-Hernández G, López-Velazquez G, Perez-Montfort R, et al. (2002) Susceptibility to proteolysis of triosephosphate isomerase from two pathogenic parasites. Characterization of an enzyme with an intact and a nicked monomer. Proteins 48: 580–590.
2. Zomosa-Signoret V, Hernández-Alcántara G, Reyes-Vivas H, Martínez-Martínez E, Garza-Ramos G, et al. (2003) Control of the reactivation of homodimeric triosephosphate isomerase from unfolded monomers. Biochemistry 42: 3311–3318.
3. Tellez-Valencia A, Avila-Ríos S, Perez-Montfort R, Rodríguez-Romero A, Tuena de Gómez-Puyou M, et al. (2002) Highly specific inactivation of triosephosphate isomerase from Trypanosoma cruzi by agents that act on the dimer interface. Biochem Biophys Res Com 295: 958–963.
4. Maldonado E, Moreno A, Panneerselvam K, Ostoa-Saloma P, Garza-Ramos G, et al. (1997) Crystallization and preliminary X-Ray analysis of triosephosphate isomerase from Trypanosoma cruzi. Prot Pept Lett 4: 139–144.
5. Maldonado E, Soriano-García M, Moreno A, Cabrera N, Garza-Ramos G, et al. (1998) Differences in the intersubunit contacts in triosephosphate isomerase from two closely related pathogenic trypanosomes. J Mol Biol 283: 193–203.
6. Ostoa-Saloma P, Garza-Ramos G, Ramírez J, Becker I, Berzunza M, et al. (1997) Cloning, expression and characterization of triosephosphate isomerase from Trypanosoma cruzi. Eur J Biochem 244: 700–705.
7. Garza-Ramos G, Cabrera N, Saavedra-Lira E, Tuena de Gómez-Puyou M, Ostoa-Saloma P, et al. (1998) Sulfhydryl reagent susceptibility in proteins with high sequence similarity: triosephosphate isomerase from Trypanosoma brucei, T. cruzi, and Leishmania mexicana. Eur J Biochem 253: 684–691.
8. Perez-Montfort R, Garza-Ramos G, Hernández-Alcántara G, Reyes-Vivas H, Gao XG, et al. (1999) Derivatization of the interface cysteine of triosephosphate isomerase from Trypanosoma brucei and Trypanosoma cruzi as probe of the interrelationship between the catalytic sites and the dimer interface. Biochemistry 38: 4114–4120.
9. Gómez-Puyou A, Saavedra-Lira E, Becker I, Zubillaga R, Rojo-Dominguez A, et al. (1995) Using evolutionary changes to achieve species specific inhibition of enzyme action. Studies with triosephosphate isomerase. Chemistry and Biology 2: 847–855.
10. Garza-Ramos G, Perez-Montfort R, Rojo-Domínguez A, Tuena de Gómez-Puyou M, Gómez-Puyou A (1996) Species specific inhibition of homologous enzymes by modification of nonconserved amino acids. The cysteines of triosephosphate isomerase. Eur J Biochem 241: 114–120.
11. Cabrera N, Hernández-Alcántara G, Mendoza-Hernandez G, Gómez-Puyou A, Perez-Montfort R (2008) Key residues of loop 3 in the interaction with the interface residue at position 14 in triosephosphate isomerase from Trypanosoma brucei. Biochemistry 47: 3499–3506.
12. Maity H, Maity M, Krishna MM, Mayne L, Englander SW (2005) Protein folding: the stepwise assembly of foldon units. Proc Natl Acad Sci USA 102: 4741–4746.
13. Freire E (1999) The propagation of binding interactions to remote sites in proteins: an analysis of the monoclonal antibody D1.3 to lysozyme. Proc Natl Acad Sci USA 96: 10118–10122.
14. Halabi N, Rivoire O, Leibler S, Rangantahan R (2009) Protein sectors: evolutionary units of three-dimensional structure. Cell 138: 774–786.
15. He Y, Chen Y, Alexander P, Bryan PN, Orban J (2008) NMR structures of two designed proteins with high sequence identity but different fold and function. Proc Natl Acad Sci USA 105: 14412–14417.
16. Yuan SM, Clarke ND (1998) A hybrid sequence approach to the paracelsus challenge. Proteins 30: 136–143.
17. Capra JA, Singh M (2008) Characterization and prediction of residues determining protein functional specificity. Bioinformatics 24: 1473–1480.
18. Law PY, Wong YH, Loh HH (1999) Mutational analysis of the structure and function of opioid receptors. Biopolymers 51: 440–455.
19. Sadelain M, Brentjens R, Riviere I (2009) The promise and potential pitfalls of chimeric antigen receptors. Curr Opin Immunol 21: 215–223.
20. Yin D, Gavi S, Wang H, Malbon CC (2004) Probing receptor structure/function with chimeric G-protein-coupled receptors. Mol Pharmacol 65: 1323–1332.
21. Perez-Montfort R, Tuena de Gómez-Puyou M, Gómez-Puyou A (2002) The interfaces of oligomeric proteins as targets for drug design against enzymes from parasites. Curr Top Med Chem 2: 457–470.
22. Krissinel E, Henrick K (2007) Inference of macromolecular assemblies from crystalline state. J Mol Biol 372: 774–797.
23. Malabanan MM, Amyes TL, Richard JP (2010) A role for flexible loops in enzyme catalysis. Curr Opin Struct Biol 20: 702–710.
24. Reyes-Vivas H, Hernández-Alcántara G, López-Velazquez G, Cabrera N, Perez-Montfort R, et al. (2001) Factors that control the reactivity of the interface cysteine of triosephosphate isomerase from Trypanosoma brucei and Trypanosoma cruzi. Biochemistry 40: 3134–3140.
25. Borchert TV, Pratt K, Zeelen JP, Callens M, Noble ME, et al. (1993) Overexpression of trypanosomal triosephosphate isomerase in Escherichia coli and characterization of a dimer-interface mutant. Eur J Biochem 211: 703–710.

26. Leslie AGW (1992) Recent changes to the MOSFLM package for processing film and image plate data. Joint CCP4 + ESF-EAMCB Newsletter on Protein Crystallography 26.
27. Collaborative-Computational-Project-4 (1994) The CCP4 suite: programs for protein crystallography. Acta Crystallogr D50: 760–763.
28. McCoy AJ, Grosse-Kunstleve RW, Adams PD, Winn MD, Storoni LC, et al. (2007) Phaser crystallographic software. J Appl Crystallogr 40: 658–674.
29. Murshudov GN, Vagin AA, Dodson EJ (1997) Refinement of macromolecular structures by the maximum-likelihood method. Acta Crystallogr D53: 240–255.
30. Adams PD, Afonine PV, Bunkoczi G, Chen VB, Davis IW, et al. (2010) PHENIX: a comprehensive Python-based system for macromolecular structure solution. Acta Crystallogr D Biol Crystallogr 66: 213–221.

ChemPubSoc Europe

DOI: 10.1002/cmdc.201500385

CHEMMEDCHEM Full Papers

SPECIAL ISSUE

Potent and Selective Inhibitors of *Trypanosoma cruzi* Triosephosphate Isomerase with Concomitant Inhibition of Cruzipain: Inhibition of Parasite Growth through Multitarget Activity

Elena Aguilera,[a] Javier Varela,[a] Estefanía Birriel,[a] Elva Serna,[b] Susana Torres,[b] Gloria Yaluff,[b] Ninfa Vera de Bilbao,[b] Beatriz Aguirre-López,[c] Nallely Cabrera,[c] Selma Díaz Mazariegos,[c] Marieta Tuena de Gómez-Puyou,[c] Armando Gómez-Puyou,[c] Ruy Pérez-Montfort,[c] Lucia Minini,[d] Alicia Merlino,[d] Hugo Cerecetto,[a, e] Mercedes González,[a] and Guzmán Alvarez*[a, f]

Dedicated to the memory of Armando Gómez-Puyou—an exemplary scientist and friend.

Triosephosphate isomerase (TIM) is an essential *Trypanosoma cruzi* enzyme and one of the few validated drug targets for Chagas disease. The known inhibitors of this enzyme behave poorly or have low activity in the parasite. In this work, we used symmetrical diarylideneketones derived from structures with trypanosomicidal activity. We obtained an enzymatic inhibitor with an IC_{50} value of 86 nM without inhibition effects on the mammalian enzyme. These molecules also affected cruzipain, another essential proteolytic enzyme of the parasite. This dual activity is important to avoid resistance problems. The compounds were studied in vitro against the epimastigote form of the parasite, and nonspecific toxicity to mammalian cells was also evaluated. As a proof of concept, three of the best derivatives were also assayed in vivo. Some of these derivatives showed higher in vitro trypanosomicidal activity than the reference drugs and were effective in protecting infected mice. In addition, these molecules could be obtained by a simple and economic green synthetic route, which is an important feature in the research and development of future drugs for neglected diseases.

Introduction

Chagas disease is caused by the parasite *Trypanosoma cruzi*. It remains the major parasitic disease in Latin America, despite recent advances in the control of its vector-borne and transfusion-mediated transmission.[1] Moreover, migration of infected people has spread the disease to non-endemic areas, presenting a new worldwide challenge.[2] The chemotherapy regime employed to control the parasitic infection employs old and nonspecific drugs, such as Nifurtimox and Benznidazole, and requires long-term treatment that can give rise to severe side effects.[3] Although Nifurtimox and Benznidazole are able to eliminate patent parasitemia and decrease serological titers in acute and early chronic infections, they are not active against all *T. cruzi* strains, exhibit low efficiency in long-term chronic infections, and are mutagenic.[4] Unfortunately, due to a perceived deficit in potential revenue, most pharmaceutical companies have neglected this disease despite the urgent need for new drugs.

A variety of molecular targets has been identified for designing new drugs, among which are metabolites formed during sterol biosynthesis, glycolysis, and DNA synthesis.[5,6] An important characteristic of *T. cruzi* is its dependence on glycolysis as an energy source for cellular survival.[7] Thus, enzymes of this

[a] *E. Aguilera, J. Varela, E. Birriel, Dr. H. Cerecetto, Dr. M. González, Dr. G. Alvarez*
Grupo de Química Medicinal, Facultad de Ciencias
Universidad de la República, Iguá 4225, Montevideo, 11600 (Uruguay)

[b] *E. Serna, S. Torres, G. Yaluff, Dr. N. V. de Bilbao*
Departamento de Medicina Tropical
Instituto de Investigaciones en Ciencias de la Salud
Universidad Nacional de Asunción, Asunción, 2511 (Paraguay)

[c] *B. Aguirre-López, N. Cabrera, S. Díaz Mazariegos, Dr. M. T. de Gómez-Puyou, Dr. A. Gómez-Puyou, Dr. R. Pérez-Montfort*
Departamento de Bioquímica y Biología Estructural
Instituto de Fisiología Celular
Universidad Nacional Autónoma de México, México DF, 04510 (México)

[d] *L. Minini, Dr. A. Merlino*
Laboratorio de Química Teórica y Computacional, Facultad de Ciencias
Universidad de la República, Iguá 4225, Montevideo, 11600 (Uruguay)

[e] *Dr. H. Cerecetto*
Área de Radiofarmacia, Centro de Investigaciones Nucleares
Facultad de Ciencias, Universidad de la República
Iguá 4225, Montevideo, 11600 (Uruguay)

[f] *Dr. G. Alvarez*
Laboratorio de Moléculas Bioactivas
Centro Universitario Regional Litoral Norte
Universidad de la República, Rute 3 km 363, Paysandú, 60000 (Uruguay)
E-mail: guzmanalvarezlqo@gmail.com

Supporting information and ORCID(s) from the author(s) for this article are available on the WWW under http://dx.doi.org/10.1002/cmdc.201500385.

This article is part of a Special Issue on Polypharmacology and Multitarget Drugs. To view the complete issue, visit: http://onlinelibrary.wiley.com/doi/10.1002/cmdc.v11.12/issuetoc.

© 2016 Wiley-VCH Verlag GmbH & Co. KGaA, Weinheim

pathway represent excellent targets for research of small molecules that could inhibit them selectively and affect their metabolic function.

In this sense, *T. cruzi* triosephosphate isomerase (*Tc*TIM) has been proposed as a validated target for drug design against this parasite.[8] TIM catalyzes the isomerization of glyceraldehyde-3-phosphate and dihydroxyacetone phosphate in the fifth step of the glycolytic pathway. Structurally, most known TIMs are homodimers, with each monomer consisting of eight parallel β-strands, surrounded by eight α-helices and forming a barrel. An important feature of the TIM active site is the concerted closure of loop 6 and loop 7 on ligand binding, shielding the catalytic site from bulk solvent. The buried active site stabilizes the enediolate intermediate. The catalytic residue Glu167 is at the top of loop 6. On closure of loop 6, the Glu167 carboxylate moiety moves approximately 2 Å towards the substrate. The dynamic properties of the Glu167 side chain in the enzyme–substrate complex are a key feature of the proton shuttling mechanism. Two proton shuttling mechanisms, the classical and the criss-cross mechanism, are responsible for the interconversion of the substrates of this enolizing enzyme. The interface between monomers occupies a significant portion of the molecular surface area of each monomer, approximately 1496 Å^2 for *Tc*TIM.[9] Interestingly, TIM is active only as a dimer; therefore, the use of small molecules to target its interface may potentially induce structural modifications and alter the dimer, leading to enzyme inactivation.[10] TIM from *homo sapiens* (*Hs*TIM) and the *T. cruzi* enzyme have the same catalytic residues. However, the identity of the approximately 32 interfacial residues of *Tc*TIM and *Hs*TIM is 52%, whereas the identity of those residues between *Tc*TIM and TIM from *Trypanosoma brucei* (*Tb*TIM) is approximately 82%.[11] Therefore, it is theoretically possible to find molecules that have high specificity for the interface of the enzymes from these parasites.[11] As part of an ongoing program in the research for molecules that could provide leads in the design of a new drug for the treatment of Chagas disease, in a previous work, we undertook a massive screening for *Tc*TIM inhibitors. Initially, we performed a primary screening of 230 compounds from an in-house chemical library.[12] The IC_{50} and the selectivity for *Tc*TIM were then determined for the best inhibitors, and we found that some of the best inhibitors of *Tc*TIM were symmetric molecules (Figure 1 A).[12]

Also a lot of simple molecules with structural symmetry have shown trypanosomicidal activity, like curcumin derivatives and others with more complex structures.[13–16] In addition, results obtained in a previous study using a phenotypic screening of *T. cruzi* on near 80 new thiazolyl derivatives allowed the identification of a new bioactive structural motif.[17]

In order to obtain derivatives with inhibitory action on *Tc*TIM and with good activity against *T. cruzi*, we selected frameworks from the diarylideneketone and furylthiazolidine systems (Prototype I and Prototype II in Figure 1 B, respectively), and redesigned the synthesis to obtain simpler and symmetrical molecules. In particular, we replaced the diarylidene system (Figure 1 B) with the furylidene motif previously described to have good trypanosomicidal activity.[12, 13, 16, 17]

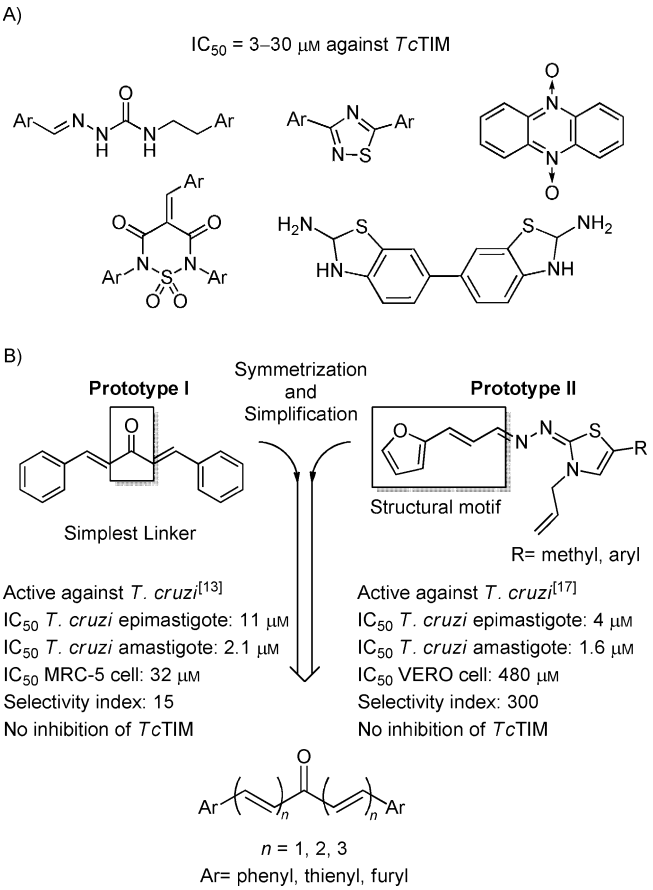

Figure 1. A) Symmetric inhibitors of *Tc*TIM previously reported; Ar denotes an aryl group. B) Trypanosomicidal structures used as basis for designing new and simpler symmetric diarylideneketone from dibenzalketone (Prototype I) and furylthiazolidines (Prototype II) with some of their biological data.[12, 13, 17]

Results and Discussion

Synthesis of diarylideneketones

The scope of the design of these molecules was the presence of the pharmacophore identified in the previous work: the furylpropenyl fragment.[14] We synthesized 23 derivatives (Tables 1 and 2) with good to excellent yields (60–100%). The synthesis was carried out with environmentally friendly solvents. In most cases, the purification was done by crystallization from ethanol. Consequently, these compounds follow the principles of green chemistry with simple, economical, and environmentally friendly synthesis.[17] For example, the synthesis of one of the most active compounds was performed using furfural, which can be obtained from rice husk (a waste material from the food industry), acetone, ethanol, sodium hydroxide, and water—all reagents being inexpensive and easy to acquire.[18–20]

Anti-*T. cruzi* activity in vitro

The derivatives were initially tested in vitro against the epimastigote form of *T. cruzi*, Tulahuen 2 strain, discrete typing unit (DTU) Tc VI. The compounds were incorporated into the culture

© 2016 Wiley-VCH Verlag GmbH & Co. KGaA, Weinheim

Table 1. Compounds derived from prototype II. Structures of the newly developed compounds, their trypanosomicidal activity against epimastigotes of *Trypanosoma cruzi*, and cytotoxicity against mammalian cells.

Compd	Structure	IC_{50} [μM] *T. cruzi*[a]	IC_{50} [μM] J774.1[b]	SI[c]
Prototype II	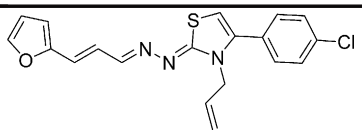	4.2 ± 0.4[d]	120 ± 5[d]	28[d]
1	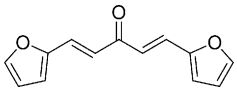	23.9 ± 1.5	115 ± 6	5
2	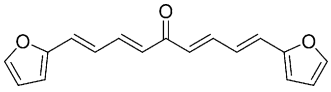	5.0 ± 0.7	60 ± 3	12
3	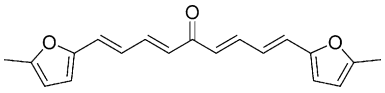	9.4 ± 1.4	ND[e]	–
4	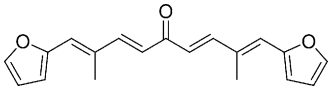	8.2 ± 2.0	33 ± 5	4
5	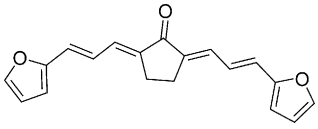	5.4 ± 1.6	19 ± 2	4
6	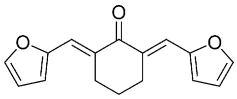	7.3 ± 1.6	115 ± 5	16
7	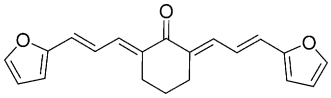	0.6 ± 0.2	10 ± 2	17
8	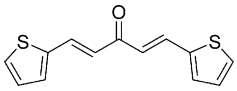	5.0 ± 0.8	38 ± 4	8
9	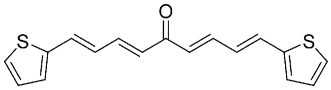	12.6 ± 1.4	188 ± 6	15
10	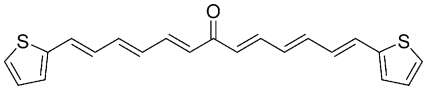	> 25	ND[e]	–
11	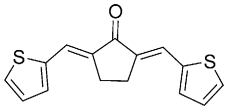	6.5 ± 1.1	ND[e]	–
12	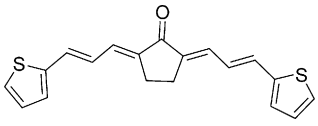	0.04 ± 0.01	15 ± 4	375
13	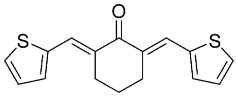	3.6 ± 0.9	73 ± 4	20
14	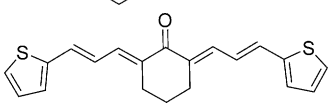	0.6 ± 0.2	20 ± 1	33

milieu at a final concentration of 25 μM, and their ability to inhibit the parasite growth was evaluated and compared to the control (without drug) on day 5. The IC_{50} was determined for the most active derivatives and for Nifurtimox used as the reference drug (Table 1and 2). The 58% of the synthesized molecules displayed good to excellent trypanosomicidal activity ($IC_{50} < 25$ μM). In addition, compounds **7**, **12**, and **14**, with IC_{50} in the submicromolar and nanomolar range, exhibited enhanced trypanosomicidal activity relative to Nifurtimox and their parent compounds Prototype I and Prototype II. We confirmed that the incorporation of a furylacroleine fragment increased the trypanosomicidal activity (comparing the activities of compounds **2** and **1**, and **2** and **15**).

Symmetry played a key role in the anti-*T. cruzi* activity of these molecules (based on the activities of compound **23** and the Prototype I). The number of conjugated double bonds, present between the aryl and carbonyl moieties, caused different effects in the trypanosomicidal activity. For example, for the heteroaryl cyclic ketones, the increase in the number of double bonds increased the bioactivity (as seen for the activities of derivative **6** compared with **7**, derivative **11** compared with **12**, or derivative **13** compared with **14**). With the exception of derivatives **1** and **2**, the contrary occurred in the linear ketones (shown by the activities of derivative **8** compared with **9** and **10**, or Prototype I and **15**). Additionally, the data suggest that the incorporation of an electron donor group (like methyl) to the system decreases trypanosomicidal activity (activities of derivative **2** compared to **3** and **4**). In the case of the cycloheptanones, the compounds without the α,β-ketone system, and the compounds without

© 2016 Wiley-VCH Verlag GmbH & Co. KGaA, Weinheim

Table 1. (Continued)

Compd	Structure	IC_{50} [μM] *T. cruzi*[a]	IC_{50} [μM] J774.1[b]	SI[c]
Nifurtimox	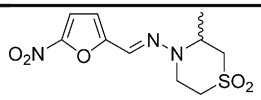	8±1	316±23	40

Compound concentration required to inhibit [a] 50% epimastigote growth of *T. cruzi*, Tulahuen 2 strain or [b] murine macrophages; data represent the mean±SD of two independent experiments performed in triplicate. [c] Selectivity index (SI): IC_{50} against mammalian cells/IC_{50} against *T. cruzi*. [d] Data from Ref. [17]. [e] ND: not determined.

Table 2. Compounds derived from prototype I, the simplest form. Structures of known compounds, their trypanosomicidal activity against epimastigotes of *Trypanosoma cruzi*, and cytotoxicity against mammalian cells.[16]

Compd	Structure	IC_{50} [μM] *T. cruzi*[a]	IC_{50} [μM] J774.1[b]	SI[c]
Prototype I[d]	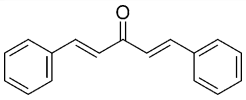	7.2±0.8	22±5	3
15	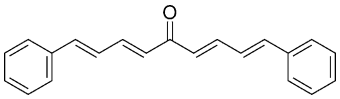	11.0±1.3	50±5	5
16	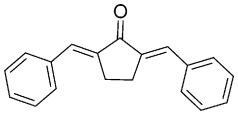	15.9±1.2	ND[e]	–
17	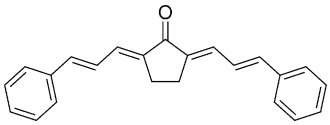	>25	ND[e]	–
18	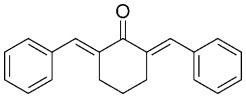	5.1±0.3	115±5	23
19	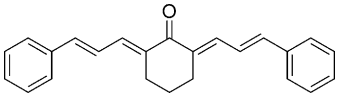	14.2±2.7	168±6	12
20	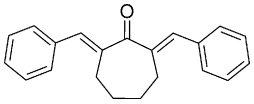	>25	ND[e]	–
21	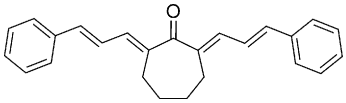	>25	ND[e]	–
22	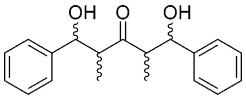	>25	ND[e]	–
23	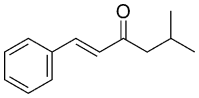	>25	ND[e]	–
Nifurtimox	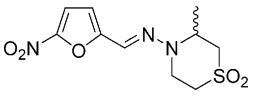	8±1	316±23	40

Compound concentration required to inhibit [a] 50% epimastigote growth of *T. cruzi*, Tulahuen 2 strain or [b] murine macrophages; data represent the mean±SD of two independent experiments performed in triplicate. [c] Selectivity index (SI): IC_{50} against mammalian cells/IC_{50} against *T. cruzi*. [d] Data from Ref. [16]. [e] ND: not determined.

symmetry (compounds **20**–**23**, Table 2), the anti-*T. cruzi* activity decreases dramatically. Furyl-cyclohexanone **7**, thienyl-cyclopentanone **12**, and thienyl-cyclohexanone **14** have trypanosomicidal activity in the submicromolar and nanomolar range. In particular, compound **12** was 200 times more potent than Nifurtimox.

Nonspecific toxicity in mammalian cells in vitro

To explore the selectivity of these new derivatives against *T. cruzi*, we evaluated the nonspecific mammalian cell toxicity in vitro using J774.1 mouse macrophages. The evaluated compounds were selected taking into account their anti-*T. cruzi* activity, and their selectivity indexes were calculated as the ratio between the IC_{50} for mammalian cells and the IC_{50} for *T. cruzi*. The most potent compound against *T. cruzi* (compound **12**) showed an excellent selectivity index (SI), and was 375 times more active against *T. cruzi* than the mammalian cells and near tenfold more selective than the reference drug (Table 1and 2). Comparing the Prototype I with the cyclohexanone **18**, we saw that the flexibility restriction of the molecule by addition of a cycle causes a 7-fold increase in selectivity. Moreover, the extra double bond in derivative **2** relative to **1**, derivative **9** to **8**, derivative **14** to **13**, or derivative **15** to Prototype I, also caused an increase in the selectivity.

Treatment of *T. cruzi*-infected mice

Compounds **2**, **7**, and **12** were evaluated in vivo in a murine model of acute Chagas disease. The chosen compounds for this in vivo assay were the most structurally representative and active molecules of the family of

© 2016 Wiley-VCH Verlag GmbH & Co. KGaA, Weinheim

compounds, with lower nonspecific toxicity and good trypanosomicidal activity. Compound **14** was not tested in vivo because it was a less potent inhibitor of TIM than compound **7** (see below). Benznidazole was used as the reference drug. For optimum oral administration we selected a microemulsion as vehicle which previously demonstrated good bioavailability with compounds like Prototype II.[17] For the experiment, eight male BALB/c mice, infected with CL Brener clone, DTU Tc VI, were treated orally, by intragastric cannula, during 15 days with compounds **2**, **7**, and **12** at 192 μmol kg^{-1} body weight/day (the optimal dose previously established for Prototype II)[17] and compound **7** at 384 μmol kg^{-1} body weight/day in the microemulsion, or Benznidazole at 192 μmol kg^{-1} body weight/day in saline solution. The course of the infection was monitored by counting blood parasites and animal survival, and was followed during 60 days postinfection, in two independent experiments. Derivative **2** led to a significant decrease of the parasitemia (over 50% in the maximum peak of parasitemia and in the second peak, Figure 2) and 83% survival of the treated mice (versus 50% for untreated animals in the same assay). To avoid this fact, a longer duration of treatment could reverse this situation. In other experiments, derivative **7** at the two analyzed doses showed significant decrease of the parasitemia level, but no differences were observed in the double dose (×2) treatment. Derivative **7**, mainly at the lower assayed dose, was able to shift the maximum parasitemia peaks, from day 21 to 28, and day 38 to 45. Additionally, derivative **7** produced a survival of 100% of the animals during the assay. Derivative **12** showed some toxicity achieving significantly reduced parasitemia, although there was a 40% survival of the animals. This goes in contrast to the shown in vitro selectivity index (Table 1). Additionally, derivative **12** was able to abolish the second maximum peak of parasitemia.

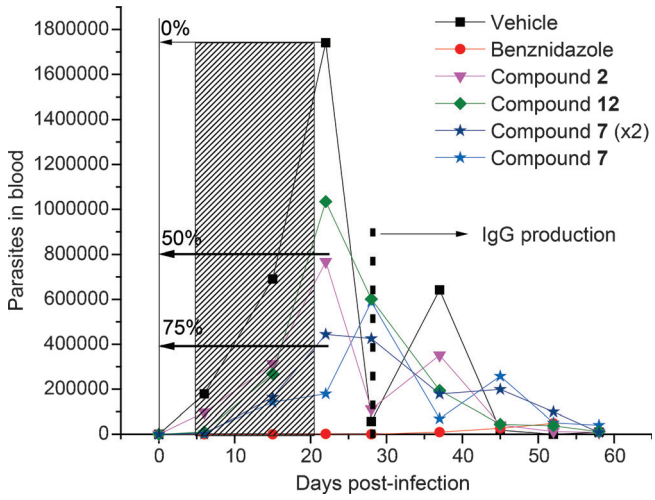

Figure 2. In vivo study of compounds **2**, **7**, and **12** in the acute model of Chagas disease. Curve of parasitemia (parasites per mL of blood) at days postinfection was compared with the control untreated mice (vehicle). The shaded zone shows the treatment period (15 days), and the dashed line marked with IgG shows the start of immune system protection (around 30 days postinfection). Treatments with compound **2** at 192 μmol kg^{-1} body weight/day, compound **7** at 192 or 384 μmol kg^{-1} body weight/day, compound **12** at 192 μmol kg^{-1} body weight/day, and Benznidazole at 192 μmol kg^{-1} body weight/day are shown. Each point represents the average parasitemia of eight mice in each group every seven days. The percentage was calculated from the decrease in the parasitemia peak related to the maximum peak, corresponding to the group of untreated mice. The use of eight mice determines that the results are statistically correct.

Inhibition of triosephosphate isomerase

In order to investigate if these compounds act on *Tc*TIM, we initially tested all of them against the enzyme at a concentration of 25 μM using percentages of inhibition higher than 70% as an arbitrary cut-off point. Some compounds precipitated at 25 μM, leading to variability in the data inhibition at this point. We could not reach 100% inhibition for this reason. Using this cut-off, we detected one new inhibitor (derivative **7**) of *Tc*TIM with better inhibition capacity than the thiadiazolone inhibitor previously described by our group (Table 3).[21,22] Derivative **7** was 40 times more potent than the thiadiazolone and in our knowledge is the best *Tc*TIM inhibitor described until now. Additionally, derivatives **1**, **2**, **4**, **12**, **13**, **14**, and **17** also displayed good IC_{50} but higher than the corresponding values for derivative **7**. It is worth noting that the lack of the extra double bond in compound **1** causes a little decrease in the inhibitory capacity compared with compound **2**. The symmetry of the molecules and the size and the type of the heteroatom present in the aryl ring are important for the inhibition of *Tc*TIM (see molecular docking results in the section below).

To test the selectivity of the inhibition, derivatives **2**, **7**, and **12** were assayed on *Tb*TIM and *Hs*TIM. These compounds were unable to inactivate *Tb*TIM or *Hs*TIM at concentrations higher than 100 μM (see example for **7** in Figure 3). These results confirmed the selectivity and the specificity of these molecules for *Tc*TIM. The destabilization of the dimer was studied using size-exclusion chromatography of *Tc*TIM, in the absence and presence of derivative **7**. We compared the effect of derivative **7** with a monomerization agent like methyl methanethiosulfonate (MMTS).[7] This study showed that the enzyme always elutes as a dimer (Figure S1 in the Supporting Information). These results indicated that the cause of inhibition of *Tc*TIM by derivative **7** does not involve the disruption of the dimer.

Inhibition of cruzipain

When we observed that the activity of the studied compounds in the parasite was not explained only by the TIM inhibition, we decided to explore another target. In order to investigate if the studied compounds were also inhibitors of another molecular target in the parasite, we tested their activity on cruzipain. Cruzipain is a cysteine protease of *T. cruzi* that has been validated as a target because inhibitors of this enzyme affect the evolution of the pathology.[6] We initially tested all derivatives against the enzyme at a concentration of 100 μM using percentages of inhibition higher than 30% as an arbitrary cut-off point. Using this cut-off, we detected two new inhibitors (derivatives **7** and **14**) of cruzipain (Table 4). This enzyme was purified from epimastigotes, and it is important to highlight that the activity in this type of enzyme is more representative than

© 2016 Wiley-VCH Verlag GmbH & Co. KGaA, Weinheim

Table 3. IC_{50} values against *T. cruzi* triosephosphate isomerase (*Tc*TIM) of the best enzymatic inhibitors.

Compd	Structure	IC_{50} [μM][a]
Prototype II	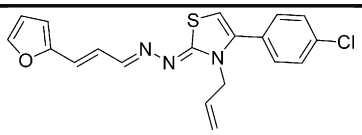	>25
1	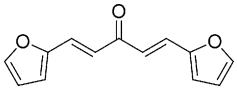	5±1
2	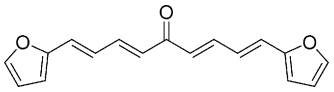	3.0±0.7
4	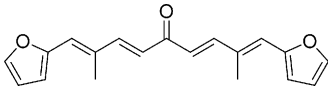	3.3±0.5
7	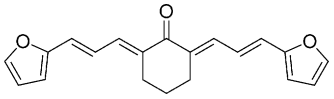	0.086±0.007
12	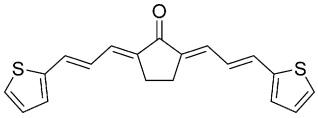	4.7±0.8
13	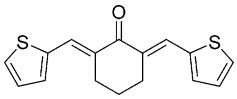	6±1
14	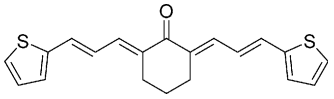	7±1
Prototype I	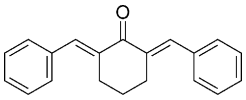	>25
17	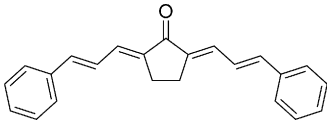	7±1
Thiadiazolone[b]	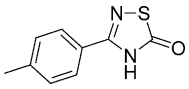	3.5±0.5

[a] IC_{50} values against *Tc*TIM; data represent the mean±SD of two independent experiments performed in triplicate. [b] Inhibitor described previously.[18,19]

the activities in the recombinant version of the enzyme (called cruzain). In the recombinant version one can find inhibitors in the nanomolar range, but in the version purified from epimastigotes (called cruzipain) in the micromolar range.[23,32] We found other derivatives with moderate activity in cruzipain: compounds **2**, **8**, **18**, and **19**. The other tested compounds did not affect the enzyme at a concentration of 100 μM.

We think that the trypanosomicidal activity of the studied compounds could also be explained by affecting other targets like trypanothione reductase,[16] and/or glutatione *S*-tranferase, since we have found inhibition of the last enzyme in other parasites (data not shown).

Molecular docking studies

Molecular docking studies were performed after inhibition experiments to investigate the binding mode of three inhibitors of *Tc*TIM, derivatives **1**, **2**, and **7**, and one derivative with no ability to inhibit *Tc*TIM, derivative **9**. The binding mode of derivative **2** to *Hs*TIM was also analyzed in order to explain its selectivity for *Tc*TIM. The predicted binding modes of derivatives **1**, **2**, **7**, and **9** to *Tc*TIM are shown in Figure 4A–D, and the docking model for derivative **2** with *Hs*TIM is shown in Figure 5.

As illustrated in Figure 4, derivatives **2** (4B) and **7** (4C) bind to the dimer interface. These compounds, having an additional double bond relative to compound **1** (4A), demonstrate the importance of the distance between the two aryl rings as a requirement to bind to the dimer interface. Additionally, the predicted binding mode for derivative **1** (Figure 4A) explains its lower activity, since it binds to a loop at the surface of the enzyme and, thus, can be easily removed from this site due to *Tc*TIM dynamics in solution.[36] Comparing the binding modes of derivative **2** and **9** (Figure 4D), it can be seen that the active compound **2** is stabilized in the binding cleft by strong hydrogen-bond interactions. The furyl oxygen of the inhibitor is hydrogen bonded to the backbone nitrogen of Gly100, and the carbonyl oxygen of the inhibitor interacts with Arg95 side chain (3.0 Å and 2.9 Å, respectively). These interactions were absent in compound **9**. Therefore, besides the conjugate double bonds, the presence of a furyl ring in the molecule is a structural requirement to adequately position the molecule to exert its inhibitory activity against *Tc*TIM. On the other hand, derivative **7**, which inhibits the enzyme in the nanomolar range, is also located in at the interface establishing hydrophobic interactions with Tyr99 and Phe72 of both monomers, and the furyl rings also provide π-cation and π–π-type interactions with residues of Lys110 (monomer A) and Phe72 (monomer B), respectively (Figure 4C). Interestingly, residue Phe72 is located in loop 3, which is involved in maintaining the integrity of the

© 2016 Wiley-VCH Verlag GmbH & Co. KGaA, Weinheim

Table 4. IC_{50} values against cruzipain of the best enzymatic inhibitors of *T. cruzi* triosephosphate isomerase (*Tc*TIM).

Compd	Structure	IC_{50} [μM][a]	Inhibition [%][b]
2	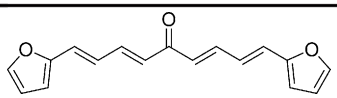	–	48%
7	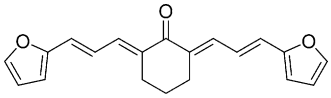	37.0 ± 1.1	–
8	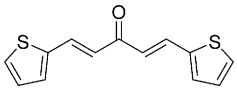	–	49%
12	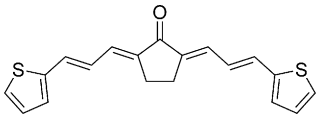	42 ± 2	–
18	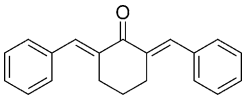	–	38%[c]
19	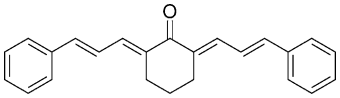	–	40%

[a] IC_{50} values against cruzipain; data represent the mean ± SD of two independent experiments performed in triplicate. [b] Percent inhibition of *Tc*TIM at a compound concentration of 100 μM. [c] According to Ref. [16], at 100 μM, this compound inhibits 31% of the activity of recombinant cruzain.

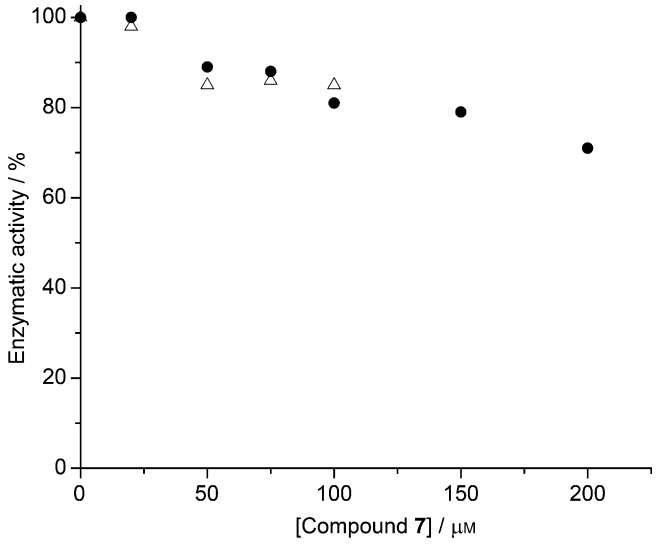

Figure 3. Enzyme inhibition studies. *Hs*TIM (●) and *Tb*TIM (△) activity vs. concentration of compound **7**. Data points represent the mean for triplicates in two independent experiments.

dimer. Comparing derivatives **2** and **7**, one can see that derivative **7** has a restricted movement and a defined orientation because of the chair-like conformation of the cyclohexyl moiety. This orientation increases the π–π interactions. The predicted binding mode of derivative **2** to *Hs*TIM is shown in Figure 5. Clearly, derivative **2** was unable to bind to the dimer interface in *Hs*TIM. Instead, it interacts weakly on the enzyme's surface, which could explain the selectivity of this compound for *Tc*TIM.

Integration of the data

We found three molecules with improved in vitro trypanosomicidal activity in the nanomolar range: compounds **7**, **12**, and **14**. These molecules were more active than the reference drug (Nifurtimox).

Analyzing the whole population of compounds and from the small differences in their structures, it can be said that those containing furyl and thienyl rings are the most active compounds, and the optimal number of conjugated double bonds is four, for the symmetric forms. Also, the movement restriction of the α-carbonyl-carbon improves trypanosomicidal activity. Moreover, this restriction of rotation seems to increase the selectivity. The lack of symmetry leads to loss of trypanosomicidal activity, as seen when comparing compounds **18** with **20** and **23**. Derivatives **2**, **7**, and **12** were able to protect infected animals with *T. cruzi*.

Enzymatic inhibition assays showed that one of the biological targets of derivatives **2** and **7** is *Tc*TIM, an essential enzyme for the metabolism of amastigotes and epimastigotes. A positive qualitative correlation between inhibition of *Tc*TIM and trypanosomicidal activity in vitro was observed. Moreover, compounds **2** and **7** lacked inhibitory activity against *Hs*TIM and *Tb*TIM. Structurally *Tb*TIM is 80% similar to *Tc*TIM, and we demonstrated that it is possible to obtain molecules with specific inhibition of *Tc*TIM besides this apparently small difference between them. The mechanism of inhibition does not involve disruption of the dimer as the other inhibitors previously reported.[24,25] Initially, it was thought that inhibitors targeting the dimer interface caused destabilization and loss of activity. As observed for the MMTS and its analogs, they interact at the interface at Cys15, which is critical for stability.[7,11] Molecular docking studies were consistent with the experimental data, suggest the mechanisms of inhibition, and could explain the selectivity for these novel compounds. Docking results also suggest a possible site of interaction between the inhibitors and *Tc*TIM. It can be seen that the interaction at the interface is located near loop 6 and loop 7, critical loops for the movement of the active site and substrate input. Thus, the inhibitors may stabilize the dimer and prevent the movement necessary for catalysis. Compound **7** was the most potent inhibitor,

© 2016 Wiley-VCH Verlag GmbH & Co. KGaA, Weinheim

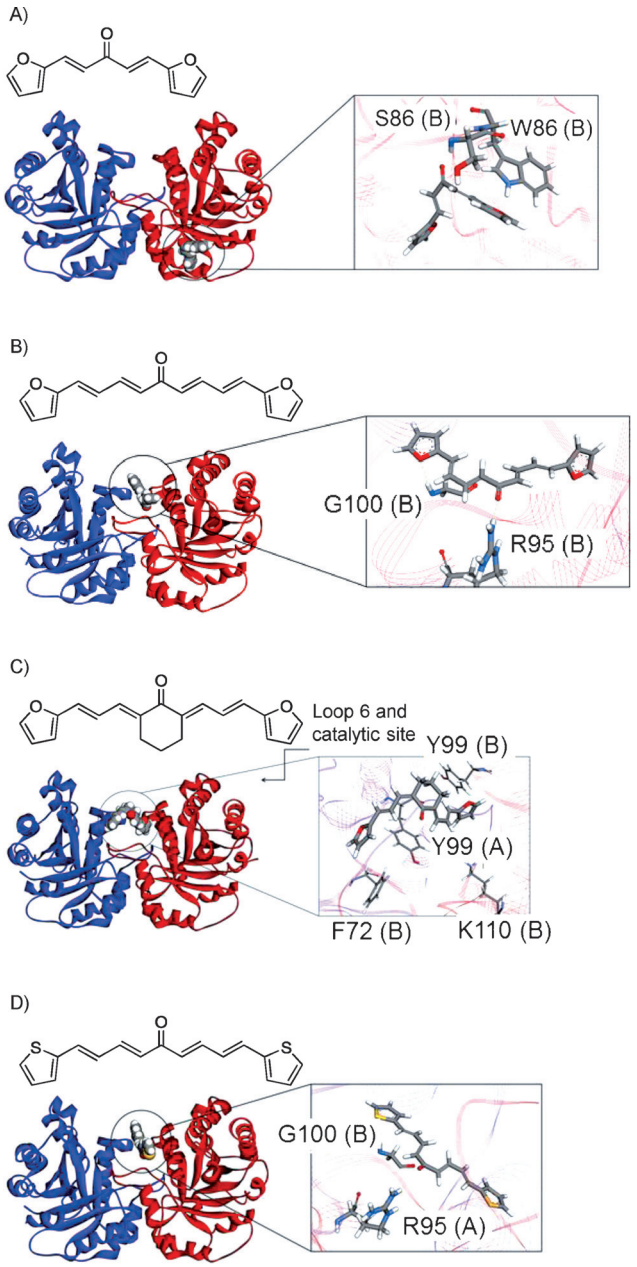

Figure 4. Predicted binding modes. A) Compound **1** did not interact in the interface (too short) and was a moderate inhibitor. B) Compound **2** interacted with the interface and was a good inhibitor. C) Compound **7** interacted with the interface more closely at the critical loop and was the best inhibitor. D) Compound **9** interacted in the interface superficially and was not an inhibitor.

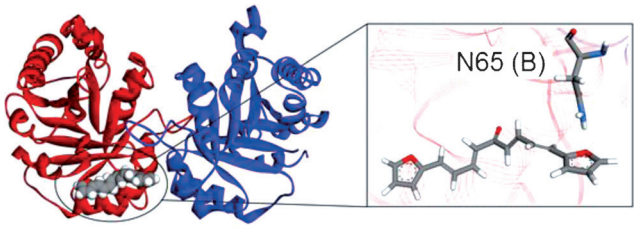

Figure 5. Predicted binding mode of derivative **2** to *Hs*TIM. Derivative **2** did not interact in the interface and did not inhibit the enzyme.

which is 41 times better than the thiadiazolone previously described.[21,22] Additionally, it has in vitro trypanosomicidal activity in the nanomolar range, which is 13 times more active than the reference drug.

Cruzipain inhibition assays showed that another biological target of derivatives **7** and **12** is this essential enzyme. In addition, a positive qualitative correlation between inhibition of cruzipain and trypanosomicidal activity was observed in vitro.

We can hypothesize that the trypanosomicidal activity of derivatives **7** and **12** involve the inhibition of at least two biological targets: *Tc*TIM and cruzipain. Other mechanisms are probably derived from the furylacroleine fragment, a previously described pharmacophore.[17] This fragment could be acting as a substrate for a specific oxidoreductase in the parasite, with the generation of toxic molecules.[26,27] Another target reported for diarylideneketones[13,16] is the thiol metabolism dependent on trypanothione reductase, a flavoenzyme that maintains bis-glutathionylspermidine (trypanothione) and monoglutathionylspermidine in their reduced state. This thiol system replaces the glutathione/glutathione-reductase system (present in mammalian hosts) and is widely accepted as a target for the development of novel therapies to treat trypanosomiasis and leishmaniasis. Finally, another potential target is glutathione *S*-transferase, as part of the same metabolic pathway aforementioned.

Since these compounds are molecules directed to multiple targets, it makes the generation of resistant parasites less likely. In this way, less evolutionary pressure on the parasitic population is generated, thereby lowering the probability of generation of resistance.[28]

Conclusions

A series of highly potent and selective *T. cruzi* growth inhibitors was successfully described. These compounds are structurally different from known compounds, which are less potent and have toxicity liabilities.[12–19] Among them, the most promising compound, derivative **7**, showed efficacy in vivo in the acute model of Chagas disease, with absence of in vivo toxicity and was able to inhibit *Tc*TIM and cruzipain. These results support the progress of this compound as a low-cost multitarget drug candidate.

Experimental Section

General procedure for the synthesis of diarylideneketones 1–21.[29] All characterization data, appearances, yields, spectroscopic data, procedures, and elemental microanalyses are available in the Supporting Information.

In vitro anti-*T. cruzi* test.[17] *T. cruzi* epimastigotes (Tulahuen 2 strain) were grown at 28 °C in brain–heart infusion (BHI)-tryptose milieu supplemented with 5% fetal bovine serum. Cells from a 10-day-old culture (stationary phase) were inoculated into 50 mL of fresh milieu to give an initial concentration of 1×10^6 cells mL^{-1}. Cell growth was followed by measuring the absorbance of the culture at 600 nm every day. Before inoculation, the milieu was supplemented with the indicated quantity (for a first evaluation 25 μM

© 2016 Wiley-VCH Verlag GmbH & Co. KGaA, Weinheim

was used) of the drug from a stock solution in dimethylsulfoxide (DMSO). The final concentration of DMSO in the culture milieu never exceeded 0.4%. Cultures with nontreated epimastigotes and 0.4% DMSO were included as negative controls, while cultures with 8 μM of Nifurtimox were used as positive controls. The percentage of growth inhibition (PGI) was calculated as follows: PGI (%) = $\{1-[(A_p-A_{0p})/(A_c-A_{0c})]\}\times 100$, where $A_p = A_{600}$ of the culture containing the drug at day 5; $A_{0p} = A_{600}$ of the culture containing the drug just after adding the inoculum (day 0); $A_c = A_{600}$ of the culture in the absence of drug (negative control) at day 5; $A_{0c} = A_{600}$ in the absence of the drug at day 0. In order to determine the 50% inhibitory concentration (IC_{50}) values, parasite growth was followed in the absence (negative control) and presence of increasing concentrations of the corresponding drug. At day 5, the absorbance of the culture was measured and related to the control. The IC_{50} value was taken as the concentration of drug needed to decrease the absorbance ratio to 50%. All IC_{50} values in this work were obtained by analysis with the program OriginLab8.5, using sigmoidal regression (PGI vs. logarithm of the compound concentration) and triplicate samples. The positive control PGI was always around 50%.

Nonspecific cytotoxicity assay.[17] J774.1 murine macrophage cells (ATCC, USA) were grown in Dulbecco's Modified Eagle's Medium (DMEM) culture milieu containing 4 mM L-glutamine and supplemented with 10% heat-inactivated fetal calf serum. The cells were seeded in a 96-well plate (5×10^4 cells in 200 μL culture medium) and incubated at 37 °C in a 5% CO_2 atmosphere for 48 h, to allow cell adhesion prior to drug testing. Afterwards, cells were exposed for 48 h to the compounds (12.5–400 μM) or vehicle for control (0.4% DMSO), and additional controls (cells in milieu) were used in each test. Cell viability was then assessed by measuring the mitochondria-dependent reduction of MTT (3-(4,5-dimethylthiazol-2-yl)-2,5-diphenyltetrazolium bromide) to formazan. For this purpose, MTT in sterile PBS (0.2% glucose) pH 7.4 was added to the macrophages to achieve a final concentration of 0.1 mg mL^{-1} and the cells were incubated at 37 °C for 3 h. After removing the milieu, formazan crystals were dissolved in DMSO (180 μL) and MTT buffer (20 μL, 0.1 M glycine, 0.1 M NaCl, 0.5 mM EDTA, pH 10.5), and the absorbance at 560 nm was measured. The IC_{50} was defined as the drug concentration at which 50% of the cells were viable, relative to the control (no drug added), and was determined by analysis using OriginLab8.5 sigmoidal regression (% of viable cells vs. logarithm of the compound concentration) for triplicate samples.

Formulation for in vivo assays.[14,17,30] The lipid-based drug delivery system was prepared using 1.0 g of surfactant (460 mg polyoxyl-40 hydrogenated castor oil, 360 mg of sodium oleate, and 180 mg of soya phosphatidylcholine), 1.0 g of cholesterol, and phosphate buffer enough to make 10 mL of the vehicle. Preparation: each compound was pulverized in a porcelain mortar and mixed with cholesterol, phosphatidylcholine, and polyoxyl-40 hydrogenated castor oil. The mixture was dissolved in $CHCl_3$, and this was evaporated under vacuum to dryness. To ensure complete removal of the $CHCl_3$, a stream of N_2 was passed through the vial for 5 min. In parallel, sodium oleate was dissolved in phosphate buffer and shaken for 12 h at rt in an orbital shaker. This solution was then added to the mix containing the compounds, and the mixture was homogenized and immersed in an ultrasonic bath at full power for 30–60 min until the desired homogeneity and consistency were reached.

In vivo anti-*T. cruzi* activity (acute model).[14,17,31] BALB/c male mice (30 days old, 25–30 g) were infected by intraperitoneal injections of 5×10^3 blood trypomastigotes (CL Brener). One group (eight animals) was used as control (inoculated orally with the vehicle), and two groups of animals were treated with the studied derivatives (eight animals) or Benznidazole (seven animals), respectively. The first parasitemia developed five days postinfection (week 1), and the treatment began seven days later (when 80% of the animals were infected). Compounds were administered orally, using the aforementioned formulation, 0.2 mL at 50 mg kg^{-1} body weight/day, during 15 days (daily, once a day). Parasitemia, in control and treated mice, was determined in tail-vein blood once a week after the first administration during 60 days, and the mortality rate was recorded. The number of parasites (trypomastigotes form) in blood were counted manually in an optical microscope (at 40× magnification). The numbers of parasites in blood were averaged for each group, and the number of parasites in blood vs. time post-infection in days was graphed. The experimental protocols with animals were evaluated and supervised by the local Ethics Committee, and the research adhered to the Principles of Laboratory Animal Care. These recommend five to eight animals per group for a good relation between the number of parasites and errors.

Expression and purification of TIMs. *Tc*TIM, *Tb*TIM, and *Hs*TIM were expressed in *Escherichia coli* and purified as described in the literature.[7–11] After purification, the enzymes were dissolved in 100 mM triethanolamine, 10 mM EDTA ,and 1 mM dithiothreitol (DTT, pH 8) and were precipitated with $(NH_4)_2SO_4$ (75% saturation) for storage at 4 °C. Before use, extensive dialysis against 100 mM triethanolamine, 10 mM EDTA (pH 7.4) was performed. The purity of the protein was analyzed by SDS-PAGE electrophoresis (TIM monomer is 27 kDa). Protein concentration was determined by absorbance readings at 280 nm. The ε ($M^{-1}cm^{-1}$) were 36440 for *Tc*TIM, 33460 for *Tb*TIM, and for *Hs*TIM concentration was determined by Bradford's method, using the Bio-Rad protein assay, with bovine serum albumin as standard.

TIM enzymatic activity and inhibition assays.[14,21,22] Enzymatic activity was determined following the conversion of glyceraldehyde 3-phosphate (GAP) into dihydroxyacetone phosphate. The decrease in absorbance at 340 nm due to oxidation of NADH in a coupled enzyme assay was followed in a multicell Hewlett–Packard spectrophotometer at 25 °C. The reaction mixture (1 mL, pH 7.4) contained 100 mM triethanolamine, 10 mM EDTA, 0.2 mM NADH, 1 mM GAP, and 0.9 units of α-glycerol phosphate dehydrogenase. The reaction was initiated by addition of 1.0 nM of the corresponding TIM or the corresponding TIM preincubated with the studied compounds (from the mixture as described below). In these cases of the inhibition assays, the enzymes at 1.0 μM were preincubated for 2 h at 37 °C with the studied compounds (at different concentrations) in 10% DMSO. The average specific activity of *Tc*TIM with 1 mM GAP as substrate was 3400 μmol (min mg)$^{-1}$ as 100% of activity. The IC_{50} was defined as the drug concentration at which there is only 50% of the initial velocity, relative to the control (no drug added), and was determined by analysis using OriginLab8.5 sigmoidal regression (% of enzymatic activity vs. logarithm of the compound concentration). All assays were done in triplicate, and the average error for each measurement did not exceed 10%.

Cruzipain enzymatic activity and inhibition assays.[23,32] Cruzipain was purified according to the work of Cazzulo et al.[33] Cruzipain (2.5 μM $\varepsilon = 58285\ M^{-1}cm^{-1}$) was incubated in 50 mM acetate buffer pH 5.5 with 50 mM DTT, and 100 μM inhibitor was added, and the solution was shaken for 15 min at 27 °C. The derivatives were added diluted in DMSO, and the controls contained the same sol-

© 2016 Wiley-VCH Verlag GmbH & Co. KGaA, Weinheim

vent concentration. The concentration of DMSO never exceeded 1% in the reaction milieu. E-64 was used as a positive control of inhibition.[32b] Then, the fluorogenic substrate Z-Phe-Arg-AMC (100 μM) was added, and the fluorescence was measured during 10 min at intervals of 3 s (excitation at 350 nm and emission at 460 nm) using a Varioskan Flash Spectrophotometer. From the slope of the negative control, we calculated the total (100%) enzyme activity, while the slopes obtained in the presence of the compounds yielded the percentage of remaining enzyme activity. The percentage of enzyme inhibition was determined as 100% of remaining enzyme activity. The experiments were done in triplicate for two independent experiments.

Dimerization check by size-exclusion fast protein liquid chromatography.[9] *Tc*TIM at a concentration of 8.0 μM in the presence and absence of 10 μM of the studied compound was incubated at 37 °C for 2 h and analyzed immediately in a Superdex 200 10/300 GL (GE Healthcare Life Sciences) column that was previously equilibrated with 100 mM triethanolamine and 10 mM EDTA, pH 7.4. The flow in the column was set to 0.5 mL min^{-1} in an ÄKTA Purifier UV 900 (GE Healthcare Life Sciences). To determine the elution volume of the monomer, *Tc*TIM, at the same concentration of 8.0 μM, was incubated for 2 h at 25 °C with 100 μM MMTS and analyzed immediately in the same column and conditions. The enzymatic activity of each samples were verified before the chromatography.

Ligand–protein molecular docking.[34–40] The geometrical structures of the synthesized compounds were fully optimized in aqueous solution at the PM6 semi-empirical level using IEF-PCM (integral equation formalism polarizable continuum model) with bond atomic radius. Molecular docking calculations were carried out with Autodock 4.2 using the implemented empirical free energy function and the Lamarckian Genetic Algorithm. In order to take into account protein flexibility, the average protein structures for *Tc*TIM[34] and *Hs*TIM[35] (obtained by previous molecular dynamic simulations) were used to perform ligand–protein docking.[36] The AutoDockTools package was employed to generate the docking input files and to analyze the docking results. Gasteiger–Marsilli charges were used for proteins and ligands.[37] Since the location of the compounds in the enzyme was unknown, a grid map with 124×126×126 points and a grid-point spacing of 0.6 Å was applied in order to explore the entire protein surface. The maps were centered on the macromolecule. Each docking consisted of 50 independent runs, with an initial population of 150 individuals, a maximum number of 2.5×10^5 energy evaluations, and a maximum number of 27000 generations. Default values were used for the remaining parameters. Results differing by less than 2.0 Å in root-square deviation were grouped into the same cluster.

Acknowledgements

The authors would like to thank the Comisión Sectorial de Investigación Científica (CSIC) of the Universidad de la República (UdelaR), Montevideo, Uruguay (CSIC–N° 661) for financial support. E. A. thanks the Agencia Nacional de Investigación e Innovación (ANII), Uruguay and the CSIC for her scholarships. This work was also supported by grants from the Consejo Nacional de Ciencia y Tecnología (CONACyT), México (167823 to R. P.-M.) and the Dirección General de Asuntos del Personal Académico (DGAPA–UNAM), México (IN221812 to RP-M).

Keywords: Chagas disease · cruzipain · enzyme inhibitors · multitarget drugs · triosephosphate isomerase · *Trypanosoma cruzi*

[1] C. J. Schofield, J. Jannin, R. Salvatella, *Trends Parasitol.* **2006**, *22*, 583–588.
[2] L. Kapelusznik, D. Varela, S. P. Montgomery, A. N. Shah, F. J. Steurer, D. Rubinstein, S. H. Factor, *Clin. Infect. Dis.* **2013**, *57*, e7.
[3] J. R. Coura, J. Borges-Pereira, *Rev. Soc. Bras. Med. Trop.* **2012**, *45*, 286–296.
[4] M. Cabrera, M. L. Lavaggi, P. Hernández, A. Merlino, M. González, H. Cerecetto, *Toxicol. Lett.* **2009**, *190*, 140–149.
[5] D. Smirlis, M. B. Soares, *Subcell. Biochem.* **2014**, *74*, 43–76.
[6] A. Merlino, M. González, H. Cerecetto, *Curr. Enzyme Inhib.* **2010**, *6*, 195–210.
[7] A. Gómez-Puyou, E. Saavedra-Lira, I. Becker, R. A. Zubillaga, A. Rojo-Domínguez, R. Pérez-Montfort, *Chem. Biol.* **1995**, *2*, 847–855.
[8] A. A. Cortés-Figueroa, A. Pérez-Torres, A. Salaiza, N. Cabrera, N. Escalona-Montaño, A. Rondán, A. Aguirre-García, M. Gómez-Puyou, A. Pérez-Montfort, R. Becker, *Parasitol. Res.* **2008**, *102*, 635–643.
[9] E. Maldonado, M. Soriano-García, A. Moreno, R. Perez-Montfort, *J. Mol. Biol.* **1998**, *283*, 193–203.
[10] V. Olivares-Illana, A. Rodríguez-Romero, I. Becker, M. Berzunza, A. Gómez-Puyou, *PLoS Neglected Trop. Dis.* **2007**, *1*, e1.
[11] V. Olivares-Illana, R. Pérez-Montfort, F. López-Calahorra, M. Costas, A. Rodríguez-Romero, M. Tuena de Gómez-Puyou, A. Gómez Puyou, *Biochemistry* **2006**, *45*, 2556–2560.
[12] G. Álvarez, B. Aguirre-López, J. Varela, M. Cabrera, A. Merlino, G. V. López, M. L. Lavaggi, W. Porcal, R. Di Maio, M. González, H. Cerecetto, N. Cabrera, R. Pérez-Montfort, M. Tuena de Gómez-Puyou, A. Gómez-Puyou, *Eur. J. Med. Chem.* **2010**, *45*, 5767–5772.
[13] E. Davioud-Charvet, I. N. Wenzel, T. J. J. Müller, G. Hanquet, D. A. Lanfranchi, F. Leroux, T. Gendron, (Centre National De La Recherche Scientifique, Paris, France), , **2011**, WO2011/033115 A2.
[14] G. Álvarez, J. Martínez, J. Varela, E. Birriel, E. Cruces, M. Gabay, S. M. Leal, P. Escobar, B. Aguirre-López, N. Cabrera, M. Tuena de Gómez-Puyou, A. Gómez-Puyou, R. Pérez-Montfort, G. Yaluff, S. Torres, E. Serna, N. Vera de Bilbao, M. González, H. Cerecetto, *Eur. J. Med. Chem.* **2015**, *100*, 246–256.
[15] a) T. L. Deepika, K. Kannabiran, V. G. Khanna, G. Rajakumar, A. A. Rahuman, *Parasitol. Res.* **2012**, *111*, 1151–1163; b) D. Saleheen, M. M. Yasinzai, *Biol. Pharm. Bull.* **2002**, *25*, 386–389.
[16] S. F. Braga, E. V. P. Alves, S. R. Ferreira, J. R. B. Fradico, P. S. Lage, M. C. Duarte, T. G. Ribeiro, P. A. S. Júnior, A. J. Romanha, M. L. Tonini, M. Steindel, E. F. Coelho, R. B. de Oliveira, *Eur. J. Med. Chem.* **2014**, *71*, 282–289.
[17] G. Álvarez, J. Varela, P. Márquez, M. Gabay, C. E. Arias Rivas, K. Cuchilla, G. A. Echeverría, O. E. Piro, M. Chorilli, S. M. Leal, P. Escobar, E. Serna, S. Torres, G. Yaluff, N. I. Vera de Bilbao, M. González, H. Cerecetto, *J. Med. Chem.* **2014**, *57*, 3984–3999.
[18] P. T. Anastas, J. C. Warner, *Green Chemistry: Theory and Practice*, Oxford University Press, New York, **1998**, 30.
[19] J. A. Dumesic, Y. Roman-Leshkov, **2007**, (Wisconsin Alumini Research Foundation, Madison, USA), EP2164928 A1.
[20] H. I. El-Subbagh, S. M. Abu-Zaid, M. Mahran, F. A. Badria, A. M. Al-Obaid, *J. Med. Chem.* **2000**, *43*, 2915–2921.
[21] G. Alvarez, B. Aguirre-López, N. Cabrera, E. B. Marins, L. Tinoco, C. I. Batthyány, M. Tuena de Gómez-Puyou, A. Gómez-Puyou, R. Pérez-Montfort, H. Cerecetto, M. González, *J. Enzyme Inhib. Med. Chem.* **2013**, *28*, 981–989.
[22] G. Alvarez, J. Martínez, B. Aguirre-López, N. Cabrera, L. Pérez-Díaz, M. Tuena de Gómez-Puyou, A. Gómez-Puyou, R. Pérez-Montfort, B. Garat, A. Merlino, M. González, H. Cerecetto, *J. Enzyme Inhib. Med. Chem.* **2014**, *29*, 198–204.
[23] a) A. Merlino, D. Benitez, S. Chavez, J. Da Cunha, P. Hernández, L. Tinoco, M. González, *MedChemComm* **2010**, *1*, 216; c) A. Merlino, D. Benitez, N. Campillo, J. Páez, L. Tinoco, M. González, H. Cerecetto, *MedChemComm* **2012**, *3*, 90–101; b) D. M. E. Caputto, L. E. Fabian, D. Benítez, A. Merlino, N. Ríos, H. Cerecetto, G. Y. Moltrasio, A. G. Moglioni, M. González, L. M. Finkielsztein, *Bioorg. Med. Chem.* **2011**, *19*, 6818–6826.

© 2016 Wiley-VCH Verlag GmbH & Co. KGaA, Weinheim

[24] A. K. Yadav, M. Kumar, M. Verma, M. Kumar, M. Kumar, *Basic Res. J. Med. Clin. Sci.* **2014**, *3*, 62 – 66.
[25] Z. Kurkcuoglu, D. Findik, E. D. Akten, P. Doruker, *Biophys. J.* **2015**, *109*, 1169 – 1178.
[26] H. S. Toogood, N. S. Scrutton, *ChemCatChem* **2010**, *2*, 892 – 914.
[27] A. Trochine, G. Álvarez, S. Corre, P. Faral-Tello, R. Durán, C. I. Batthyany, H. Cerecetto, M. González, C. Robello, *Exp. Parasitol.* **2014**, *140*, 33 – 38.
[28] J. J. Lu, Y. T. Wang, *PLoS One* **2012**, *7*, e40262.
[29] a) J. R. Dimmock, G. Y. Kao, *J. Pharm. Sci.* **1994**, *83*, 852 – 858; b) J. S. Yadav, J. Sarma, *Synth. Commun.* **2002**, *32*, 893 – 896; c) A. Barakat, H. K. Fun, *Molecules* **2015**, *20*, 13240 – 13263; d) I. Huber, I. Zupkó, I. Kovács, P. Perjési, *Monatsh. Chem.* **2015**, *146*, 973 – 981.
[30] T. P. Formariz, LA. Chiavacci, M. V. Scarpa, A. A. Silva-Júnior, E. S. Egito, C. H. Terrugi, C. M. Franzini, V. H. Sarmento, A. G. Oliveira, *Colloids Surf. B* **2010**, *77*, 47 – 53.
[31] D. B. Morton, P. H. Griffiths, *Vet. Rec.* **1985**, *116*, 431 – 436.
[32] a) M. Couto, C. Sánchez, B. Dávila, V. Machín, J. Varela, G. Álvarez, M. Cabrera, L. Celano, B. Aguirre-López, N. Cabrera, M. Tuena de Gómez-Puyou, A. Gómez-Puyou, R. Pérez-Montfort, H. Cerecetto, M. González, *Molecules* **2015**, *20*, 14595 – 14610; b) N. Fujii, J. P. Mallari, E. J. Hansell, Z. Mackey, P. Doyle, Y. Zhou, J. H. McKerrow, K. Guy, *Bioorg. Med. Chem. Lett.* **2005**, *15*, 121 – 123.
[33] C. Labriola, M. Sousa, J. J. Cazzulo, *Biol. Res.* **1993**, *26*, 101 – 107.
[34] P. Ostoa-Saloma, G. Garza-Ramos, R. Pérez-Montfort, *Eur. J. Biochem.* **1997**, *244*, 700 – 705.
[35] V. Mainfroid, S. C. Mande, K. Goraj, *Biochemistry* **1996**, *35*, 4110 – 4117.
[36] L. Minini, L. G. Álvarez, G. M. González, H. Cerecetto, A. Merlino, *J. Mol. Graphics Modell.* **2015**, *58*, 40 – 49.
[37] T. V. Borchert, R. K. Wierenga, *Structure* **1993**, *1*, 205 – 213.
[38] J. Gasteiger, M. Marsili, *Tetrahedron* **1980**, *36*, 3219 – 3228.
[39] G. M. Morris, R. K. Belew, D. S. Goodsell, A. J. Olson, *J. Comput. Chem.* **2009**, *30*, 2785 – 2791.
[40] X. G. Gao, E. Maldonado, A. Gómez-Puyou, A. Rodríguez-Romero, *Proc. Natl. Acad. Sci. USA* **1999**, *96*, 10062 – 10067.

Received: August 31, 2015
Published online on October 23, 2015

© 2016 Wiley-VCH Verlag GmbH & Co. KGaA, Weinheim

Biochemical and Biophysical Research Communications 503 (2018) 3017–3022

Contents lists available at ScienceDirect

Biochemical and Biophysical Research Communications

journal homepage: www.elsevier.com/locate/ybbrc

A strategy based on thermal flexibility to design triosephosphate isomerase proteins with increased or decreased kinetic stability

Andrea G. Quezada [a, *], Nallely Cabrera [b], Ángel Piñeiro [c], A. Jessica Díaz-Salazar [a], Selma Díaz-Mazariegos [b], Sergio Romero-Romero [d], Ruy Pérez-Montfort [b], Miguel Costas [a, **]

[a] Laboratorio de Biofisicoquímica, Departamento de Fisicoquímica, Facultad de Química, Universidad Nacional Autónoma de México, México City 04510, Mexico
[b] Departamento de Bioquímica y Biología Estructural, Instituto de Fisiología Celular, Universidad Nacional Autónoma de México, México City, 04510, Mexico
[c] Soft Matter and Molecular Biophysics Group, Departamento de Física Aplicada, Facultad de Física, Universidad de Santiago de Compostela, Campus Vida s/n, E-15782, Santiago de Compostela, Spain
[d] Laboratorio de Fisicoquímica e Ingeniería de Proteínas, Departamento de Bioquímica, Facultad de Medicina, Universidad Nacional Autónoma de México, México City, 04510, Mexico

ARTICLE INFO

Article history:
Received 26 July 2018
Accepted 11 August 2018
Available online 22 August 2018

Keywords:
Protein kinetic stability
Protein flexibility
Design strategy
Protein half-life
Differential scanning calorimetry
Triosephosphate isomerase

ABSTRACT

Kinetic stability of proteins determines their susceptibility to irreversibly unfold in a time-dependent process, and therefore its half-life. A residue displacement analysis of temperature-induced unfolding molecular dynamics simulations was recently employed to define the thermal flexibility of proteins. This property was found to be correlated with the activation energy barrier (E_{act}) separating the native from the transition state in the denaturation process. The E_{act} was determined from the application of a two-state irreversible model to temperature unfolding experiments using differential scanning calorimetry (DSC). The contribution of each residue to the thermal flexibility of proteins is used here to propose multiple mutations in triosephosphate isomerase (TIM) from *Trypanosoma brucei* (TbTIM) and *Trypanosoma cruzi* (TcTIM), two parasites closely related by evolution. These two enzymes, taken as model systems, have practically identical structure but large differences in their kinetic stability. We constructed two functional TIM variants with more than twice and less than half the activation energy of their respective wild-type reference structures. The results show that the proposed strategy is able to identify the crucial residues for the kinetic stability in these enzymes. As it occurs with other protein properties reflecting their complex behavior, kinetic stability appears to be the consequence of an extensive network of inter-residue interactions, acting in a concerted manner. The proposed strategy to design variants can be used with other proteins, to increase or decrease their functional half-life.

© 2018 Elsevier Inc. All rights reserved.

1. Introduction

Protein stability has two main facets. One is the thermodynamic stability, which is measured by the free energy change upon unfolding and that can only be considered when the denaturation process, induced by temperature, pressure or a chemical agent, is reversible. The second facet is the kinetic stability, which refers to the time-dependence of an irreversible protein denaturation process. There have been many efforts to understand, predict and ultimately modify the thermodynamic stability of proteins [1,2]. In contrast, less work has been devoted to reach those same goals in regard to protein kinetic stability, even though it has many biological and practical roles. Among these roles are the resistance to proteolysis, the prevention of aggregation or premature degradation and the regulation of cellular processes by controlling the trigger and timing of molecular motion [3]. Protein kinetic stability is also a key parameter to understand the balance between function and stability as shaped by evolution in cell-relevant time scales. The disruption of this balance in the crowded cell medium may result in a variety of pathological conditions [4,5]. In addition, it may play a relevant role as a control mechanism of the circadian clock [6,7].

* Corresponding author.
** Corresponding author.
E-mail addresses: agutierrez@email.ifc.unam.mx (A.G. Quezada), costasmi@unam.mx (M. Costas).

https://doi.org/10.1016/j.bbrc.2018.08.087
0006-291X/© 2018 Elsevier Inc. All rights reserved.

Finally, it is an important parameter to predict and enhance the half-life of proteins with biotechnological and biomedical applications [8,9].

Protein kinetic stability determines the susceptibility of a protein to irreversible unfolding in a time-dependent process [10]. In the framework of the transition state theory, it can be quantified by an activation energy barrier (E_{act}) between the native state and the transition state that ultimately leads to non-functional forms, unable to fold back to the native state. The larger this barrier is, the more kinetically stable the protein is. E_{act} might be very large, virtually trapping the protein in a specific conformation state for enough time to endow it with a remarkably long half-life, as is the case for α-lytic protease [11]. For this kind of kinetically hyperstable proteins the measurement of their denaturation kinetics is quite elaborate and difficult [12,13]. For a large number of other proteins the denaturation process can be described by a rate constant that is measurable in the laboratory with conventional techniques [4]. In particular, assuming that the temperature dependence of the rate constant follows the Arrhenius equation, E_{act} can be conveniently obtained using Differential Scanning Calorimetry (DSC) [10].

The E_{act} values have been interpreted in terms of desolvation/solvation barriers for the protein folding/unfolding processes [8,14], their role being to reduce protein flexibility and increase folding/unfolding cooperativity [15,16]. On the other hand, protein flexibility has been estimated using several strategies [17–20]. Two broad definitions have been considered in the literature, namely the "static" and the "dynamic" flexibilities [21]. The former pertains to the conformational diversity and number of fluctuation conformations in the equilibrium ensemble, while the later refer to how quickly the protein can hop between different conformations. Recently, we have defined protein thermal flexibility as a measure of the increment of the conformational space available to the protein when energy is provided upon an increase in temperature [22]. A quantitative measure of protein thermal flexibility was obtained using a residue displacement analysis of temperature-induced unfolding molecular dynamics (MD) simulations at several temperatures, providing the temperature gradient of the total displacement (TGD). Using as model systems two triosephosphate isomerases (TIM) from two parasites closely related by evolution (*Trypanosoma brucei* (TbTIM) and *Trypanosoma cruzi* (TcTIM)), we demonstrated that there is a correlation between protein kinetic stability (as measured by E_{act} obtained from DSC experiments) and thermal flexibility (as given by TGD from multi-temperature MDs) [22]. Based on this correlation, in this work we propose and test a strategy to design new functional triosephosphate isomerase proteins with decreased or increased kinetics stabilities. The proposed method is here restricted to two TIM proteins but it could eventually be extended to any other protein. Moreover, we intend to contribute to the understanding of the molecular basis of kinetic stability.

2. Materials and methods

2.1. Construction, gene design, expression, purification and activity assays for the TIM variants

The DNA sequences with the NCBI ID numbers X03921 (TbTIM) and U53867 (TcTIM) were used for the design of the 6 mutant proteins studied in this work: Tb35hi, Tc35lo, Tb11hi, Tc11lo, Tb9hi and Tb5hi. Tb35hi has 35 mutations distributed over the sequence of wild-type TbTIM (see Table 1); Tc35lo has 35 mutations inserted into the sequence of wild-type TcTIM; Tb11hi and Tc11lo have 11 mutations between the $(\beta\alpha)_4$ and the $(\beta\alpha)_5$ domains of wild-type TbTIM and wild-type TcTIM, respectively. Tb9hi and Tb5hi, have 9 and 5 mutations in the $(\beta\alpha)_5$ domain, and between the $(\beta\alpha)_5$ and $(\beta\alpha)_6$ domains of wild-type TbTIM, respectively. Enzyme activity was determined in the direction of glyceraldehyde 3-phosphate (GAP) to dihydroxyacetone phosphate (DHAP) by a coupled assay with α-glycerophosphate dehydrogenase (α-GDH), following β-nicotinamide adenine dinucleotide (NADH) oxidation by absorbance changes at 340 nm [23]. The data were adjusted to the Michaelis-Menten model and the values of K_M and V_{max} were calculated by non-linear regression. To calculate the catalytic efficiency, the value of K_M was corrected considering that there is only 4% of free GAP in the solution [24]. A complete account of the chemicals and methodologies employed is given in the Supplementary Material.

Table 1
Mutations in TbTIM.

	Mutation[a]	Type[e]		Mutation[a]	Type[e]
1	S20L	nc	19	V141A[b,c]	sc
2	S22V	nc	20	I 147L[b,c]	c
3	E23P	nc	21	I 150V[b,c]	c
4	D26E	c	22	K152Q[b,c]	c
5	S43P	nc	23	K155S[b,c,d]	sc
6	V46L	c	24	A157E[c]	nc
7	A69T	c	25	D158A[c,d]	nc
8	F86Y	c	26	A160S[c,d]	c
9	N89S	sc	27	K161R[c,d]	c
10	I91V	c	28	S195 R	nc
11	A100L[b]	nc	29	A200T	c
12	D111E[b]	c	30	E205Q[d]	c
13	A115Q[b]	nc	31	N215T	sc
14	V117C[b]	nc	32	G216A	sc
15	S119A	c	33	Q225 M	nc
16	A125V	sc	34	V228I	c
17	L131N[b]	nc	35	Q250K	c
18	Q132E[b]	c			

Mutations in the sequence of TbTIM used to construct variants: [a]Tb35hi, [b]Tb11hi, [c]Tb9hi and [d]Tb5hi. To construct variants Tc11lo and Tc35lo the mutations performed in the sequence of TcTIM are those specified exchanging the indicated amino acids and correcting the sequence position by adding one, *i.e.* L21S, V23S *etcetera*. [e]Type of mutation performed according to CLUSTAL [30]: non conservative (nc), semi conservative (sc) and conservative (c).

2.2. Differential scanning calorimetry

DSC experiments were performed using a VP-DSC capillary calorimeter (Microcal, Malvern). The protein concentration was 0.4 mg/mL (determined from the absorbance at 280 nm using a Cary 50 spectrophotometer), with samples prepared by exhaustive dialysis against 100 mM TEA and 10 mM EDTA (pH 7.4). The calorimetric traces (scanning rates ranged from 0.5 to 3 K/min) were fitted to the two-state irreversible model [8,14,25] using home-made software. This model assumes that upon heating, the native protein (N) undergoes a conformational transition to a final state (F), which is unable to fold back. The kinetic conversion between these two states is described by a first-order rate constant k whose temperature dependence is assumed to follow the Arrhenius equation:

$$k = exp\left[-\frac{E_{act}}{R}\left(\frac{1}{T} - \frac{1}{T^*}\right)\right] \quad (1)$$

where E_{act} being the activation energy value, and T^* is the

temperature at which the rate constant equals 1 min^{-1}. In this model, the apparent heat capacity is written in terms of the mole fraction of native state (X_N) and its temperature dependence (dX_N/dT) as [8]:

$$C_P^{APP} = C_P^{PRE} + \left(C_P^{POST} - C_P^{PRE}\right)(1 - X_N) - \Delta H\left(\frac{dX_N}{dT}\right) \quad (2)$$

with X_N and dX_N/dT being given by:

$$X_N = exp\left[- exp\left(\frac{E_{act}\Delta T}{RT_m^2}\right)\right] \quad (3)$$

$$\frac{dX_N}{dT} = -\frac{E_{act}}{RT_m^2} exp\left(\frac{E_{act}\Delta T}{RT_m^2}\right) exp\left[- exp\left(\frac{E_{act}\Delta T}{RT_m^2}\right)\right] \quad (4)$$

where C_p^{PRE} and C_p^{POST} are the pre- and post-transition baselines which were taken to be linear functions of temperature, ΔH is the denaturation enthalpy (N to F transition), T_m is the temperature corresponding to the maximum of the unfolding transition, E_{act} is the activation energy barrier separating the native state from the transition state and $\Delta T = T - T_m$. Each individual experimental DSC profile (*i.e.* for every scan rate employed) was fitted with Eqs. (2)–(4), and the E_{act} value obtained from Eq. (1) using an Arrhenius plot (ln *k v.s.* 1/T).

3. Results and discussion

Triosephosphate isomerases (TIM) from *Trypanosoma brucei* (TbTIM) and *Trypanosoma cruzi* (TcTIM), two parasites closely related by evolution, are used here as model systems. These two enzymes are obligated homodimers with 74% sequence identity, and their three-dimensional structures superpose with a RMSD value of less than 1 Å. Nevertheless, they show remarkably different behaviors in several aspects [26–29]. In particular, the activation energy value for TcTIM is twice that of TbTIM [14], *i.e.* these two enzymes have very different energetic barriers for irreversible denaturation with only small changes in structure. Therefore, they are excellent models to study the molecular basis of kinetic stability. The large difference between E_{act} values obtained from DSC experiments (822 ± 30 kJ/mol for TcTIM and 434 ± 26 kJ/mol for TbTIM) have been explained in terms of their different thermal flexibilities as measured by their TGD values obtained from MD simulations (2.12 ± 0.19 Å/K for TcTIM and 1.50 ± 0.10 Å/K for TbTIM) [22]. The methodology based on short-length, high-temperature, all-atom non-equilibrium MD simulations at high temperature reported in Ref. [22] allows the calculation of TGD for any protein as a whole, as well as to evaluate the contributions to TGD of each individual residue in its sequence (TGD_{res}). Fig. 1A shows the average individual residue contributions (TGD_{res}) of the two subunits, to the overall TGD values for TcTIM and TbTIM.

The determination of the individual contributions for every residue to the thermal flexibilities of TcTIM and TbTIM allows the design of TIM variants with different TGD values. We first identified the positions and residues that are different in TcTIM and TbTIM and that differ in their TGD_{res} values. The aligned sequences and the 65 differences between them are given in Fig. S1 (Supplementary). Then, we constructed TIM mutants by substituting a residue with a small TGD_{res} value in one protein with the residue having a large TGD_{res} value in the other protein, and *viceversa*. The variants constructed using this strategy are reported in Table 1. The protein Tb35hi was constructed performing 35 mutations over the whole TbTIM sequence (the protein with smaller TGD). Hence, this variant has all the residues with high TGD_{res} values (Fig. 1A). On the other hand, Tc35lo was built mutating the same 35 residues in the TcTIM sequence (the protein with larger TGD) and therefore this variant carries all the residues with low TGD_{res} values (Fig. 1A). The only criterion employed to perform the mutations was the TGD_{res} individual values, the resulting residue replacement being spread over the whole protein (Fig. 1B). In addition, four other variants were constructed focusing on those residues whose TGD_{res} values differ the most between TcTIM and TbTIM: Tb11hi, Tc11lo with 11 mutations, Tb9hi with 9 mutations and Tb5hi with 5 mutations (Table 1). All six variants had TIM activity (Supplementary Table T1), and their catalytic efficiencies (k_{cat}/K_M) were within the $\mu \pm \sigma$ interval (μ being the mean and σ the standard deviation) calculated using data from 23 wild-type TIMs reported in the literature (Supplementary Fig. S2 and Table T2). In consequence, they are correctly folded and are catalytically competent proteins.

Scanning-rate-dependent DSC measurements were used to characterize the kinetics of the denaturation and to determine the activation energy values for the six TIM variants. The E_{act} values for the wild-type TcTIM and TbTIM proteins have been previously reported and discussed in detail [14]. The DSC profiles of all the variants showed that their thermal denaturation is scan-rate dependent and is irreversible, *i.e.* no signal was observed after cooling and reheating the samples. As an example, Fig. 2A shows the DSC profiles for Tb35hi which are well described by the two-state irreversible model (Materials and Methods). The compliance of the model with the calorimetric profiles obtained experimentally indicates that the kinetically relevant transition is dimeric, as was the case for wild-type TcTIM and TbTIM [14], the E104D mutants of several TIMs [25] and specific proline mutations [31]. The activation energies were obtained (Supplementary Table T1) from the slopes of the Arrhenius plots as that displayed in Fig. 2B. For the other variants the fitted calorimetric profiles and the corresponding Arrhenius plots are given in the Supplementary Material (Figs. S3 and S4). The E_{act} values for all the variants are given in Supplementary Table T1, together with the temperatures corresponding to the maximum of each transition (T_m) and the estimated half-life times.

The activation energies for wild-type TcTIM and TbTIM and the six studied variants are compared in Fig. 3. The 35 mutations introduced in the sequence of TcTIM (Table 1) have a very important influence on E_{act}, *i.e.* the kinetic stability of the construct Tc35lo is half that of the original wild-type protein. Clearly, the decrease of the thermal flexibility of the protein by the introduction of residues with low TGD_{res} values in TcTIM (Fig. 1*A*) reduces its kinetic stability. Tc35lo is an exceptionally unstable TIM that during the purification procedures had a great propensity to form aggregates, a fact that is most probably a reflection of its small kinetic stability. Despite many modifications of the usual TIM purification protocols, we were unable to obtain a His-tag free Tc35lo. In contrast, the tagged protein was soluble for approximately 7 h, which allowed us perform the DSC experiment. Hence, the E_{act} value shown in Fig. 3 corresponds to Tc35lo with the His-tag. Nevertheless, a His-tagged Tb35hi revealed that the presence of a His-tag has no significant effect on the E_{act} value of this protein (only 2% difference with respect to the Tb35hi without His-tag (Supplementary Table T1)). Therefore, the E_{act} value of Tc35lo with a His-tag is comparable to the E_{act} values for the other proteins reported in this work. The introduction of 11 residues with low TGD_{res} values to the sequence of TcTIM (Fig. 1 and Table 1) to construct Tc11lo also decreased the E_{act} (Fig. 3), showing again that the selection of individual mutations based on their TGD values has an important effect on the kinetic stability. Overall, the results for Tc35lo and Tc11lo illustrate the well-known fact that it is much easier to disrupt the stability of a protein than to enhance it.

The 35 mutations introduced in the sequence of TbTIM (Fig. 1

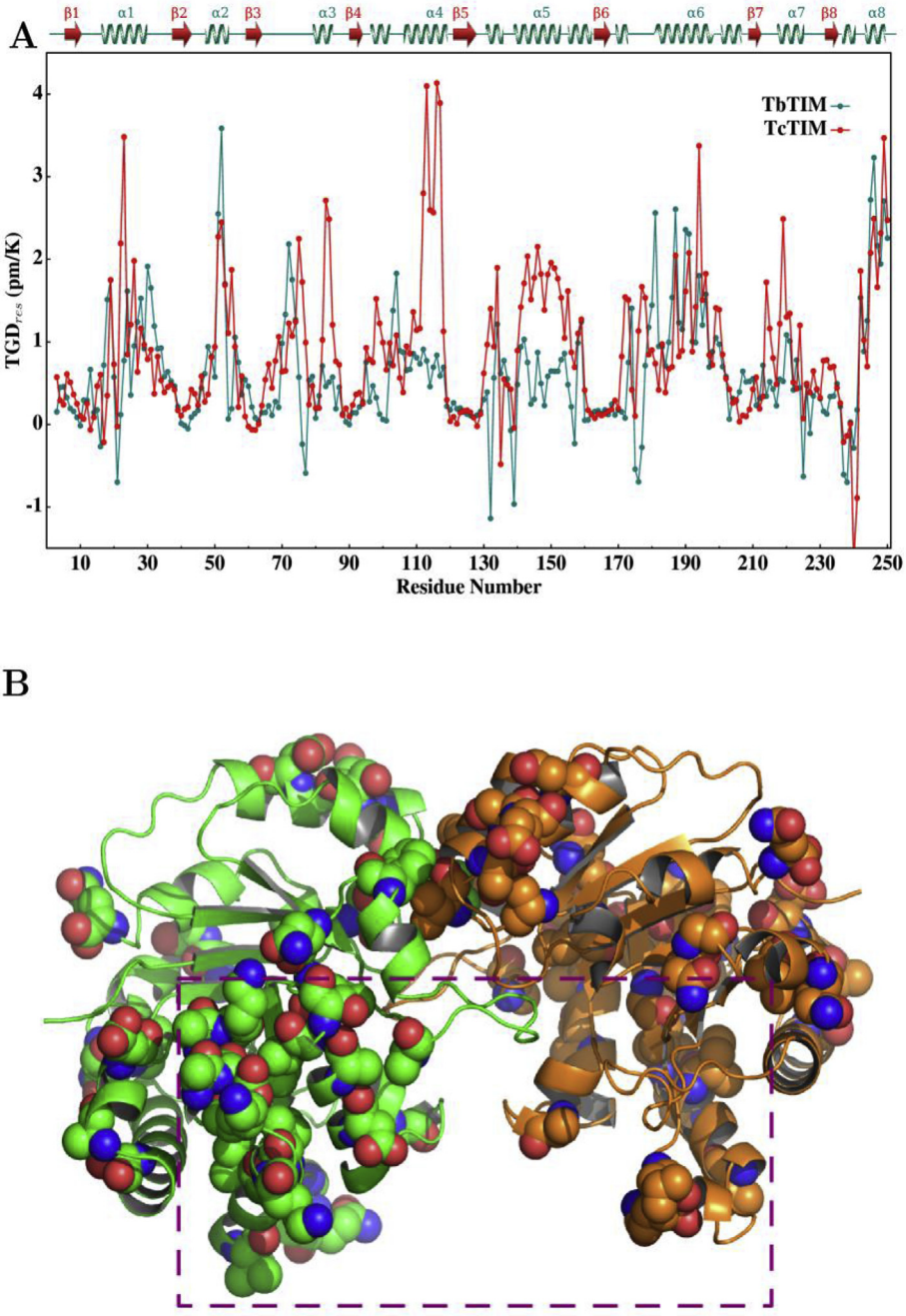

Fig. 1. A. TGD$_{res}$ values for each residue (average for both subunits) of TcTIM and TbTIM (modified figure from Ref. [22]). The secondary structure is depicted at the top of the plot. A summary of the analysis required to determine the TGD$_{res}$ values is described in the Supplementary Material and, in full detail, in Ref. [22]. **B.** TbTIM dimeric structure (PDBID: 5TIM) depicting the 35 residues mutated to produce Tb35hi (Table 1). The equivalent residues were mutated in TcTIM to produce Tc35lo (Table 1). Residues in alpha 4 and alpha 5 helices, which contribute the most in the difference in TGD between both wild type proteins (2.12 ± 0.19 Å/K for TcTIM and 1.50 ± 0.10 Å/K for TbTIM), are shown within the box.

and Table 1) have a large impact in the E_{act}, *i.e.* the kinetic stability of the construct Tb35hi is twice that of the original wild-type protein. Clearly, the introduction of mutations with large TGD$_{res}$ identified from MD simulations of the two wild-type triosephosphate isomerases (Fig. 1) successfully increases the kinetic stability and the half-life time (Supplementary Table T1). Fig. 3 also shows that introducing a smaller number of mutations to construct the Tb5hi, Tb9hi and Tb11hi does not increase the E_{act}, despite the mutations being those corresponding to the residues that have the highest TGD$_{res}$ values (Fig. 1). A clear avenue for future work is to gain insight into this non cumulative effect constructing other TIM variants. Despite this, the results for Tb35hi show the proposed strategy is able to identify the crucial residues for the kinetic stability of triosephosphate isomerases.

It should be emphasized that the only criterion used to choose the 35 mutations in Table 1 was the thermal flexibility TGD$_{res}$ obtained from the residue displacement analysis of multi-temperature MD simulations (Fig. 1A). The 35 mutations performed to construct Tb35hi and Tc35lo represent 14% of the total number of the residues of each TIM monomer, and 54% of the residues that are different between wild-type TcTIM and wild-type TbTIM. 17 of the 35 substitutions (49%) are conservative, 6 (17%) are

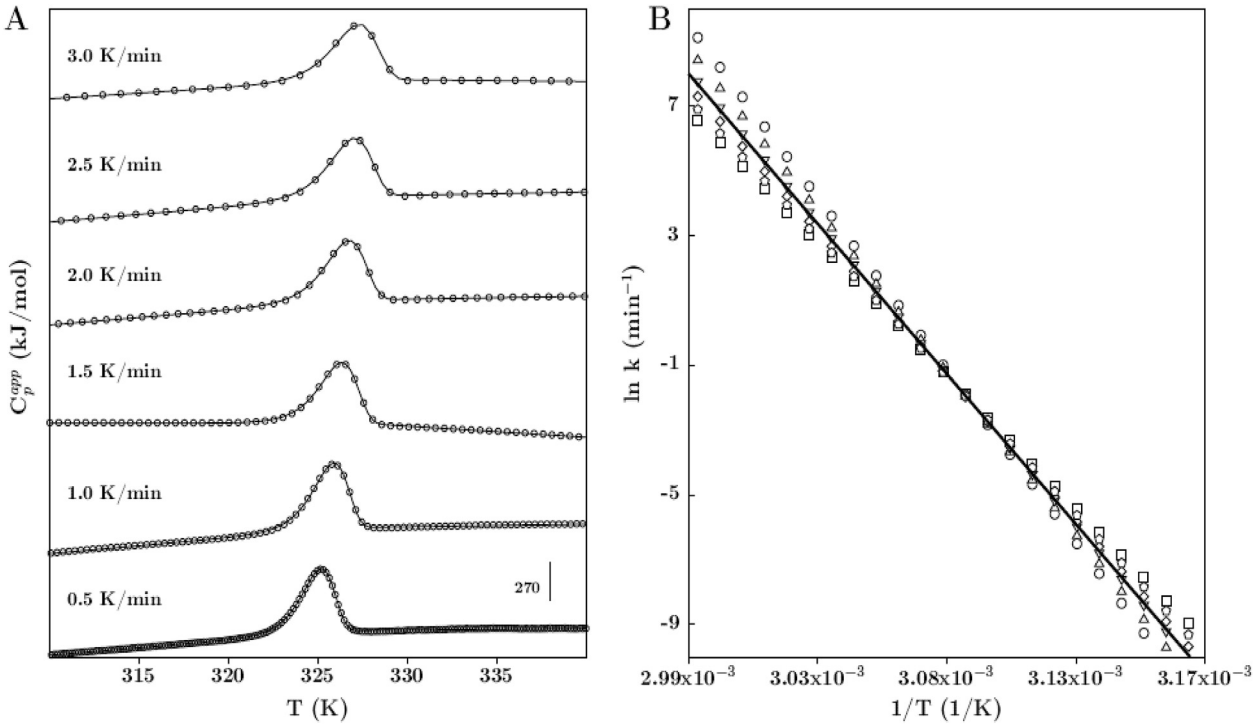

Fig. 2. A. Experimental DSC thermogram for the TIM variant Tb35hi at the indicated scan rates and at 0.4 mg/mL. Symbols represent the apparent heat capacity and continuous lines represent the fitting to the two-state irreversible model (Materials and Methods). The profiles have been shifted in the y axis for clarity. **B.** Arrhenius plot. Symbols correspond to the different scan rates indicated in A. The straight line is the best fit for all the points, its slope providing the activation energy E_{act} value (Supplementary Table T1).

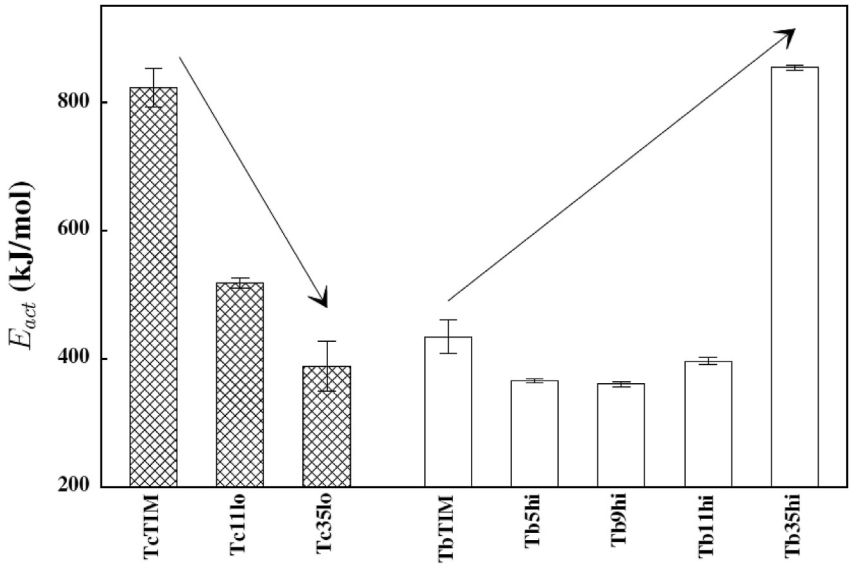

Fig. 3. Comparison between the activation energies for wild-type TcTIM and wild-type TbTIM (from Ref. [22] and for the six variants studied in this work (Supplementary Table T1). The arrows indicate the increase and decrease in kinetic stability in going from wild-type TbTIM to Tb35hi and from wild-type TcTIM to Tc35lo, respectively.

semi-conservative and 12 (34%) are non-conservative (Table 1), *i.e.* there is no clear prevalence of any given type of mutation. However, the slight predominance of semi conservative and conservative substitutions (51%) is consistent with the fact that these substitutions are more prone to occur during evolution. Further, 34% of the 35 mutations were performed on residues that have 30% or more of their Accessible Surface Area exposed to the solvent media, and hence can be considered as part of the protein surface [32]. Without ruling out that protein kinetic stability can be importantly affected by point mutations, the results for Tb35hi and Tc35lo indicate that an increased or decreased thermal flexibility, leading to an increased or decreased kinetic stability, is more the result of concerted effects between many residues that occur in a global spatial context, than of the chemical identity and particular position in the structure of the involved amino acids. Hence, as it is the case with other protein properties, kinetic stability is also the consequence of an extensive network of inter-residue interactions, acting in a concerted manner. In summary, we have shown that

using a strategy based on the calculation of residue thermal flexibility (TGD_{res}) from low consuming computational resources MD simulations, it is possible to successfully convert a wild-type triosephosphate isomerase with a small E_{act} value into a variant with a large kinetic stability, without losing function. For many other proteins, this is certainly a desirable goal for biotechnological applications and might assist in improving the present knowledge on how evolution reached the balance between protein function and stability.

Conflicts of interest

The authors declare no conflict of interest.

Acknowledgements

We thank Drs. Luis Olguín and Alejandro Fernández for their comments and critical review of the manuscript. We also thank Unidad de Biología Molecular at the Instituto de Fisiología Celular-UNAM (Dr. Laura Ongay, Ms. Guadalupe Codiz and Ms. Minerva Mora) for technical support. This work was supported by grant 5000-9018 from PAIP-FQ-UNAM to M.C., grant 254694 from CONACyT-México to R.P.-M., and grant MAT2015-71826-P from MINECO-Spain to Á.P.

Appendix A. Supplementary data

Supplementary data related to this article can be found at https://doi.org/10.1016/j.bbrc.2018.08.087.

References

[1] R. Guerois, J.E. Nielsen, L. Serrano, Predicting changes in the stability of proteins and protein complexes: a study of more than 1000 mutations, J. Mol. Biol. 320 (2002) 369–387.
[2] A. Goldenzweig, S. Fleishman, Principles of protein stability and their application in computational design, Annu. Rev. Biochem. 87 (2018) 105–129.
[3] W. Colón, J. Church, J. Sen, J. Thibeault, H. Trasatti, K. Xia, Biological roles of protein kinetic stability, Biochemistry 56 (2017) 6179–6186.
[4] I.M. Plaza Del Pino, B. Ibarra-Molero, J.M. Sanchez-Ruiz, Lower kinetic limit to protein thermal stability: a proposal regarding protein stability in vivo and its relation with misfolding diseases, Proteins Struct. Funct. Genet. 40 (2000) 58–70.
[5] J.S. Valastyan, S. Lindquist, Mechanisms of protein-folding diseases at a glance, Dis. Model. Mech. 7 (2014) 9–14.
[6] P. Ruoff, J.J. Loros, J.C. Dunlap, The relationship between FRQ-protein stability and temperature compensation in the Neurospora circadian clock, Proc. Natl. Acad. Sci. U.S.A. 102 (2005) 17681–17686.
[7] Di Wu, Q. Hu, Z. Yan, W. Chen, C. Yan, X. Huang, J. Zhang, P. Yang, H. Deng, J. Wang, X. Deng, Y. Shi, Structural basis of ultraviolet-B perception by UVR8, Nature 484 (2012) 214–219.
[8] D. Rodriguez-Larrea, S. Minning, T.V. Borchert, J.M. Sanchez-Ruiz, Role of solvation barriers in protein kinetic stability, J. Mol. Biol. 360 (2006) 715–724.
[9] R.M. Ionescu, J. Vlasak, C. Price, M. Kirchmeier, Contribution of variable domains to the stability of humanized IgG1 monoclonal antibodies, J. Pharmacol. Sci. 97 (2008) 1414–1426.
[10] J.M. Sanchez-Ruiz, Protein kinetic stability, Biophys. Chem. 148 (2010) 1–15.
[11] E.L. Cunningham, S.S. Jaswal, J.L. Sohl, D.A. Agard, Kinetic stability as a mechanism for protease longevity, Proc. Natl. Acad. Sci. U.S.A. 96 (1999) 11008–11014.
[12] K. Xia, M. Manning, H. Hesham, Q. Lin, C. Bystroff, W. Colón, Identifying the subproteome of kinetically stable proteins via diagonal 2D SDS/PAGE, Proc. Natl. Acad. Sci. U.S.A. 104 (2007) 17329–17334.
[13] C. Park, S. Zhou, J. Gilmore, S. Marqusee, Energetics-based protein profiling on a proteomic scale: identification of proteins resistant to proteolysis, J. Mol. Biol. 368 (2007) 1426–1437.
[14] M. Costas, D. Rodríguez-Larrea, L. De Maria, T.V. Borchert, A. Gómez-Puyou, J.M. Sanchez-Ruiz, Between-species variation in the kinetic stability of TIM proteins linked to solvation-barrier free energies, J. Mol. Biol. 385 (2009) 924–937.
[15] Z. Liu, H.S. Chan, Solvation and desolvation effects in protein folding: native flexibility, kinetic cooperativity and enthalpic barriers under isostability conditions, Phys. Biol. 9 (2005) S75–S85.
[16] M.S. Cheung, A.E. García, J.N. Onuchic, Protein folding mediated by solvation: water expulsion and formation of the hydrophobic core occur after the structural collapse, Proc. Natl. Acad. Sci. 99 (2002) 685–690.
[17] N.C. Benson, V. Daggett, Dynameomics: large-scale assessment of native protein flexibility, Protein Sci. 17 (2008) 2038–2050.
[18] M. Jamroz, A. Kolinski, S. Kmiecik, CABS-flex : server for fast simulation of protein structure fluctuations 41 (2013) 427–431.
[19] J. Ma, Usefulness and limitations of normal mode analysis in modeling dynamics of biomolecular complexes, Structure 13 (2005) 373–380.
[20] M.L. Teodoro, G.N. Phillips, L.E. Kavraki, Understanding protein flexibility through dimensionality reduction, J. Comput. Biol. 10 (2003) 617–634.
[21] K.E. Tang, K.A. Dill, Native protein fluctuations: the conformational-motion temperature and the inverse correlation of protein flexibility with protein stability, J. Biomol. Struct. Dyn. 16 (1998) 397–411.
[22] A.G. Quezada, A.J. Díaz-Salazar, N. Cabrera, R. Pérez-Montfort, Á. Piñeiro, M. Costas, Interplay between protein thermal flexibility and kinetic stability, Structure 25 (2017) 167–179.
[23] B. Plaut, J.R. Knowles, pH-dependence of the triose phosphate isomerase reaction, Biochem. J. 129 (1972) 311–320.
[24] D.R. Trentham, C.H. McMurray, C.I. Pogson, The active chemical state of d-glyceraldehyde 3-phosphate in its reactions with d-glyceraldehyde 3-phosphate dehydrogenase, aldolase and triose phosphate isomerase, Biochem. J. 114 (1969) 19–24.
[25] Y. Aguirre, N. Cabrera, B. Aguirre, R. Pérez-Montfort, A. Hernandez-Santoyo, H. Reyes-Vivas, S. Enríquez-Flores, M. de Gómez-Puyou, A. Gómez-Puyou, J.M. Sanchez-Ruiz, M. Costas, Different contribution of conserved amino acids to the global properties of triosephosphate isomerases, Proteins 82 (2014) 323–335.
[26] I. García-Torres, N. Cabrera, A. Torres-Larios, M. Rodríguez-Bolaños, S. Díaz-Mazariegos, A. Gómez-Puyou, R. Perez-Montfort, Identification of amino acids that account for long-range interactions in two triosephosphate isomerases from pathogenic trypanosomes, PLoS One 6 (2011), e18791.
[27] V. Guzman-Luna, G. Garza-Ramos, The folding pathway of glycosomal triosephosphate isomerase: structural insights into equilibrium intermediates, Proteins Struct. Funct. Bioinforma. 80 (2012) 1669–1682.
[28] M. Rodríguez-Bolaños, N. Cabrera, R. Perez-Montfort, Identification of the critical residues responsible for differential reactivation of the triosephosphate isomerases of two trypanosomes, Open Biol 6 (2016) pii: 160161.
[29] S. Díaz-Mazariegos, N. Cabrera, R. Perez-Montfort, Three unrelated and unexpected amino acids determine the susceptibility of the interface cysteine to a sulfhydryl reagent in the triosephosphate isomerases of two trypanosomes, PLoS One 13 (2018), e0189525.
[30] M. Goujon, H. McWilliam, W. Li, F. Valentin, S. Squizzato, J. Paern, R. Lopez, A new bioinformatics analysis tools framework at EMBL–EBI, Nucleic Acids Res. 38 (2010) W695–W699.
[31] V. Guzmán-Luna, A.G. Quezada, A.J. Díaz-Salazar, N. Cabrera, R. Pérez-Montfort, M. Costas, The effect of specific proline residues on the kinetic stability of the triosephosphate isomerases of two trypanosomes, Proteins Struct. Funct. Bioinforma. 85 (2017) 571–579.
[32] G. Nicolas, P.M. C, SWISS-MODEL and the Swiss-Pdb Viewer: an environment for comparative protein modeling, Electrophoresis 18 (2005) 2714–2723.